MERCURY EMISSION BEHAVIOR DURING ISOLATED COAL PARTICLE COMBUSTION

A Dissertation

by

MADHU BABU PUCHAKAYALA

Submitted to the Office of Graduate Studies of
Texas A&M University
in partial fulfillment of the requirements for the degree of

DOCTOR OF PHILOSOPHY

December 2006

Major Subject: Mechanical Engineering

MERCURY EMISSION BEHAVIOR DURING ISOLATED COAL PARTICLE COMBUSTION

A Dissertation

by

MADHU BABU PUCHAKAYALA

Submitted to the Office of Graduate Studies of
Texas A&M University
in partial fulfillment of the requirements for the degree of

DOCTOR OF PHILOSOPHY

Approved by:

Chair of Committee,	Kalyan Annamalai
Committee Members,	N. K. Anand
	Bing Guo
	Yassin A. Hassan
Head of the Department,	Dennis O' Neal

December 2006

Major Subject: Mechanical Engineering

ABSTRACT

Mercury Emission Behavior during Isolated Coal

Particle Combustion. (December 2006)

Madhu Babu Puchakayala, B.Tech., Indian Institute of Technology, Madras, India;

M.Tech., Indian Institute of Technology, Madras, India

Chair of Advisory Committee: Dr. Kalyan Annamalai

Of all the trace elements emitted during coal combustion, mercury is most problematic. Mercury from the atmosphere enters into oceanic and terrestrial waters. Part of the inorganic Hg in water is converted into organic Hg (CH_3Hg), which is toxic and bioaccumulates in human and animal tissue.

The largest source of human-caused mercury air emissions in the U.S is from combustion coal, a dominant fuel used for power generation. The Hg emitted from plants primarily occurs in two forms: elemental Hg and oxidized Hg (Hg^{2+}). The coal chlorine content and ash composition, gas temperature, residence time and presence of different gases will decide the speciation of Hg into Hg^0 and Hg^{2+}. For Wyoming coal the concentrations of mercury and chlorine in coal are 120ppb and 140ppb.

In order to understand the basic process of formulation of $HgCl_2$ and Hg^0 a numerical model is developed in the current work to simulate in the detail i) heating ii) transient pyrolysis of coal and evolution of mercury and chlorine, iii) gas phase oxidation iv) reaction chemistry of Hg and v) heterogeneous oxidation of carbon during

isolated coal particle combustion. The model assumes that mercury and chlorine are released as a part of volatiles in the form of elemental mercury and HCl. Homogenous reaction are implemented for the oxidation of mercury. Heterogeneous Hg reactions are ignored. The model investigates the effect of different parameters on the extent of mercury oxidation; particle size, ambient temperature, volatile matter, blending coal with high chlorine coal and feedlot biomass etc,.

Mercury oxidation is increased when the coal is blended with feedlot biomass and high chlorine coal and Hg % conversion to $HgCl_2$ increased from 10% to 90% when 20% FB is blended with coal. The ambient temperature has a negative effect on mercury oxidation, an increase in ambient temperature resulted in a decrease in the mercury oxidation. The percentage of oxidized mercury increases from 9% to 50% when the chlorine concentration is increased from 100ppm to 1000ppm. When the temperature is decreased from 1950 K to 950 K, the percentage of mercury oxidized increased from 3% to 27%.

To My Parents and Sister

ACKNOWLEDGEMENTS

I would like to express my deep appreciation to Dr. Kalyan Annamalai for the patience he has shown me, opinions he has shared with me and the guidance and support he has given me for the past few years. They have been invaluable. In addition, I would like to thank Dr. N K Anand, Dr. Bing Guo and Dr. Yassin A Hassan for taking the time to serve on my committee. This material was prepared with the support of the Texas Commission on Environmental Quality (TCEQ) and partly from DOE- Golden, Colorado. However, any findings, conclusions, or recommendations expressed herein are those of the author and do not necessarily reflect the view of TCEQ and the DOE.

TABLE OF CONTENTS

Page

Page

Page

LIST OF FIGURES

Page

Page

Page

LIST OF TABLES

Page

1 INTRODUCTION

Mercury is emitted from a wide variety of natural and man-made sources. Alkali and metal processing, incineration of coal, and medical and other waste, and mining of gold and mercury contribute greatly to mercury concentrations in some areas, but atmospheric deposition is the dominant source of mercury over most of the landscape. Once in the atmosphere, mercury is widely disseminated and can circulate for years, accounting for its wide-spread distribution. Natural sources of atmospheric mercury include volcanoes, geologic deposits of mercury, and volatilization from the ocean. Although all rocks, sediments, water, and soils naturally contain small but varying amounts of mercury, scientists have found some local mineral occurrences and thermal springs that are naturally high in mercury.

Health effects due to mercury depend on the form of mercury exposure. Exposure to elemental mercury may lead to lung injury, and nervous system failure. Symptoms of high exposures to inorganic mercury can be memory loss, skin rashes, muscle weakness, etc.

The principal anthropogenic source of mercury is from power plants, cement kilns, waste incineration, etc. Conventional cleaning devices are fairly effective in capturing the oxidized mercury compounds, such as mercury chloride ($HgCl_2$), but are very poor in removing the elemental mercury (Hg^0). Therefore, the mercury content of solid fuels is

---

This document follows the style of Combustion and Flame.

generally emitted to the atmosphere in its elemental form, subsequently settling on agricultural lands and lakes. Mercury can be converted by micro-organism into its especially toxic organic form, methyl mercury that can enter the food chain.

Pulverized coal combustion is the most commonly used method in coal-fired power plants. Figure 1.1 shows a schematic of a typical coal fired power plant. The coal is ground (pulverized) to a fine powder, so that less than 2% is +300 μm and 70-75% is below 75 μm, for a bituminous coal. By way of hot air, the dust is blown into the combustion chamber of the steam generator. In the piping system of the steam generator, the water is converted to steam at high pressures. The steam drives the turbine which in turn powers the connected generator. The steam is, after it has expended its energy in the turbine, liquefied in the condenser at ambient temperature. This water is returned to the steam generator over the heater and the supply pumps. The cooling water circuit is used to transmit the heat from the condenser to the atmosphere. If the warming capacity of the river is insufficient, then the discharged heat can be transmitted to the air in part or completely by way of a cooling tower. During the combustion of coal, products as a result of combustions result (CO_2, SO_2, NO_x, ash, slag, gypsum). Initially, the nitrogen oxides contained in the flue gas are reduced in a catalyzer. Subsequently, the flue gas is made dust free in an electro-filter to be additionally cleaned in a flue gas desulphurization plant. The ash removed from the steam generator and the electro filter can be used in the construction industry.

The coal-fired electric power plants are the largest source of human-caused mercury air emissions in the U.S. While world wide emission is 1900 tons per year from natural

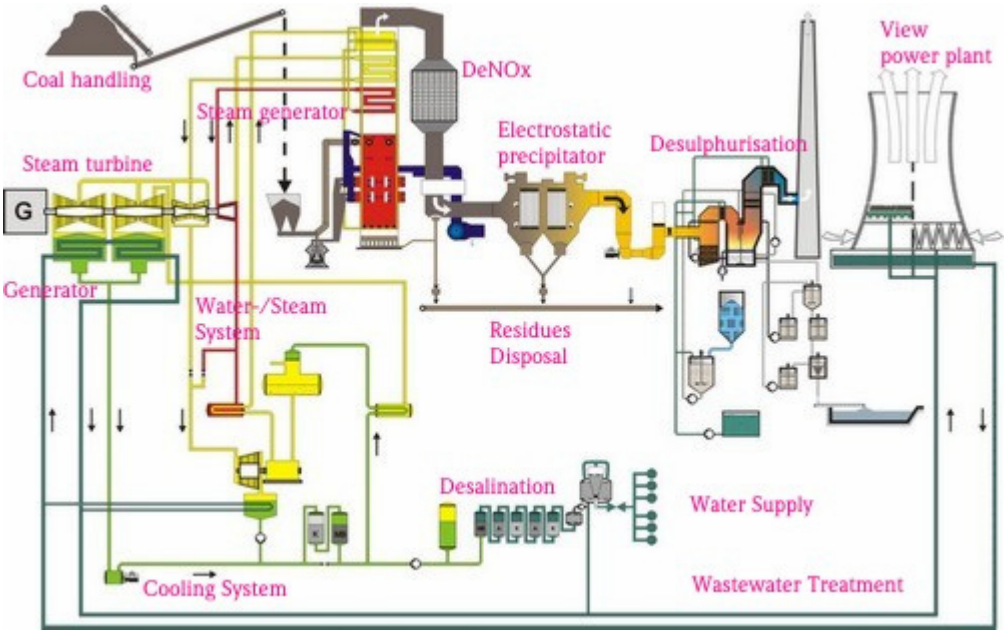

Fig. 1.1. Schematic of a coal fired power plant [1]

and anthropogenic sources [2], the 1165 coal fired utilities produce only about 48 tons of Hg every year [3, 4]. Figure 1.2 shows the data compiled on Hg vs. in various types of coals. The data is taken from the US Coal resource database. . Figure 1.3 shows the mercury loading over the United States atmosphere [5]. Mercury loading over the Texas region is very high compared to others. Out of the top ten power plants which contribute to mercury pollution, five are present in Texas.

Mercury in the environment can exist in three forms: elemental mercury (Hg^0), inorganic mercury (Hg^+) and organic mercury (Hg^{++}).Its very important to know the concentration of the above forms of mercury in flue gases. The technical word associated is speciation. It is essential to know the speciation of Hg in flue gases. The elemental Hg is non reactive and less soluble in water, which constitutes a global environmental issue. The oxidized forms of mercury (Hg^+ and Hg^{++}) are soluble in water,

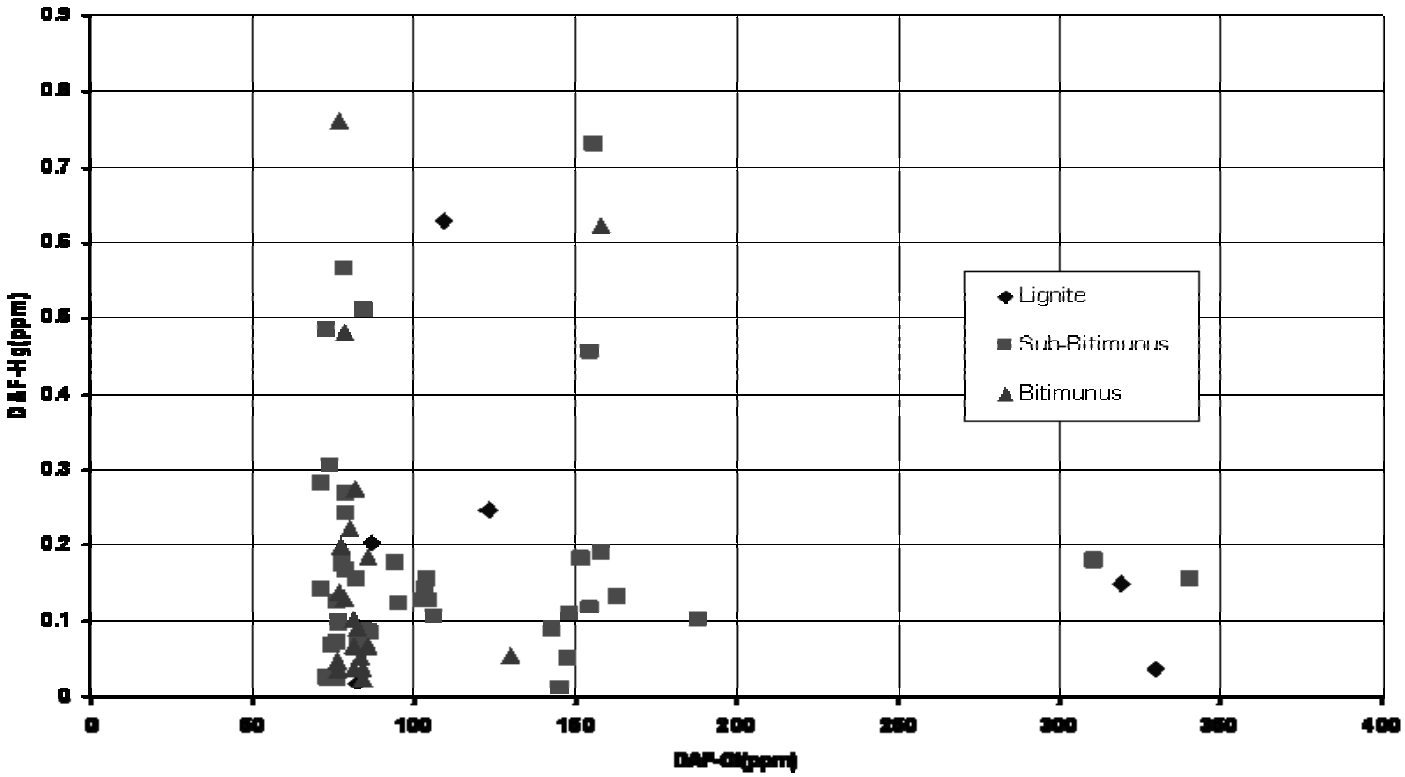

Fig. 1.2. Hg and Cl concentrations in coal on DAF basis

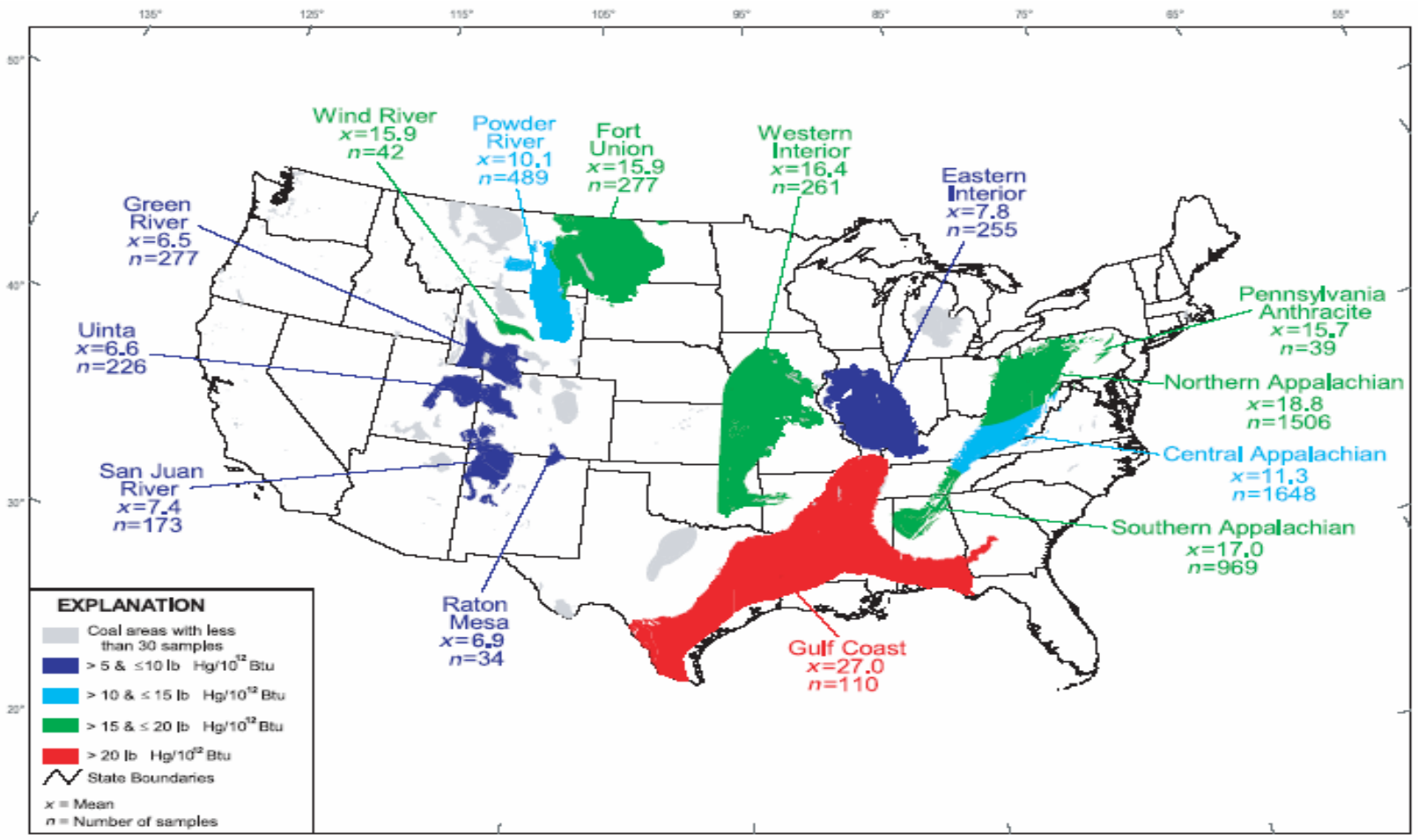

Fig. 1.3. Mercury loading (x in lb per 10^{12} BTU) [5]

this produces risk to humans and the environment. On the contrary, since they are soluble in water, they can be captured. Hence it's very essential to capture the elemental mercury. The Hg vapor in flue gasses is captured by oxidizing it with the chlorine present in the coal and/or by injecting chlorine. EPA's Clean Air Mercury Rule (CAMR) established the regulations call for reduction of Hg emissions inn two phases: from 48 tons 38 tons in Phase I and to 15 tons in Phase II [6]. The Phase I controls begins in 2010 with 38 Tons in cap while Phase II begins in 2018. Phase I is based on co-benefit reductions through conventional Air Pollution Control Devices (APCD) for reduction of SO_2 (e.g. wet scrubbers), NO_x and particulate matter (PM) emissions from coal fired flue gases required under Clean Air Interstate Rule (CAIR). For example, the Selective Catalytic Reduction (SCR) used for NO_x control can also oxidize elemental Hg. The coal chlorine content and ash composition, gas temperature, residence time and presence of different gases will decide the speciation of Hg. The extent of oxidation depends on the concentration of chlorine in flue gases. As shown in the Fig. 1.4, the fraction of elemental Hg emission of coal-fired boilers decreases with increase in Cl content of coal[7].

Mercury loading is defined as the amount of Hg (kg) per Giga joule Typically the Hg in coal is vaporized as elemental Hg, yielding Hg^0 vapor while the Hg in the flue gas exists in three different forms: elemental Hg^0 (elemental) and Hg^{2+} (oxidized form, e.g. $HgCl_2$) [8] and Hg in particulates. The elemental Hg^0 does not dissolve in water and is not usually captured in APCD while the Hg in particulates is captured in upstream of particulate control devices (PCD) (e.g. Electro static precipitator (ESP) or fabric filter

(FF)). The oxidized form dissolves in water and can be captured with water spray or in flue gas desulphurization (FGD) unit. In fact relative solubility's of Hg^0 and Hg^{2+} are 1 and 1,400,000 respectively [9]. The oxidized mercury compounds are also known to form complexes with fly ash aerosols. The particles are captured using either ESP to capture the particulate containing carbon along with Hg compounds or using wet scrubbers.

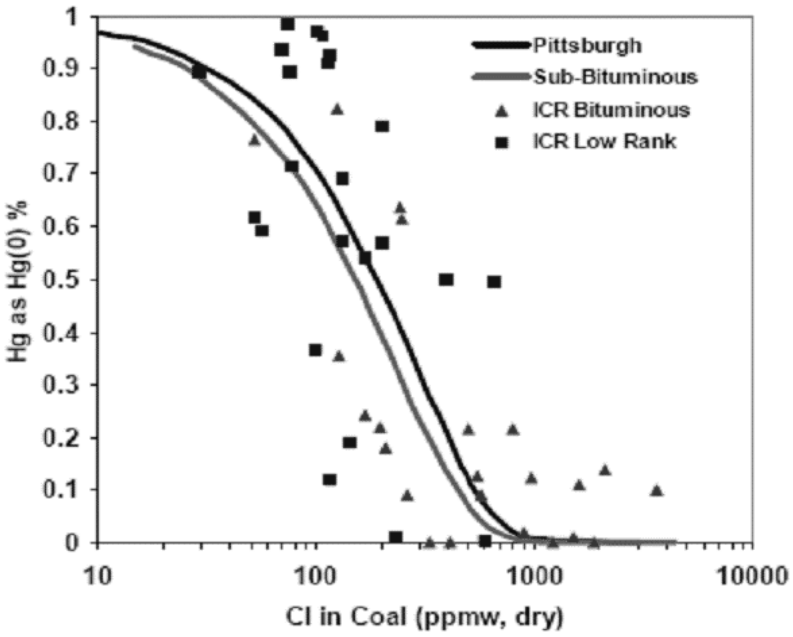

Fig. 1.4. Effect of Cl in coal on Hg emissions[7]

The oxidized mercury compounds are also known to form complexes with fly ash aerosols. The particles are captured using either ESP to capture the particulate containing carbon along with Hg compounds or using wet scrubbers. In order to form oxidized Hg,

Chlorine is required. The Cl content in Bituminous coals range from 200 to 2000 ppm (dry basis) while for low rank coals (sub-bituminous and lignite) it ranges from 20 to 200 ppm an order of magnitude lower. Typically elemental Hg content in coal is inversely proportional to Cl content of coal. Thus the low rank Sub-bituminous and lignite coals reveal lower Hg capture (3-72 %) in co-benefit" systems than higher rank bituminous coal (9-98 %) [4]. Hg removal plotted against coal chlorine content reveals increasing Hg capture with Cl due to $HgCl_2$ formation. Typically, when Cl concentration exceeds 200 ppm, Hg is captured primarily in the particulate phase. TXU Energy uses Texas Lignite and the Texas Municipal Power Agency (TMPA) near College Station uses Wyoming sub-bituminous coal as fuel. As Cl is low in sub-bituminous and lignite coals, the Hg exists primarily as elemental Hg, which is difficult to capture. In order to understand the behavior of Hg emission, the distribution of mercury species in coal combustion flue gases must be predicted using analytical models. The present research deals with development of a model for evolution of Hg, Cl and gas phase oxidation Hg reaction in addition to transient heating, pyrolysis, ignition combustion of coal particle [10]. The model is expanded to include blended coals. The effect of blending alters the VM, Hg and Cl contents. Various parameters including chlorine concentration, particle size, volatile matter, kinetic rates etc are considered in order to study their effect on mercury speciation and to determine the extent of oxidation as fraction of Hg released from coal.

2 LITERATURE REVIEW

A literature review is presented on Mercury, which is one of the trace elements emitted during the coal combustion. The first part of review covers the health effects, origin/sources and the emission statistics of Mercury. Basic reactions involved in mercury oxidation are then reviewed. Later the control technologies and its behavior in combustion environment are briefly reviewed.

2.1 Health Effects

Mercury is a naturally occurring metal that has metallic inorganic and organic forms .Inorganic mercury exists in two forms (mercuric and mercurous) and combines with other elements such as chlorine to form inorganic mercury compounds or salts. Inorganic mercury enters the air from the mining of ore, combustion of coal and the incineration of waste. Mercury can combine with organic compounds (e.g., methyl mercury, phenyl mercury, merthiolate). In mercury contaminated soil or water, the micro-organisms can organify the mercury into methyl mercury, which concentrates in the food chain. The health effects of mercury are diverse and it may depend on the form of mercury encountered and severity and the length of exposure.

2.1.1 Elemental Mercury

With large acute exposures to elemental mercury vapor may lead to lung injury. At levels below that causes lung injury, low dose or chronic inhalation may affect the nervous system. Symptoms include these: tremors; emotional changes (e.g., mood

swings, irritability, nervousness, excessive shyness); insomnia; neuromuscular changes (such as weakness, muscle atrophy, twitching); headaches; disturbances in sensations; changes in nerve responses; performance deficits on tests of cognitive function. At higher exposures there may be kidney effects, respiratory failure and death.

2.1.2 Inorganic Mercury

Exposure to inorganic mercury is mostly through ingestion. The most prominent effect is on kidneys, where mercury accumulates, leading to tubular necrosis High exposures to inorganic mercury may also result in damage to the gastrointestinal tract, the nervous system Symptoms of high exposures to inorganic mercury include: skin rashes and dermatitis; mood swings; memory loss; mental disturbances; and muscle weakness.

2.1.3 Organic Mercury

Organic mercury is more toxic than inorganic mercury. The effects of organic mercury include changes in vision, sensory disturbances in the arms and legs, cognitive disturbances, dermatitis, and muscle wasting. The developing nervous systems of the fetus and infants are considered to be susceptible to the effects of methyl mercury.

Exposure of childbearing-aged women is of particular concern because of the potential adverse neurological effects of Hg in fetuses. To determine levels of total blood Hg in childbearing-aged women and in children aged 1-5 years in the United States, CDC's National Health and Nutrition Examination Survey (NHANES) began measuring blood Hg levels in these populations in 1999. Table 2.1 shows the geometric mean and

percentiles of total blood mercury of women and children. Table 2.2 shows the percentage of women with blood mercury concentration greater than 5.8 µg/L (this is an estimated level assumed to be with no appreciable harm).

Table 2.1

Geometric means (GMs) and selected percentiles of total blood mercury (Hg) concentrations (µg/L) for women aged 16-49 years and children aged 1-5 years, by selected variables – National Health and Nutrition Examination Survey, United States, 1999-2002

				Selected percentile (95% CI)					
Variable	No.	GM	(95% CI*)	5th	(95% CI)	10th	(95% CI)	25th	(95% CI)
Women									
Race/Ethnicity									
Mexican American	1,106	0.74	(0.64–0.84)	0.10	(0.08–0.15)	0.17	(0.12–0.23)	0.34	(0.27–0.45)
White, non-Hispanic	1,377	0.87	(0.76–0.99)	0.09	(0.08–0.10)	0.15	(0.13–0.18)	0.37	(0.34–0.45)
Black, non-Hispanic	794	1.18	(1.00–1.36)	0.17	(0.12–0.25)	0.30	(0.24–0.38)	0.60	(0.55–0.73)
Age group (yrs)									
16–29	2,004	0.68	(0.60–0.76)	0.08	(0.07–0.09)	0.11	(0.09–0.14)	0.29	(0.25–0.37)
30–49	1,633	1.10	(0.97–1.24)	0.13	(0.10–0.16)	0.24	(0.20–0.29)	0.52	(0.45–0.60)
Pregnancy status									
Pregnant	629	0.75	(0.60–0.90)	0.08	(...†–0.10)	0.10	(0.08–0.20)	0.32	(0.24–0.44)
Not pregnant	2,978	0.94	(0.84–1.04)	0.10	(0.09–0.11)	0.18	(0.15–0.21)	0.41	(0.38–0.47)
Total	3,637	0.92	(0.82–1.02)	0.09	(0.09–0.11)	0.17	(0.15–0.20)	0.40	(0.36–0.47)
Children									
Race/Ethnicity									
Mexican American	526	0.35	(0.30–0.40)	...		0.08	(...–0.09)	0.13	(0.10–0.16)
White, non-Hispanic	447	0.29	(0.24–0.33)	...		0.07	(...–0.08)	0.09	(0.09–0.10)
Black, non-Hispanic	424	0.50	(0.44–0.57)	0.08	(...–0.10)	0.10	(0.09–0.13)	0.22	(0.18–0.26)
Total	1,577	0.33	(0.30–0.37)	...		0.07	(...–0.08)	0.10	(0.09–0.12)

	Selected percentile (95% CI)							
Variable	50th	(95% CI)	75th	(95% CI)	90th	(95% CI)	95th	(95% CI)
Women								
Race/Ethnicity								
Mexican American	0.73	(0.67–0.83)	1.27	(1.16–1.48)	2.38	(2.05–2.95)	3.60	(3.03–6.48)
White, non-Hispanic	0.81	(0.76–0.92)	1.69	(1.51–2.15)	3.73	(2.84–5.14)	6.17	(4.64–9.30)
Black, non-Hispanic	1.15	(1.05–1.41)	2.12	(1.86–2.70)	3.89	(3.24–5.03)	5.54	(4.27–11.08)
Age group (yrs)								
16–29	0.64	(0.55–0.77)	1.34	(1.24–1.54)	2.58	(2.28–3.13)	3.87	(3.32–7.80)
30–49	1.02	(0.91–1.19)	2.10	(1.79–2.69)	4.56	(3.74–5.76)	6.97	(5.73–11.62)
Pregnancy status								
Pregnant	0.73	(0.63–0.97)	1.50	(1.38–1.90)	3.11	(2.14–4.79)	4.86	(3.00–8.02)
Not pregnant	0.88	(0.80–1.00)	1.83	(1.65–2.11)	3.93	(3.26–4.93)	6.11	(5.12–10.90)
Total	0.86	(0.80–0.98)	1.81	(1.62–2.16)	3.89	(3.20–4.88)	6.04	(5.08–10.74)
Children								
Race/Ethnicity								
Mexican American	0.28	(0.24–0.33)	0.63	(0.56–0.81)	1.36	(1.05–1.57)	1.85	(1.60–2.66)
White, non-Hispanic	0.20	(0.17–0.25)	0.49	(0.38–0.63)	1.15	(0.80–1.49)	1.78	(1.18–2.69)
Black, non-Hispanic	0.47	(0.40–0.58)	0.88	(0.78–1.02)	1.54	(1.31–2.04)	2.37	(1.75–3.64)
Total	0.26	(0.23–0.29)	0.61	(0.56–0.70)	1.29	(1.08–1.69)	2.21	(1.80–3.66)

* Confidence Interval.
† Below the limits of Detection.

Table 2.2

Percentage of women aged 16-49 years with blood mercury (Hg) levels ≥ 5.8µg/L, by race/ethnicity − National Health and Nutrition Examination Survey, United States, 1999-2002

Race/Ethnicity	No.	% with Hg levels ≥5.8 µg/L	(95% CI*)
Mexican American	1,106	1.70	(1.04–2.79)
White, non-Hispanic	1,377	5.77	(3.71–8.97)
Black, non-Hispanic	794	4.82	(2.55–9.11)
Total	3,637	5.66	(4.04–7.95)

* Confidence Interval.

2.2 Origin/Sources of Mercury

Mercury is emitted from a wide variety of natural and man-made sources. Alkali and metal processing, incineration of coal, and medical and other waste, and mining of gold and mercury contribute greatly to mercury concentrations in some areas, but atmospheric deposition is the dominant source of mercury over most of the landscape. Once in the atmosphere, mercury is widely disseminated and can circulate for years, accounting for its wide-spread distribution. Natural sources of atmospheric mercury include volcanoes, geologic deposits of mercury, and volatilization from the ocean. Although all rocks, sediments, water, and soils naturally contain small but varying amounts of mercury, scientists have found some local mineral occurrences and thermal springs that are naturally high in mercury.

A number of combustion facilities including MSW, sewage sludge, hazardous waste and hospital incinerators and coal-fired power plants, emit mercury to the atmosphere.

Fig. 2.1 presents an overview of the combustion sources and atmospheric transport of mercury.

Mercury is a natural constituent of coal. The reported average mercury concentrations of 0.087 µg/g (ranging from0.03–0.25µg/g) in Australian coal, 0.22 µg/g (ranging from 0.09–0.51 µg/g) in eastern U.S. coal, 0.04 µg/g in Colombian coal and 0.72 µg/g (ranging from 0.14–1.78 µg/g) in Polish coal [11]. The average mercury concentrations of 0.070 µg/g in bituminous coal, 0.027 µg/g in sub-bituminous coal and 0.118 µg/g in lignite coal [12]. It was estimated that typically 0.24 µg/g of mercury occurs in Appalachian coals, 0.14 µg/g in Interior Eastern coals and 0.21 µg/g in Illinois Basin coals [13].

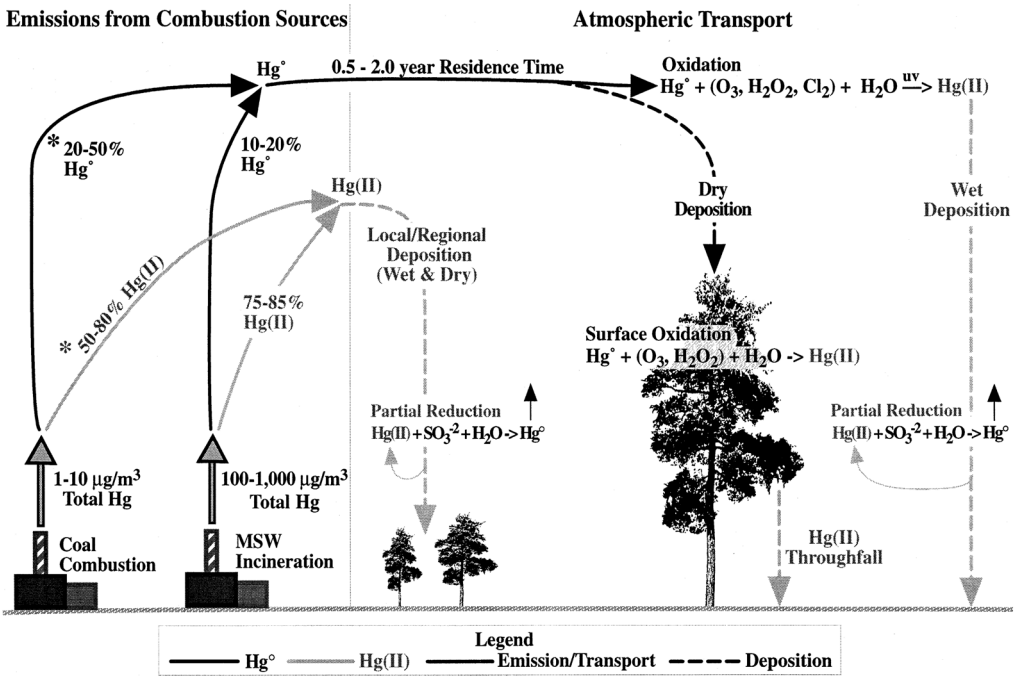

Fig. 2.1. Overview of mercury emission from combustion sources and mercuric atmospheric transport [5]

A review by the New Jersey Department of Environmental Protection and Energy (NJ DEPE) (1993) found that mean mercury concentrations in coal ranged from 0.12 to 0.28 µg/g. The average concentration of mercury is 0.056 µg/g (ranging from 0.029 µg/g- 0.114 µg/g) in high volatile bituminous coal. The concentration of mercury in coal according to the data released is given in Fig. 2.2 [6].

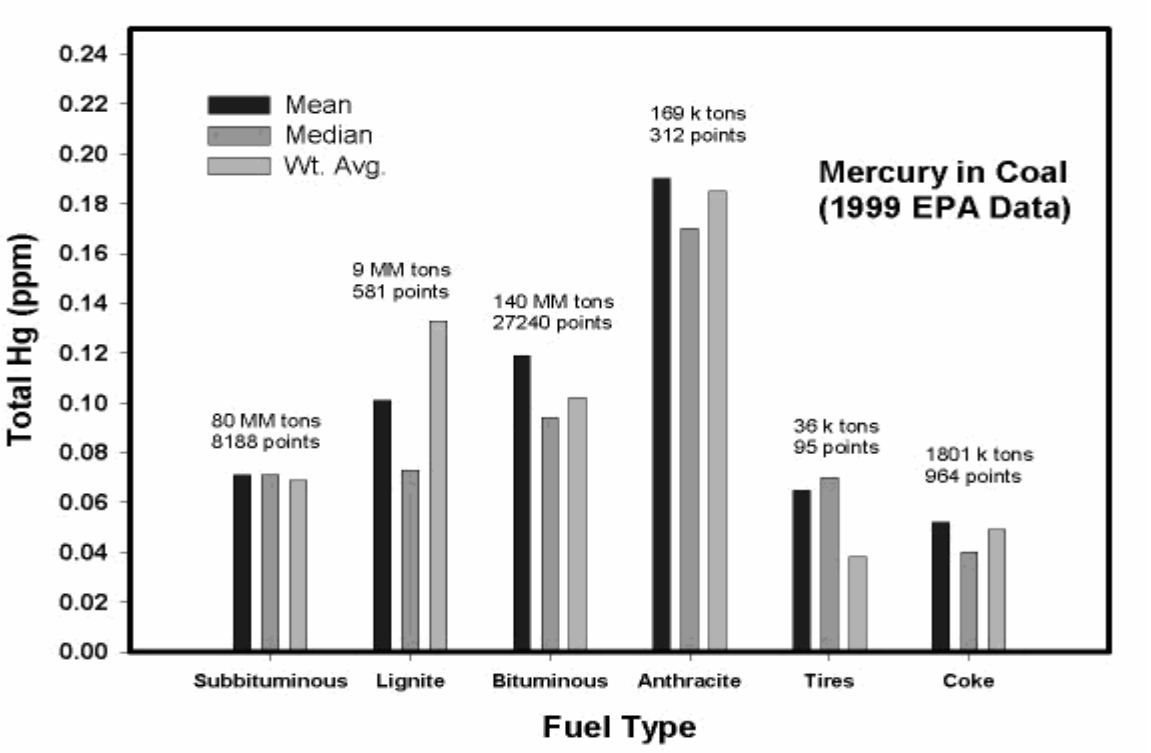

Fig. 2.2. Mercury concentrations in different types of coal [6]

The US geological has compiled a data base called COALQUAL. This database contains analysis of various coal samples. The Table 2.3 below shows the concentrations

of mercury and their calorific value in selected coal producing regions in the United States.

Table 2.3

Median and mean values for mercury concentrations and calorific values

	Mercury			Calorific value			Mercury Loading
	(ppm)			(Btu/lb)			(lb per 10^{12} BTU)
Coal-producing region	**Median**	**Mean**	**No.**	**Median**	**Mean**	**No. of Samples**	
Appalachian:							
Northern	0.19	0.24	1,613	12,570	12,440	1,506	19.29
Central	0.1	0.15	1,747	13,360	13,210	1,648	11.36
Southern	0.18	0.21	975	12,850	12,760	969	16.46
Eastern Interior	0.07	0.1	289	11,510	11,450	255	8.73
Fort Union	0.08	0.1	300	6,280	6,360	277	15.72
Green River	0.06	0.09	388	9,940	9,560	264	9.41
Gulf Coast	0.13	0.16	141	6,440	6,470	110	24.73
Pennsylvania Anthracite	0.1	0.1	51	12,860	12,520	39	7.99
Powder River	0.06	0.08	612	8,050	8,090	489	9.89
Raton Mesa	0.05	0.09	40	12,500	12,300	34	7.32
San Juan River	0.04	0.08	192	9,340	9,610	173	8.32
Uinta	0.04	0.07	253	11,280	10,810	226	6.48
Western Interior	0.14	0.18	286	11,320	11,420	261	15.76
Wind River	0.08	0.15	42	9,580	9,560	42	15.69

2.3 Emission Statistics

In 1990, more than two-thirds of the US anthropogenic mercury emissions came from three source categories: coal fired power plants, municipal waste combustion and medical waste incineration. After the 1990 Clean Air Act Amendment, the mercury emissions have decreased by 45% over a span of nine years. Fig. 2.3 below shows the anthropogenic mercury emission from different sources.

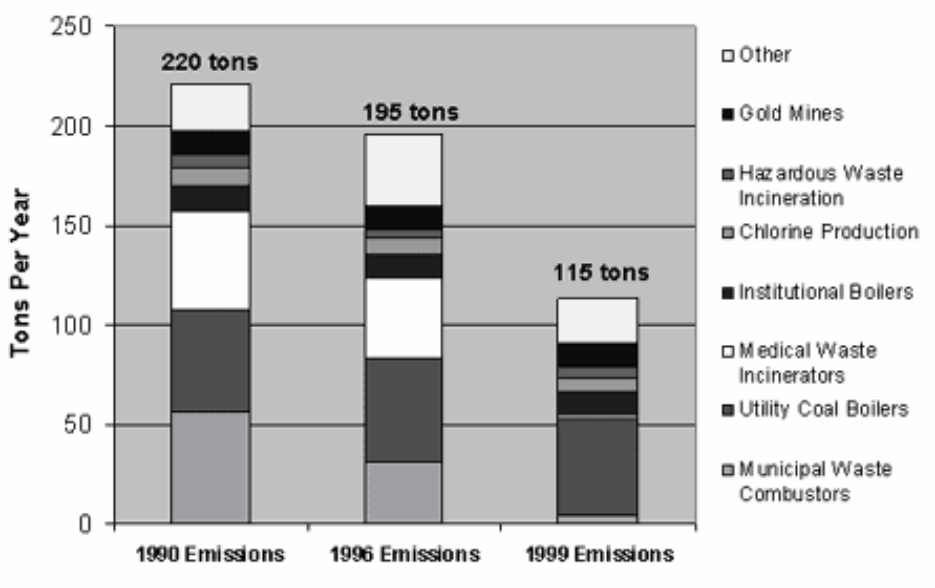

Fig. 2.3. U.S. emissions of human caused mercury [6]

According to Toxics release inventory program, 2002 which is a publicly available EPA data base, the on-site disposal of mercury compounds from electrical utilities located in Texas is reported to be 13,415 pounds. EPA reports for 2001 shows that the total mercury deposits in US from all sources are 144.23 tons. Out of which 45 tons are from US utilities. By implementing various environmental acts like CAIR, Clean Air

Mercury etc, they plan to reduce the mercury emissions by 70%. From the data reported by the SEED (Sustainable Energy and Economic Development) 2002, Texas has the 5 of the worst 10 mercury polluting power plants Table 2.4 shows a list of top seven power plants located in Texas which cause mercury pollution .

Table 2.4

Top 7 power plants in Texas which have higher mercury emissions

National Rank	Plant	2002 Mercury air Emissions(lbs)
1	Limestone (Center point)	1,800
2	Monticello (TXU)	1,324
6	W.A.Parish (Center Point)	1,100
8	Martin Lake (TXU)	1,027
9	Pirkey (AEP)	1,000
16	Fayette (LCRA)	811
30	Deely / Spruce (CPS)	636

2.4 Mercury Behavior in Combustion Environment

The fate of Hg in combustion environment is very important to know in order to control the emissions. The coal chlorine content and ash composition, gas temperature, residence time and presence of different gases will decide the speciation of Hg. The elemental Hg is un-reactive and slightly soluble in water when compared to oxidized forms of mercury.

Experiments [14] are conducted to study the fate and behavior mercury in power plants. Experiments showed that 43% of Hg present in the coal is found in the flue gases in the vapor phase. The concentration of Hg in fly ash particles is low. With the presence

of HCl, Hg^0 (partly) is converted into $HgCl_2$ at temperatures less than 500-800^{0}C. And $HgCl_2$ which is less volatile begins to condense on fly-ash particles which are indicated by the equilibrium calculations. According to the one of the test conducted it was found that 53% of the Hg presented in a water soluble form, mostly in the form of $HgCl_2$. However, it is still in the vapor phase due to the high temperature of flue gases (140-150^{0}C).

Distribution of mercury species in coal combustion flue gases has been calculated using equilibrium calculations [15]. It was demonstrated that the gas phase equilibrium for mercury-containing species in coal-fired power plant exhaust is not valid at temperatures below 500^{0}C [16]. The most important for the oxidation of mercury in the post-combustion gases is the chlorine-contained species. The conversion of HCl to Cl_2 in flue gas is kinetically limited. Since equilibrium is not considered here, constrained equilibrium and kinetic models are used for calculations. The calculations are done for four different coals and various species are considered. Equlibrium results show that all of the Hg exists in the form $HgCl_2$ below 450^{0}C. And above 700^{0}C, 99% of the Hg exist as gaseous Hg as shown in Fig. 2.4. The rest is in the form of HgO. The amount of Hg oxidized between the above temperatures depends on the amount of chlorine present in the coal. Mercury content of the coal has no control on the distribution of mercury species. Even though the equilibrium HCl concentration in the gas is in the range of 24 to 111ppm which is considerably low, the reaction between Hg and HCl dominates the equilibrium chemistry. Equilibrium is not attained in flue gas due to fact that flue gas cools rapidly as heat is transferred from water to steam.

Mercury speciation measurements which are taken by conducting pilot and full scale experiments [17] show that complete oxidation of elemental mercury doesn't take place as predicted by the equilibrium calculations. Other components of combustion flue gases like H_2O, SO_2, NO_2 also effect the mercury oxidation but not as compared as HCl. The formation of Cl_2 in the flue gases is favored at low temperatures.

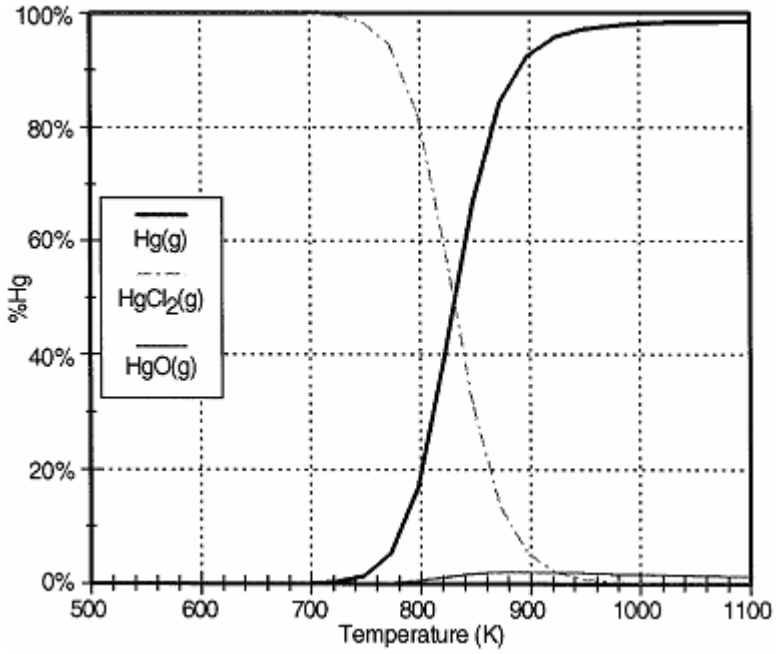

Fig. 2.4. Equilibrium mercury speciation in flue gas as function of temperature [16]

The equilibrium calculations showed that 30%-60% of chlorine is present as Cl_2 at 150^0C and rest is HCl. Various factors are considered which effect the formation of chlorine. The effects of time, initial concentration of chlorine in coal, excess of air and flue gas temperature on the production of chlorine gas are studied. Elemental Hg conversion in the presence of both HCl and Cl_2 using global kinetics is studied at

different temperatures. As the shown in the Fig. 2.5, concentration of HCl increases, fraction of Hg elemental mercury converted increases. The results are comparatively better when considered the HCl concentration. Mercury conversion is higher at slower cooling rate, which is due to long residence time at higher temperature.

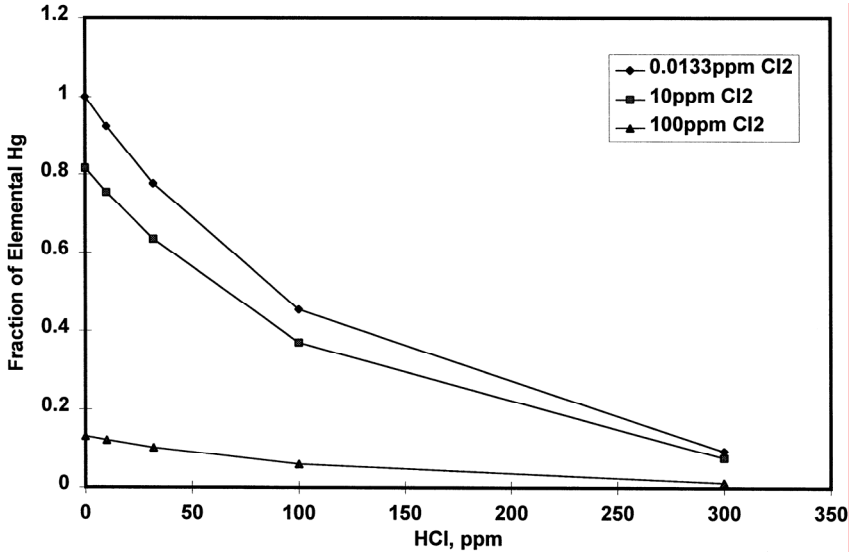

Fig. 2.5. Hg conversion as a function of Cl_2 concentration [16]

From above studies, it can be said that the most common mercury transformation which takes place is chlorination of mercury. But there are other kinds of transformation which are not as dominant as the mercury chlorination, but they significantly affect the way the mercury behaves in combustion flue gases. The interaction between the mercury and ash particles is important to consider in understanding the mercury transformation. Oxidant catalysts, nitrogenated species and some reactive species on the fly ash particles play an important factor in controlling the transformation of Hg^0 (g) to Hg (p) and Hg^{2+} X (g), where X can be Cl, S, SO_4 etc. Measurements by [18-20] indicated that the fly ash

particles adsorb mercury better than some of the adsorbing agents. Sulfur-rich ash particles are example of potential adsorbing agents.

Mercury retention in dust and the factors affecting it has been discussed [21]. The most common form which Hg takes is Hg^{2+} probably as $HgCl_2$. The amount of $HgCl_2$ formed depends upon the concentration of chlorine in coal. But as the flue gas cools, $HgCl_2$ condenses on the fly ash particles. Mercury retention on dust doesn't depend on the amount of chlorine content of the coal, but rather to the carbon content of the dust and flue gas temperature. As the carbon content increases, the mercury retention in the dust increases. In case of the flue gas temperature, the mercury retention decreases as the flue gas temperature decreases.

The mercury emissions from FBC systems fired with high chlorine coals was investigated [22]. Coals having high percentage of chlorine results in greater percentage of oxidized mercury in flue gases. Mercury is released in two stages during the coal pyrolysis. During the first stage which is around 350^0C, 35% of mercury (Elemental Hg and ionic Hg) is released. In the second stage, the organic mercury (linked or bonded to organic compounds in coal) is released during the volatilization of coal. In all a total of 60% of mercury is released in the temperature range of 350-400^0C.

2.5 Mercury Reactions

The possible reaction chemistry between mercury and chlorine [23] are given below in Table 2.5. The reaction of Hg with atomic chlorine is very fast when compared to the other forms of chlorine species.

Table 2.5

Mercury reaction chemistry

	A cm,mol,sec	Ea cal/mol
Hg+Cl+M->HgCl+M	2.40E+08	-14400
$Hg+Cl_2$->HgCl+Cl	1.39E+14	34000
$HgCl+Cl_2$->$HgCl_2$+Cl	1.39E+14	1000
HgCl+Cl+M->$HgCl_2$+M	2.19E+18	3100
Hg+HOCl->HgCl+OH	4.27E+13	19000
Hg+HCl->HgCl+H	4.94E+14	79300
HgCl+HCl->$HgCl_2$+H	4.94E+14	21500
HgCl+HOCl->$HgCl_2$+OH	4.27E+13	1000
Hg+ClO->HgO+Cl	1.38E+12	8320
$Hg+ClO_2$->HgO+ClO	1.87E+07	51270
$Hg+O_3$->$HgO+O_2$	7.02E+14	42190
$Hg+N_2O$->$HgO+N_2$	5.08E+10	59810
HgO+HCl->HgCl+OH	9.63E+04	8920
HgO+HOCl->$HgCl+HO_2$	4.11E+13	60470

2.6 Control Technologies

Mercury is difficult to remove because it is present in vapor form since it is highly volatile. It passes through most of particulate control devices which are presently installed in the power plants. The concentration of mercury in coal utility flue gas is very less when compared to the waste incineration flue gas. Due to which it is very difficult to

detect and remove. There are different ways by which the mercury emission can be reduced. The solution is not universal rather it depends on the boiler, type of coal, combustion environment, flue gas, temperature etc. Some of the ways are: Coal cleaning, Electrostatic precipitators, Wet Scrubbing, Dry Scrubbing. Figure 2.6 shows the options for enhancing mercury capture in existing air pollution controls.

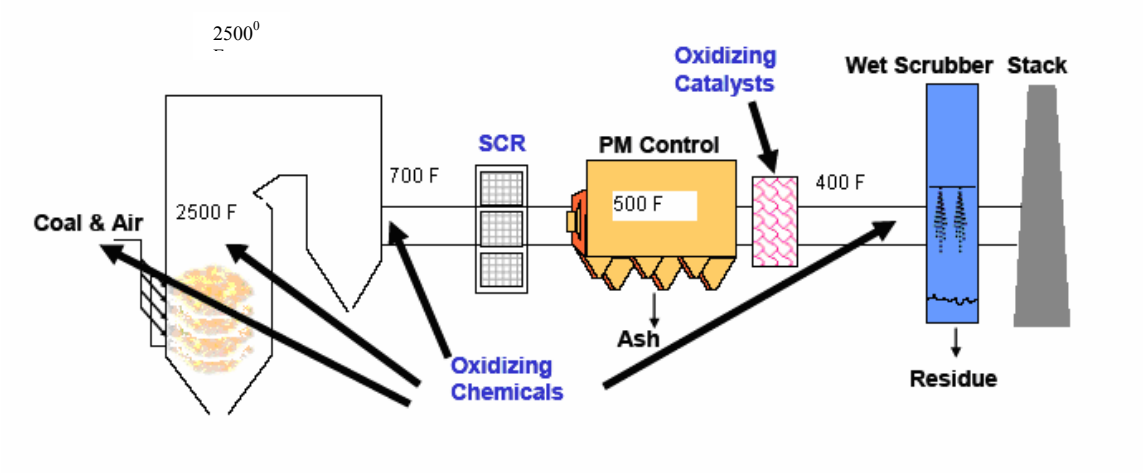

Fig. 2.6. Options for enhancing mercury capture in existing air pollution controls [6]

According to the EPA report submitted by the Air pollution Prevention Division [6], below are few of the findings on the control of mercury emissions (Fig. 2.7)

- For the same APC configuration the average mercury removal is more for bituminous coal than for others
- Mercury removal for a fabric filter is more than CS-ESP or HS-ESP for both bituminous and sub-bituminous coal

- Average mercury removal for bituminous coal-fired boilers with Spray Dryer Absorber and FF (SDA/FF) was very high (over 95%); for sub bituminous coal-fired boilers with the same control configuration mercury removal was considerably less (about 25%),which was actually less than for a FF alone (about 75%).

The tendency of high level mercury capture in bituminous coal is due to higher percentage of chlorine present in the bituminous coal and the tendency to produce to high levels of unburned carbon in the flue gas. Both these factors help us in capturing the mercury in the present air polluting equipment.

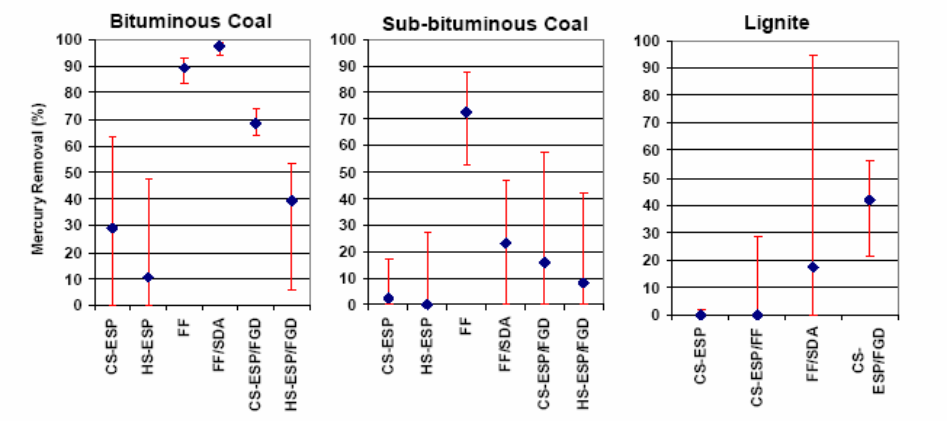

Fig. 2.7. Mercury removal rates measured for various coal types and with different air pollution control configurations [6]

Mercury capture by FGD systems fall into two categories. The wet FGD systems include the common limestone forced oxidation (LSFO) scrubber and the magnesium enhanced lime (MEL) scrubber. The dry FGD typically consists of spray dryer absorber and fabric filter. Figure 2.8 shows the % of mercury removal by various FGD systems.

Mercury in the oxidized state is expected to be captured efficiently in wet FGD systems. Data from actual facilities has shown that capture of over 90% Hg^{2+} can be expected in calcium-based wet FGD systems, though there are cases where significantly less has been measured [24]. It was suggested that this is primarily a result of scrubber equilibrium chemistry and good predictive capability for total mercury capture in wet FGD systems using a thermo-chemical equilibrium model has been discussed. It was also shown that under some conditions Hg^{2+} will be reduced to Hg^{0} and the mercury will be reemitted [25].

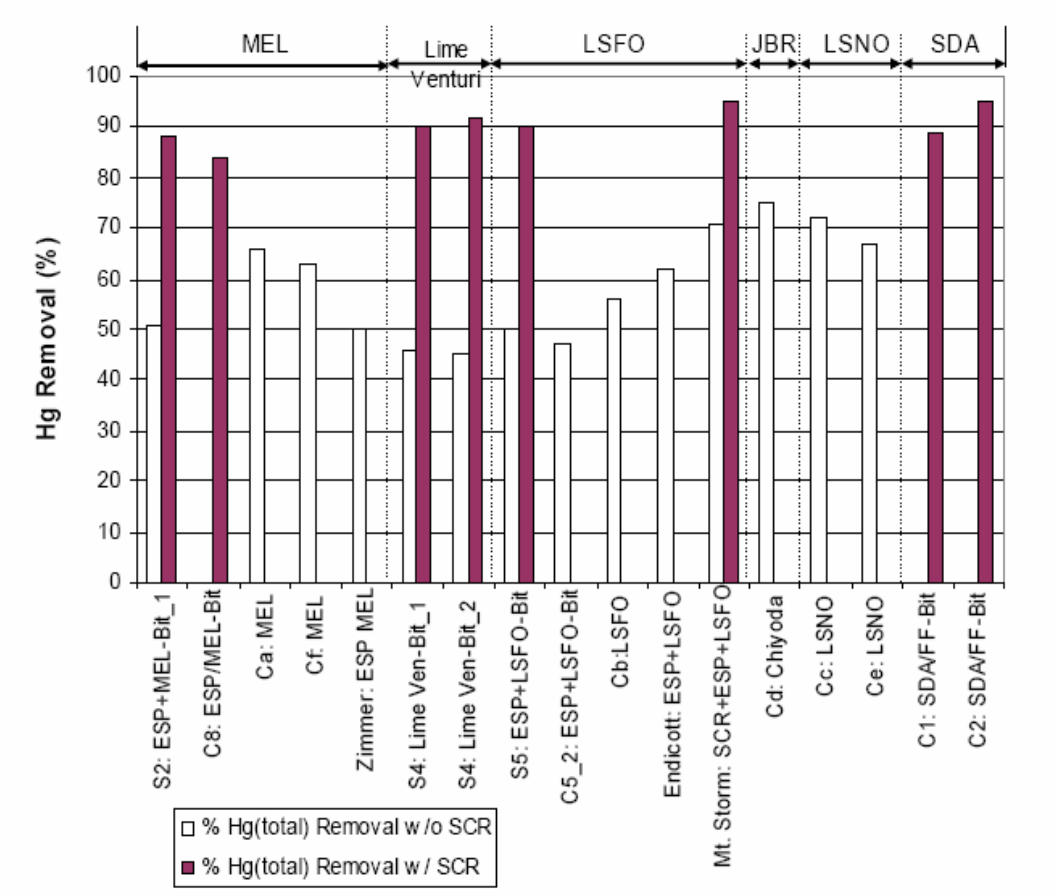

Fig. 2.8. Mercury removal of various FGD systems [24]

In some cases, the reduction of Hg^{2+} to Hg^{0} and subsequent re-emission has been abated with the help of sulfide-donating liquid reagent. So this limiting FGD scrubber chemistry and reemission of mercury may result in Hg^{2+} capture that is significantly less than 90%. The effect of scrubber chemistry and operating conditions on mercury emissions exhibited in Fig. 2.9, shows the measured mercury emissions as liquid-to-gas ratio (L/G) was varied on a 100 MMBtu/hr pilot facility with inlet mercury concentration in the range of about 10-25 $\mu g/m^3$. Higher L/G resulted in lower outlet mercury emissions which has implications for wet FGD type – Limestone Forced Oxidation having higher L/G than Magnesium Enhanced Limestone (MEL) wet FGD. Because Hg^{2+} can be captured much more effectively by wet-FGD systems, methods of increase the amount of Hg^{2+} upstream of wet FGD systems would result in more capture. In order to increase the amount of Hg^{2+}, SCR catalysts are used to promote the oxidation of elemental mercury. In order to increase the amount of Hg^{2+}, SCR catalysts are used to promote the oxidation of elemental mercury. According to results of the field tests conducted by [26], the oxidation of elemental mercury by the SCR catalysts may be affected by the following factors:

- The coal characteristics especially the chlorine content.
- Age of the catalyst.
- The temperature o f the reaction.
- The concentration of ammonia.

According [27], Mercury removals across cold-side (T = 130-180^{0}C) electrostatic precipitators (CS-ESPs) averaged 27%, compared to 4%for hot-side (T = 300-400^{0}C)

ESP (HS-ESP). Removals for fabric filters (FFs) were higher, averaging 58%, owing to additional gas–solid contact time for oxidation. Both wet and dry flue gas desulphurization (FGD) systems removed 80% to 90% of the gaseous mercury (Hg^{2+}), but elemental mercury was not affected. High mercury removals, averaging 86%, in fluidized-bed combustors with FFs were attributed to mercury capture on high-carbon fly ash. Acid gases critically influence the heterogeneous oxidation of mercury, particularly as it affects capture on sorbents. HCl, NO, and NO_2 all promote oxidation and capture both individually and in combination. However, the combination of SO_2 with NO_2 greatly reduces capture of elemental mercury on activated carbon, whereas oxidation continues on the solid surface. Figure 2.10 shows the effect of temperature and gas concentration on elemental mercury and oxidized mercury by the FGD-activated carbon.

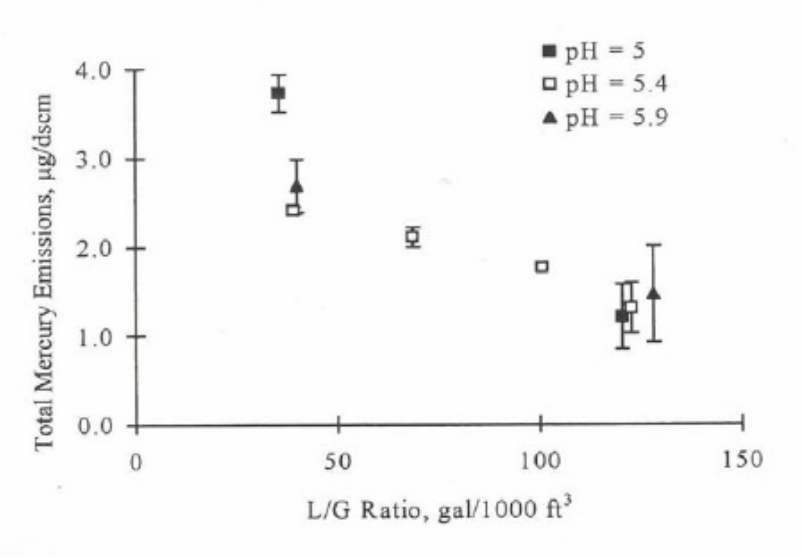

Fig. 2.9. Effect of liquid to gas ratio on mercury emission at common operating pH values [24]

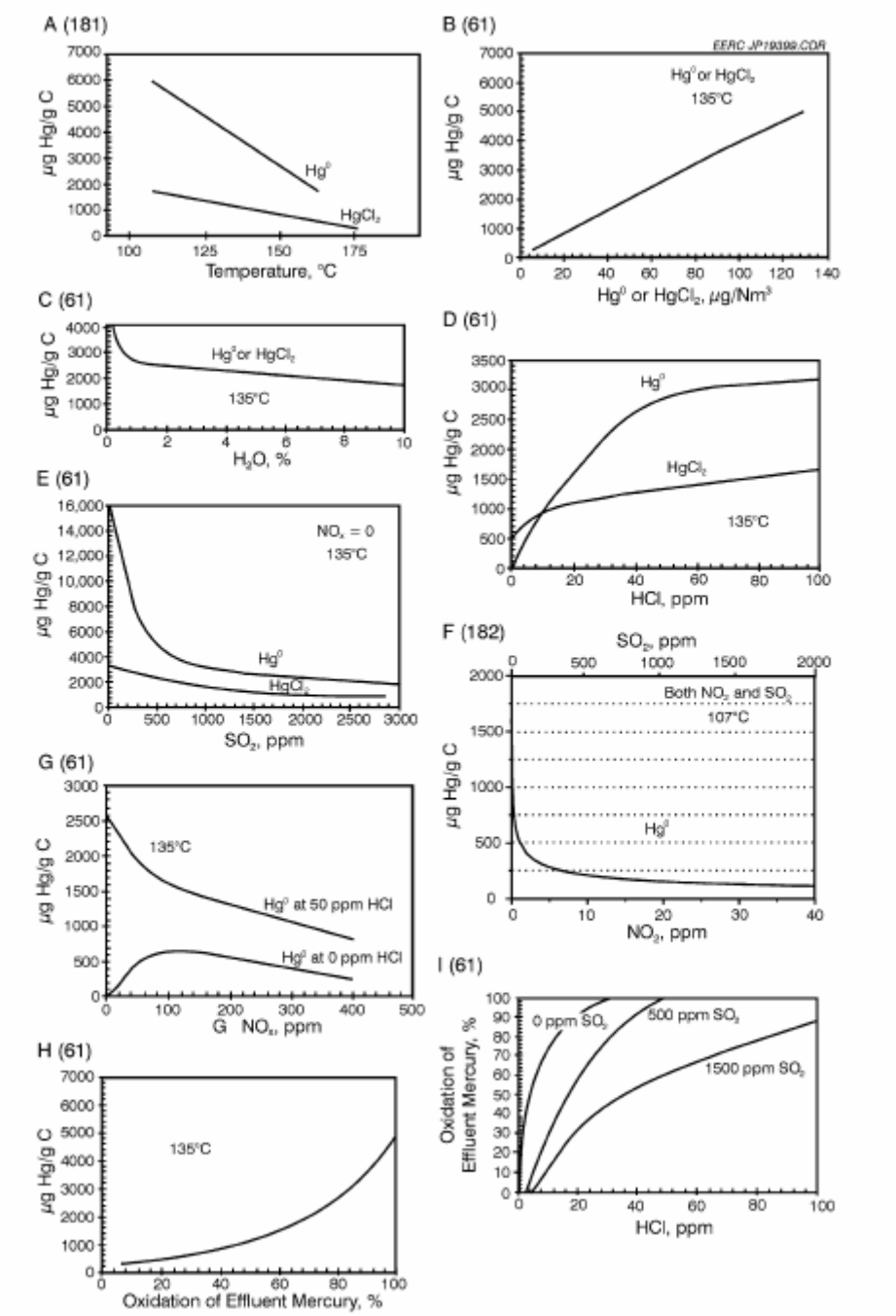

Fig. 2.10. Effect of temperature and gas concentration on elemental mercury and oxidized mercury by FGD activated carbon [27]

One of experiments [28], studies the effectiveness of activated carbon retaining the mercury in coal combustion. The performance of chemically activated carbon (sulfur loaded carbon) and thermally activated carbon are compared. Minor differences are noticed among the above. Sulfur loaded carbon retained about 70% of mercury at 120^0C when compared to thermally activated carbon which retained only about 30%. This might be due to the different mercury species present in gas phase and may be due to chemical surface modification.

Experiments [29] are conducted to study the effect of chlorine impregnated activated carbon. The results show that activated carbon impregnated by $ZnCl_2$ significantly enhanced the adsorptive capacity of mercury but in return decreased the specific area of the activated carbon. Figure 2.11 shows the amount of elemental mercury adsorbed by the impregnated carbon and simple activated carbon. Studies were also performed on the effect of temperature on adsorption of elemental mercury by the impregnated carbon and untreated sample.

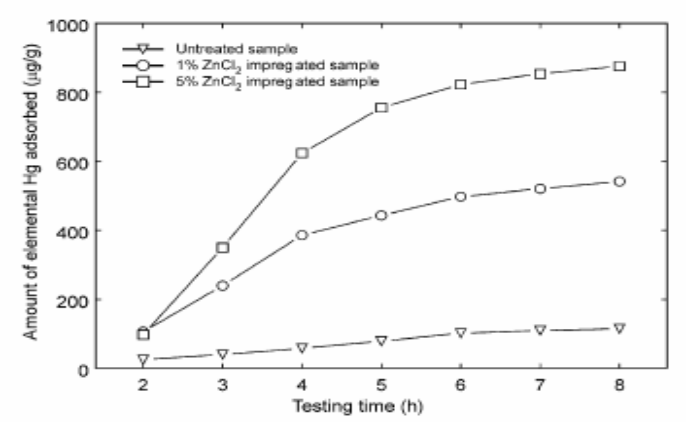

Fig. 2.11. Adsorption of elemental mercury [29]

.It was found that un-activated carbons are ineffective in capturing mercury when compared to activated carbon [30]. Carbon sorbents activated at higher temperature than the baseline temperature showed increase in mercury capture than the carbon sorbents activated at baseline temperature.

The effect of the flue gas by carbon based mercury sorbent was studied. Lignite based activated carbon (LAC) is used as a sorbent. The results showed that LAC was ineffective in the presence of flue gas components (O_2, CO_2, N_2 and H_2O). The effectiveness of LAC in the presence of SO_2 was minute. But in the presence of HCl, the sorbent showed 100% effectiveness. While in the presence of NO, initially it showed 85-95% capture which later on increased to 100% with the passage of time. It showed the same result when NO_2 was added, but the difference being it took more time to reach 100% when compared to NO [31].

Limestone is added as a sorbent and its effect on mercury emissions is studied. It has been found that limestone helps in reducing mercury emissions as it acts as a catalyst for reactions between mercury and chlorine. Apparently, the addition of limestone enhances the mercury adsorption. Figure 2.12 below shows the effect of limestone on mercury emission for two different coals having the same chlorine concentration but different sulfur concentration. In this experiment Ca/S is kept constant. In order to keep it constant different limestone feeding rates are used.

When high chlorine coal was burned nearly 55% of total fuel mercury is found in solid phase (bed and fly ash). Out of this none is found in the bed ash because of high surrounding temperature (850^0C).

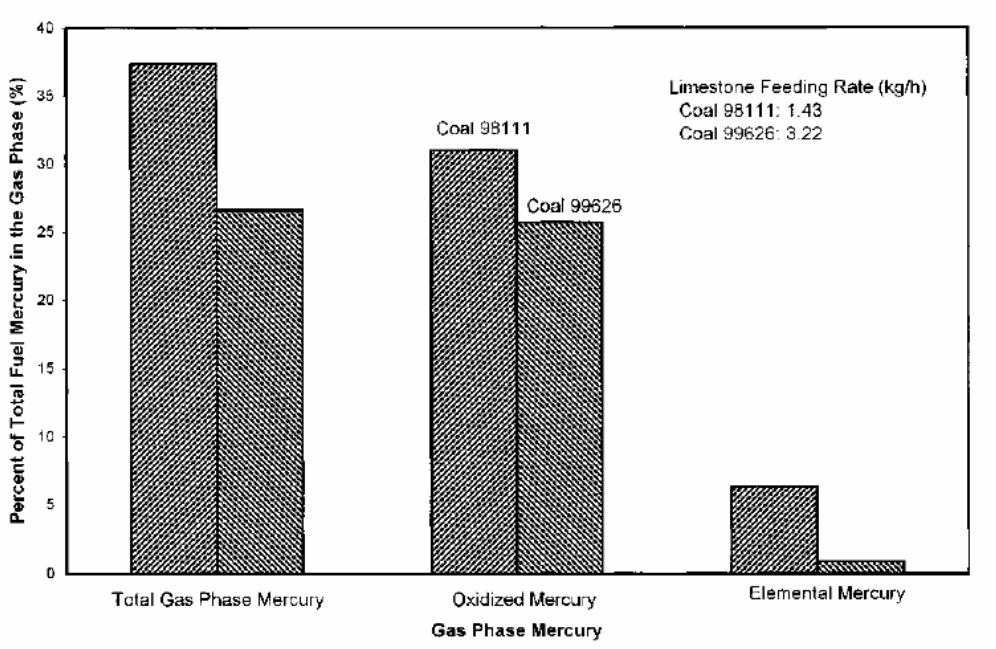

Fig. 2.12. The effect of limestone addition on mercury emission in flue gases [30]

The thermal pretreatment of low ranked coal to control mercury emissions was discussed [32]. The results showed that around 70-80% of the mercury is removed from the coal when the temperature is raised from 150-290^{0}C. Mercury does not evolve below 150^{0}C and the mercury reaches a constant value at around 270^{0}C. The mercury removal as a function of residence time shows an increase with increase of residence time.

NO_x present in the flue gas aids capturing mercury in presence of a sorbent as read in the review above. It helps in oxidizing elemental mercury. The importance of nitrogen dioxide for the oxidation of mercury in atmosphere and in combustion flue gases was studied [33]. The reactions were studied using a stopped flow technique in a temperature interval from 20-900^{0}C. The reaction exhibits a first order with respect to mercury and a

second order with respect to NO_2. From 250-500^{0}C the dependence on NO_2 is lost and partly heterogeneous reactions are proposed. The half life of mercury in atmosphere is calculated using this reaction is large (10,000 years) due to which the reaction loses its importance. The importance of this reaction is more difficult to evaluate in combustion environment as it depends on the temperature and the history of NO_2 in flue gases.

Experiments [34] were conducted to study the importance of NO in predicting the oxidation in coal derived systems. The impact of NO on homogenous oxidation is noticeable .At low concentrations of NO, it promotes Hg oxidation but at higher levels H/N/O chemistry inhibits the Hg oxidation. Figure 2.13 shows the extent of Hg oxidation for various NO levels.

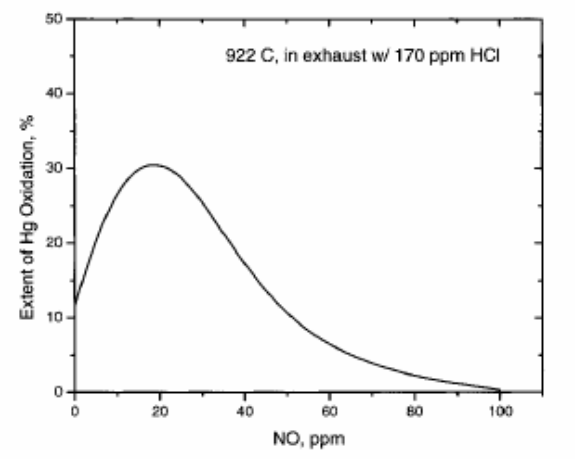

Fig. 2.13. Extent of mercury oxidation for various levels of NO concentration [34]

One of the experiments [35] studied the heterogeneous oxidation of mercury. The effect of NO_2, NO and HCl were studied individually to the baseline blend while fly ash at 180^{0}C. It is seen that NO_2 or HCl greatly enhanced the oxidation of mercury. The

effect of NO depended on whether or not NO_2 was present. Contrary to NO_2 or HCl, the presence of NO suppresses the oxidation of mercury. Figures 2.14 and 2.15 show the effect of NO_2 and NO on the oxidation of mercury.

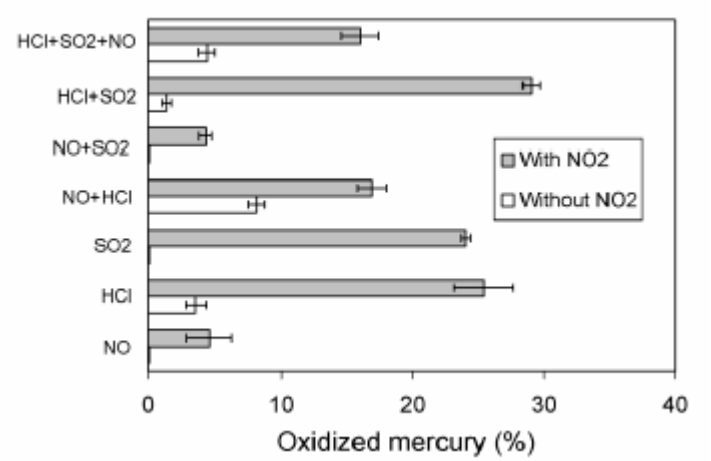

Fig. 2.14. Effect of NO_2 on the oxidation of mercury [35]

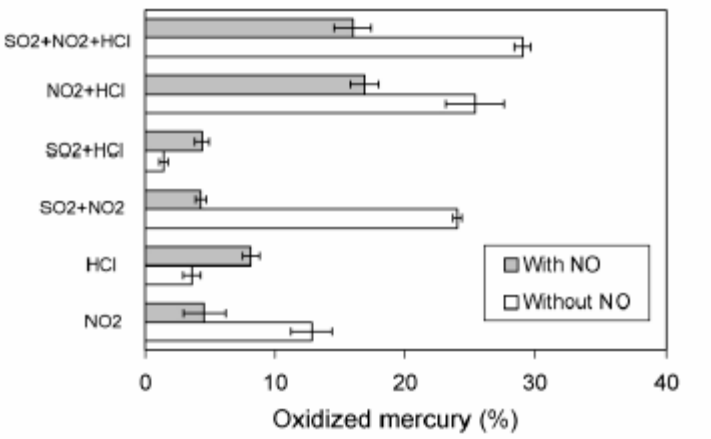

Fig. 2.15. Effect of NO on the oxidation of mercury [35]

The gases NO_2, HCl, NO, and SO_2 had strong effects on the potential of fly ash to oxidize Hg. The NO_2, HCl, and SO_2 promoted mercury oxidation, with NO_2 being the most important factor.

Co-firing tests are performed in CFBC by using sewage sludge, waste coal and limestone as fuel [36]. The mercury concentration in waste coal and sewage sludge was 0.09ppm and 0.13ppm respectively. Mercury concentration in the fuel blend is about 0.11ppm. The emission of trace elements from CFBC units are expected to be reduced because the volatilization occurs to a lesser extent as the operating temperatures are less when compared to pulverized coal combustion. The percentage of gas and particulate mercury in the flue gas prior to the bag house is found out to be 5.527 and 94.47. The respective concentrations are 2.03E-12 lb/Btu and 34.7E-12 lb/Btu. The mercury concentration in the feed stock used in co-firing is 0.11ppm and with gas emissions of 2.03E-012lb/Btu. This value meets the recently proposed emission limit of 2.0E-12 lb/Btu. This is data is taken prior to the bag house. Most of the mercury can be removed from the bag house with the help of polluting control devices.

2.7 Isolated Particle Combustion

If a single particle is placed in a hot oxidizing environment, ignition and combustion will ensure producing CO and CO_2. At high temperature, due to lack of oxygen at the particle surface, the reduction of CO_2 with carbon to CO becomes significant which subsequently oxidizes to CO_2 in gas phase. If the reduction reaction is rapid, the CO_2 concentration becomes highly negligible at the particle surface while O_2 and CO concentrations become negligible at the flame surface. If this particle is far away from

the other particle, then the particle burns in the isolated combustion mode since the combustion intensity of each particle is unaffected by the presence of the other particles.

A transient ignition is model is presented [10]. The model studies the ignition behavior of an isolated coal particle. It revealed that primary heterogeneous ignition followed by secondary homogenous ignition for small particles, but for larger particles, homogeneous ignition is the primary.

2.8 Summary

Following conclusions can be drawn after going through the above literature review:

- Equilibrium chemistry shows that $HgCl_2$ is more favorable at temperatures around $500\text{-}800^0$.
- Carbon content in the fly ash affects the amount of mercury captured in particulate form. Higher the carbon content higher is the capture.
- The effectiveness of the present control technologies on mercury captures depends on the concentration of chlorine species inn flue gas.
- The gases NO_2, HCl, NO, and SO_2 had strong effects on the potential of fly ash to oxidize Hg.

It is apparent from the review that chlorine content, residence time, porosity, temperature, presence of different species etc., effect the level and speciation of Hg. There exists no literature on Hg emission modeling from an isolated particle and the effect of VM, size, ambient temperature on the level of Hg speciation.

3 OBJECTIVES

In order to relate the % oxidized Hg with coal type, Cl content, coal particle size, combustion environment etc, more fundamental studies must be conducted in order to evaluate the parameters affecting % Hg oxidized. The overall objective of the proposed work is to model the mercury speciation under combustion conditions of isolated fuel particle.

In order to achieve the overall objective the following tasks are performed:

1. Model the Cl and Hg during evolution during pyrolysis.
2. Model the Hg oxidation reaction.
3. Modify the existing computer code.
4. Conduct the following parametric studies
    - Ambient Temperature
    - Ambient concentrations
    - Mercury and Chlorine in content in coal
    - Volatile matter
    - Particle Diameter
    - Effect of changing kinetics
    - Effect of blending with Feedlot Biomass, but heating the fuel as a single fuel particle with an equivalent Chemical formula.

4 THE MODEL AND CONSERVATION EQUATIONS

This section presents a detailed description of the model adopted. The model developed will simulate the whole processes of transient heating, pyrolysis, ignition and combustion of an isolated coal particle. The assumptions made are listed along with the various reactions used in the model. The conservation equations in the gas phase and solid phase for isolated coal particle are presented followed by the expressions for the source terms and the initial boundary conditions for the set of differential equations (conservation equations). With the definitions of reference quantities, the conservation equations are presented in non-dimensional form.

4.1 Model for Transient Combustion

Consider a cold coal particle of radius *a* suddenly placed in a hot gas containing oxygen (Fig. 4.1). The thermal wave propagates from the ambience into the coal particle. When the temperature of the coal particle reaches the pyrolysis level, thermal decomposition of the coal occurs and releases volatiles (V_I and V_{II}) that diffuse into the surrounding atmosphere. The composition and quantity of the volatile matter will vary with the rate of heating, the time of heating and the temperature reached. Homogeneous ignition may occur if the volatile concentration in the gas phase is at the flammability limit. However, if the volatile concentration is below the flammability level, the surface reaction may result in heterogeneous ignition. Thus, the ignition mode may change

depending on the relative rates of heat and mass transfer and the chemical reactions involved.

The volatiles along with CO produced by char oxidation undergo gas phase combustion; the products diffuse to the ambient. Finally the char is combusted.

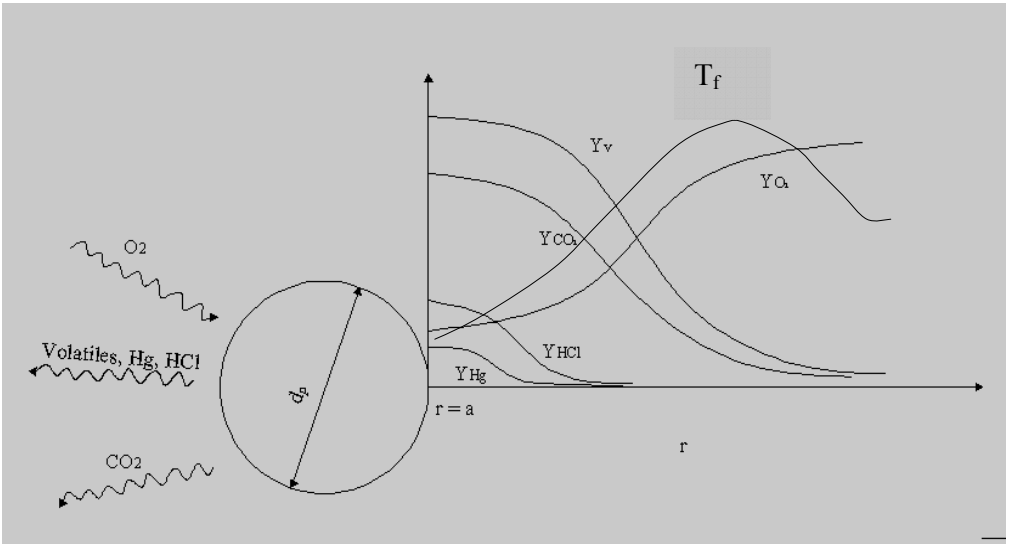

Fig. 4.1. Illustration of burning of coal particle

4.2 Assumptions

The assumptions are:

1. Spherical symmetry exists and gravitational force is neglected.
2. ρD = constant and Le = 1.
3. The coal particle is dry and ash free.
4. There is no relative motion between particle and the gas.
5. The coal particle temperature is time dependent but spatially uniform.

6. Pyrolysis occurs volumetrically with constant diameter and varying density while heterogeneous reactions occur at a particle surface with constant density and varying diameter.
7. The isothermal particle evolves volatiles uniformly throughout the particle. Devolatilization is endothermic and follows two competing routes with first order kinetics.
8. Volatile oxidation occurs by a two-step reaction. One that proceeds relatively fast and results in the production of CO and the other which proceeds at a much slower rate and results in the production of CO_2. Thus, the volatile oxidation kinetics is assumed to be same as the CO oxidation kinetics.
9. All gas phase chemical reactions for volatile, CO, CO_2, OH, H_2, and H_2O occur by a single step global reaction.
10. The ideal gas law is applicable.
11. Elemental mercury and HCl are considered to be the volatile products of mercury and chlorine respectively.
12. The Hg and Cl release rates are proportional to devolatilisation rate [37]. The proportionality constants are treated as parameters. All Hg and Cl are released with volatiles.
13. Mercury and Chlorine related compounds in gas phase are treated as trace species. Thus they do not effect the concentration of other species; further effect of heat of reactions on T_p and T_g are negligible.
14. Atomic chlorine concentration is assumed to be at equilibrium.

15. For the purpose of analysis of blended fuels, an equivalent empirical chemical formula is used for blended fuel with an equivalent volatile matter.
16. Only homogeneous Hg reactions are considered. Surface catalyzed reactions if any are ignored.
17. Heterogeneous hg reactions are ignored. Further the adsorption o f Hg on carbon surface is not considered.

4.3 Reactions

The reactions of interest are pyrolysis, char gasification, CO, volatiles oxidation and mercury-chlorine in gas phase.

4.3.1 Pyrolysis

The two–competing reactions are:

$$\text{COAL} \rightarrow (1-\alpha_I)\ \text{C (s)} + \alpha_I\ V_I$$

$$\text{COAL} \rightarrow (1-\alpha_{II})\ \text{C(s)} + \alpha_{II}\ V_{II}$$

where two types of volatiles V_I and V_{II} are evolved depending upon temperatures and heating rates.

4.3.2 Heterogeneous Reactions

$$C + \tfrac{1}{2}\ O_2 \rightarrow CO \qquad \text{(Reaction-I)}$$

$$C + O_2 \rightarrow CO_2 \qquad \text{(Reaction-II)}$$

$$C + CO_2 \rightarrow 2CO \qquad \text{(Reaction-III)}$$

$$C + H_2O \rightarrow CO + H_2 \qquad \text{(Reaction-IV)}$$

4.3.3 Homogeneous (Gas Phase) Reactions (Including Dissociation)

$CO + ½ O_2 \leftrightarrow CO$ (Reaction-V)

Volatiles, $V_I + O_2 \rightarrow CO_2 + H_2O$ (Reaction-VIa)

Volatiles, $V_{II} + O_2 \rightarrow CO_2 + H_2O$ (Reaction-VIb)

$H_2 + ½ O_2$ □ H_2O (Reaction-VIIa)

$½ H_2 + OH$□ H_2O (Reaction-VIIb)

4.3.4 Mercury Reactions

A three step reaction will be implemented for the oxidation of mercury shown in Table 4.1. Forward and backward reaction chemistry will be considered for H_2O which breaks down into OH and ½ H_2. The OH radical formed results in atomic chlorine when reacted with HCl. This atomic chlorine sets the rate oxidation of mercury. The kinetics for the three step reaction mechanism is taken from the eight reaction schemes of [23] and 90 reaction schemes of [38]. The reaction scheme will be condensed to three reactions involving Cl, OH, HgCl and HCl.

Table 4.1

Mercury reactions

	Reference	
$HCl + OH \rightarrow Cl + H_2O$	[38]	Reaction VIII
$Hg + Cl + M \rightarrow HgCl + M$	[23]	Reaction IX
$HgCl + Cl + M \rightarrow HgCl_2 + M$	[23]	Reaction X

4.4 Dimensional Form of the Conservation Equations

4.4.1 Gas Phase Conservation Equations

4.4.1.1 Mass

Assuming spherical symmetry, the mass conservation equation in spherical coordinates is given as

$$4\pi r^2\left(\frac{\partial \rho}{\partial t}\right)+\left(\frac{\partial \dot{m}}{\partial r}\right)=0 \qquad (4.1)$$

where

ρ gas phase density.

t time,

r radial distance from the particle center, and

$\dot{m}$ gas mass flow rate at “r”,

The mass flow rate ($\dot{m}$) includes the mass added/displaced through temperature gradients in the gas phase, the liberations rates of the volatiles and the carbon mass loss rate.

4.4.1.2 Species

Assuming spherical symmetry, the species conservation equation in spherical coordinates is written as

$$4\pi r^2 \rho\left(\frac{\partial Y_k}{\partial t}\right) + \dot{m}\left(\frac{\partial Y_k}{\partial r}\right) - \left[\frac{\partial}{\partial r}\left(4\pi r^2 \rho D\left(\frac{\partial Y_k}{\partial r}\right)\right)\right] = \dot{w}'''_{ch,k}\, 4\pi r^2 \tag{4.2}$$

where

k species O_2, CO, V_I, VII, CO_2, H_2O, Hg, $HgCl_2$, HgCl, Cl, HCl, etc,

Y_k mass fraction of species k,

$\dot{w}'''_{ch,k}$ volumetric gas phase source of species k, and

D diffusion coefficient.

The species k are produced or consumed in the gas phase from pyrolysis reactions and homogenous gas phase reactions.

4.4.1.3 Energy

Assuming spherical symmetry, the energy conservation in spherical coordinates is given as

$$4\pi r^2 \rho\left(\frac{\partial h_T}{\partial t}\right) + \dot{m}\left(\frac{\partial h_T}{\partial r}\right) - \left[\frac{\partial}{\partial r}\left(4\pi r^2 \rho D\left(\frac{\partial h_T}{\partial r}\right)\right)\right] = \dot{w}'''_h\, 4\pi r^2 \tag{4.3}$$

where

h_T thermal enthalpy $\left(\int_{Tref}^{T} C_p dT\right)$, and

$\dot{w}'''_h$ enthalpy production rate per unit volume of a bulk gas phase.

At the particle surface, the enthalpy production rate for the gas phase is a combination of the convective heat transfer per unit volume between the pas phase and the particle, ($\dot{q}'''_{conv}$), the enthalpy produced per unit volume as a result of chemical reactions in the gas phase ($\dot{q}'''_{ch}$) and the enthalpy gained per unit volume by the gas phase due to addition of mass from a single particle ($\dot{q}'''_{m}$). In the bulk gas phase, it is only the enthalpy produced as a result of chemical reactions in the gas phase ($\dot{q}'''_{ch}$). Each enthalpy term is expressed as follows:

$$\dot{q}'''_{ch} = \dot{m}'''_{V_{I},ch}\,\mathrm{HV_{VI}} + \dot{m}'''_{V_{II},ch}\,\mathrm{HV_{VII}} + \dot{m}'''_{CO,ch}\,\mathrm{HV_{CO}} \qquad (4.3a)$$

$$\dot{q}'''_{conv} = \mathrm{n}\,\dot{q}_{conv} \qquad \mathrm{n} = 1 \qquad (4.3b)$$

$$\dot{q}'''_{m} = \mathrm{n}\,\dot{q}_{m} \qquad \mathrm{n} = 1 \qquad (4.3c)$$

$$\dot{q}_{conv} = h\pi d_p^{\,2}\left(T_p - T_g\right) \qquad (4.3d)$$

$$\dot{q}'''_{m} = \dot{m}_p\, C_p\left(T_p - T_{ref}\right) \qquad (4.3e)$$

HV heating value,

$\dot{q}_{conv}$ convective heat transfer for a single particle,

$\dot{q}_{m}$ heat obtained by the gas phase due to addition of mass of a particle,

n particle number density (No of particles / m^3)

If $T_p > T_g$, then $\dot{q}_{conv} > 0$. Such a situation occurs if surface oxidation reactions are dominant compared with the gas phase reactions. Similarly, if the gas phase reactions are exothermic, then $\dot{q}'''_{ch} > 0$ (e.g., oxidation of volatiles).

4.4.2 Solid Phase Equations

4.4.2.1 Particle Mass (m_p)

The particle mass loss rate is express as

$$\frac{dm_p}{dt} = -\dot{m}_p \tag{4.4a}$$

$$\dot{m}_p = \dot{m}_V + \dot{m}_C + \dot{m}_{Hg} + \dot{m}_{Cl} \tag{4.4b}$$

where

dm_p/dt total rate of change of particle mass due to pyrolysis and heterogeneous reactions,

$\dot{m}_V$ total volatile loss rate,

$\dot{m}_{Hg}$ total mercury loss rate,

$\dot{m}_{Cl}$ total chlorine loss rate, and

$\dot{m}_C$ total carbon loss rate.

4.4.2.1.1 Mass Loss Rate due to Pyrolysis

The yield of volatiles depends on the rate of heating of particles and kinetics of pyrolysis. The higher the particle temperature and rate of reacting, higher the yield. A competing model explains the differing volatile yields. The competing reaction model assumes that the pyrolysis products consist of a lighter component (V_I, higher H/C ration in volatile) and a heavier component (V_{II}, lower H/C ratio in volatile). The lighter component is released at low temperatures and the heavier component is predominant pyrolysis product at high temperatures. These two reactions (I and II) proceed simultaneously and compete for hydrogen atoms. According to the competing reaction model

$$\text{COAL} \rightarrow (1-\alpha_I)\,\text{C (s)} + \alpha_I\, V_I \qquad \text{(V-I)}$$

$$\text{COAL} \rightarrow (1-\alpha_{II})\,\text{C(s)} + \alpha_{II}\, V_{II} \qquad \text{(V-II)}$$

The values of α_I and α_{II} used in the model represent the fraction of the coal that would be converted to volatile if all the volatiles are released by either reaction I or II. The kinetics of devolatilization is summarized in [39]. Pyrolysis is normally assumed to be volumetric and hence proceeds with constant particle size and variable density. A complete description of the competing reaction model is given in [40, 41].

4.4.2.1.1.1 Pyrolysis Reaction I (Low Temperature)

The mass loss rate $\dot{m}_{V,I}$ due to pyrolysis reaction I is given as

$$\dot{m}_{V,I} = \alpha_I k_{V,I} m_{cu} \tag{4.5a}$$

$$k_{V,I} = B_{V,I} \exp\left(\frac{-E_{V,I}}{R_u T_p}\right) \tag{4.5b}$$

where

α_I maximum volatile yield via pyrolysis reaction (V-I),

$k_{V,I}$ specific reaction rate constant for reaction (V-I),

$B_{V,I}$ pre-exponential factor for pyrolysis reaction (V-I), and

$E_{V,I}$ is the activation energy for pyrolysis (V-I).

The undecomposed coal (m_{cu}) can be expressed as

$$m_{cu} = m_{p,0} - \int_0^0 \left(\frac{\dot{m}_{V,I}}{\alpha_I} + \frac{\dot{m}_{V,II}}{\alpha_{II}}\right) dt \tag{4.5c}$$

where

$m_{p,0}$ initial mass of the particle,

$m_{V,I}$ mass loss rate via pyrolysis reaction (V-I), and

$m_{V,II}$ mass loss rate via pyrolysis reaction (V-II).

4.4.2.1.1.2 Pyrolysis Reaction II (High Temperature)

The mass loss rate due to pyrolysis reaction II is given in the similar form

$$\dot{m}_{V,II} = \alpha_{II} k_{V,II} m_{cu} \tag{4.6a}$$

$$k_{V,II} = B_{V,II} \exp\left(\frac{-E_{V,II}}{R_u T_p}\right) \tag{4.6b}$$

where

α_{II} maximum volatile yield via pyrolysis reaction (V-II),

$k_{V,II}$ specific reaction rate constant for reaction (V-II),

$B_{V,II}$ pre-exponential factor for pyrolysis reaction (V-II), and

$E_{V,II}$ is the activation energy for pyrolysis (V-II).

Equations (4.5a) and (4.6a) can also be written as,

$$\left(\frac{\dot{m}_{V,I}}{\dot{m}_{p,0}}\right) = \alpha_I k_{V,I} f_{cu} \tag{4.6c}$$

$$\left(\frac{\dot{m}_{V,II}}{\dot{m}_{p,0}}\right) = \alpha_{II} k_{V,II} f_{cu} \tag{4.6d}$$

And it follows from equation (4.5c)

$$f_{cu} = \frac{m_{cu}}{m_{p,0}} = 1 - \int_0^t \left(k_{V,I} + k_{V,II}\right) f_{cu}\, dt \tag{4.6e}$$

The total volatile liberation due to both reaction (V-I) and (V-II) is given as

$$\dot{m}_V = \dot{m}_{V,I} + \dot{m}_{V,II} \tag{4.6f}$$

The volatile mass loss rate contribution ($\dot{m}_V$) to the particle mass loss rate ($\dot{m}_p$) is given as

$$\dot{m}_V = (dm_p / dt)_V = -(\dot{m}_{V,I} + \dot{m}_{V,II}) \tag{4.6g}$$

4.4.2.1.1.3 Pyrolysis with Heterogeneous In-situ Combustion of Volatile

If volatiles are consumed in-situ along with the carbon, then equation (4.5c) should be modified as,

$$m_{cu} = m_{p,0} - \int_0^0 \left(\frac{\dot{m}_{V,I}}{\alpha_I} + \frac{\dot{m}_{V,II}}{\alpha_{II}} + \frac{\dot{m}_{V,S}}{VM} \right) dt \tag{4.7a}$$

where

VM instantaneous volatile fraction left in the coal, and

$\dot{m}_{V,S}$ in-situ volatile combustion rate.

By assuming the in-situ volatile combustion rate is proportional to the ratio of proximate volatile matter to the fixed carbon in the coal, the in-situ volatile combustion rate ($\dot{m}_{V,S}$) is

$$\dot{m}_{V,S} = \dot{m}_C \left(\frac{VM}{1 - VM} \right) \tag{4.7b}$$

4.4.2.1.1.4 The Q` Factor

The effect of interactions is to reduce the volatile yield. Volatile matter is measured using the standard ASTM procedure of placing a 1g sample in a covered crucible and heating it to 1200K for 7 minutes. Since the heating rate is relatively slow and the sample is dense, these conditions promote cracking reactions at char surfaces and the yield obtained is relatively low. This is termed proximate volatile yield. On the other hand, if a similar sample is heated rapidly in the dilute mode, volatile yields in excess of the proximate yield can be obtained. Thus Q' factor has been introduced to relate the actual yield to the proximate yield as

$$Q' = \frac{True \quad or \quad actual \quad yield}{proximate \quad or \quad ASTM \quad yield} \tag{4.8a}$$

Therefore, at any instant of time, Q' factor is given as

$$Q' = \frac{\dot{m}_V \quad for \quad a \quad given \quad m_{cu}}{\dot{m}_{V,I} \quad for \quad the \quad same \quad m_{cu}} \tag{4.8b}$$

where

$\dot{m}_{V,I}$ volatile liberation rate when competing reaction V_{II} is absent.

Using equations (4.5a), (4.6a) and (4.6f) in equation (4.8a), Q' becomes

$$Q' = \left(1 + \frac{k_{V,II}\alpha_{II}}{k_{V,I}\alpha_I}\right) \tag{4.8c}$$

Note that if $k_{V,II} \rightarrow 0$, then $Q` \rightarrow 1.0$ as expected

4.4.2.1.1.5 Proximate Volatile Matter (PVM)

If the proximate volatile matter in coal is traced as a function of time then

$$\frac{d\left[\left(PVM\right)m_p\right]}{dt} = -\left(\dot{m}_{V,I} + \dot{m}_{V,S}\right) \tag{4.9a}$$

$$\dot{m}_p = -\frac{dm_p}{dt} = \left(\dot{m}_p + \dot{m}_C + \dot{m}_{V,S}\right) \tag{4.9b}$$

Using equation (4.9b) in equation (4.9a) gives

$$\frac{d(PVM)}{dt} = \frac{\left(-\frac{\dot{m}_V}{Q'} - \dot{m}_{V,S} + (PVM)\,\dot{m}_p\right)}{m_p} \tag{4.9c}$$

where

$\dot{m}_V / Q'$ $\quad (= \dot{m}_{V,I})$ is the proximate volatile loss rate.

Equation (4.9c) is useful in tracking PVM as time varies. Suppose $\dot{m}_{V,S} = 0$, then for Q' = 1, the proximate volatile matter decreases more slowly than for Q' = 2.

4.4.2.1.2 Mass Loss Rate due to Heterogeneous Reactions

For heterogeneous reactions i (i=I,II, III or IV), the mass loss rate of the carbon/char is

$$\dot{m}_{C,i} = \rho_w k_{C,i} Y_{O_2,w}^{n_{O_2,i}} \pi d_p^2 \tag{4.10a}$$

$$k_{C,i} = B_{C,I} \exp\left(\frac{-E_{C,I}}{R_u T_p}\right) \tag{4.10b}$$

where

$n_{O_2,i}$ order of reaction I with respect to oxygen,

$Y_{O_2,w}$ oxygen mass fraction at the surface of the particle,

$k_{C,i}$ specific reaction rate constant for reaction i, and

$B_{C,i}$ pre-exponential factor for reaction i.

The total carbon consumption rate for a particle of size d is given as

$$\dot{m}_p = \sum_{i=1}^{N} \dot{m}_{C,i} \tag{4.10c}$$

where

N total number of reactions involving the carbon.

In order to calculate heterogeneous reactions on the particle surface, the species concentration must be determined first. The species mass fraction at the particle surface $Y_{k,w}$ is calculated as follows.

With the assumption of a first order reaction at the particle surface, the analysis of the mass transfer across the frozen film yields the following expression for the species mass fraction at the particle surface.

$$\frac{Y_{k,w}}{Y_k} = \left[\exp(X) - \sum_{l=1}^{L} \frac{\upsilon_{k,l} \rho k_{c,l} S n_l d_p \left(\exp(X) - 1\right)}{XSh\rho D} \right]^{-1} \tag{4.10d}$$

where

$$X = \frac{\dot{m}_p}{\left(Sh\rho D\pi d_p\right)} = \frac{h_m d_{p,i}}{\rho D} \tag{4.10e}$$

Sh = 2 for a quiescent atmosphere.

l total number of reaction involving species k,

v stoichiometric mass of species k per unit mass of the carbon in reaction "*l*".

h_m mass transfer coefficient,

Sn_l equals to +1 if species are produced for reaction *l*, and

Sn_l equals to -1 if species are consumed for reaction *l*.

From equation (4.10), it can be seen that the oxygen mass fraction at the particle surface ($Y_{k,w}$) is calculated in terms of the bulk gas phase mass fraction (Y_{O_2}) next to the particle by a mass balance. For example, if k=O_2, then there are two heterogeneous reactions (reaction I and II) which consume O_2 and hence L=2. Since O_2 is consumed, the sign of Sn is negative for both the reactions. When the carbon is oxidized heterogeneously, there may be in-situ combustion of volatiles. It is noted that as $X \to 0$, $Y_{k,w} \to Y_k$.

4.4.2.2 Particle Diameter (d_p)

The diameter of the particle shrinks since heterogeneous oxidation occurs at the particle surface with constant density. The relation between $\dot{m}_C$ and d_p is given as

$$\frac{d(d_p)}{dt} = -\frac{2\dot{m}_p}{\pi\rho_p d_p^2} \tag{4.11}$$

4.4.2.3 Particle Density (ρ_p)

The particle density changes with time since pyrolysis occurs volumetrically at a constant particle size. The relation between $\dot{m}_V$ and ρ_p is

$$\frac{d(d_p)}{dt} = -\frac{6\dot{m}_V}{\pi d_p^3} \tag{4.12}$$

4.4.2.4 Particle Temperature (T_p)

The particle temperature is obtained from the energy balance around a single particle.

$$m_p c_p \frac{d(d_p)}{dt} = -(\dot{q}_{conv} + \dot{q}_{rad}) + \dot{q}_{ch,p} \tag{4.13}$$

where

$\dot{q}_{ch,p}$ heat released due to heterogeneous reaction and pyrolysis,

$\dot{q}_{conv}$ convective heat transfer between the bulk gas and particle of size "d_p", and

$\dot{q}_{rad}$ radiate heat transfer between a particle of size "d_p" and ambience.

4.4.2.4.1 Convection Term

Assuming quasi-steady behavior around the particle, the overall convective heat transfer rate between the particle and the gas is given as,

$$\dot{q}_{conv} = h^o (T_p - T)\pi d_p^2 F_k F_B \tag{4.14a}$$

where

F_k Knudson correction factor,

F_B blowing correction factor, and

h^o heat transfer coefficient for a particle of size d_p, ($h^o = Nu^o\lambda/d_p$).

The blowing correction factor to the heat transfer coefficient is given as

$$F_B = \frac{(\dot{m}_p / 2\pi\rho D d_p)}{(\exp(\dot{m}_p / 2\pi\rho D d_p) - 1)} \tag{4.14b}$$

The Knudson correction factor is given as

$$F_k = 1 - \left[\frac{(l_m / d_p)}{((l_m / d_p) + 0.17)} \right] \tag{4.14c}$$

where

l_m mean free path.

Note that $F_k \rightarrow 1$ when $l_m/d_p \rightarrow 0$ or particle diameter is large compared mean free path.

4.4.2.4.2 Radiation Term

The particles transfer energy by radiation to the surroundings. The particle radiate to the ambience and hence the radiation loss is given as

$$\dot{q}_{rad} = F_R \sigma_{SB} \varepsilon (T_p^4 - T_{rad}^4)\pi d_p^2 \tag{4.15}$$

where

F_R shape factor

σ_{SB} Stefan-Boltzmann constant,

ε emissivity, and

T_{rad} radiative temperature.

4.4.2.4.3 Chemical Reaction Term

The heat liberation rate due to chemical reactions at the particle is given as

$$\dot{q}_{ch,p} = \sum_{i=1}^{N} \dot{m}_{C,i} HV_{C,i} + \dot{m}_{V,I} HV_{V,I} + \dot{m}_{V,II} HV_{V,II} + \dot{m}_{V,S} HV_{V,S} \qquad (4.16)$$

where

$HV_{C,i}$ heating value for heterogeneous reaction I (>0),

$HV_{P,I}$ latent heat of pyrolysis for the first pyrolysis reaction in the competing reaction model (<0),

$HV_{P,II}$ latent heat of pyrolysis for the second pyrolysis reaction in the competing reaction model (<0), and

$HV_{V,S}$ heating value for the in-situ volatiles.

4.4.2.5 Mass, Species, and Heat Sources

4.4.2.5.1 Mass Source ($\dot{w}_m'''$)

The gaseous mass added to the unit volume of the bulk gas phase must be equal to the mass loss of the solid particles per unit volume. Therefore, the mass source term $\dot{w}_m'''$ can be express by the solid mass loss rate of coal particles per unit volume.

$$\dot{w}_m''' = \sum n \dot{m}_p \tag{4.17}$$

In the case of single particle study, the value of "n" is 1. The mass loss rate of the coal particle ($\dot{m}_p$) occurs due to pyrolysis and heterogeneous char reactions and is given by equations (4.4), (4.5), (4.6) and (4.10).

4.4.2.5.2 Species Source ($\dot{w}_k'''$)

Species k is produced/consumed at the particle due to heterogeneous and/or pyrolysis reactions and due to homogeneous gas phase reactions. Thus species k,

$$\dot{w}_k''' = \dot{m}_{ch,p.k}''' + \dot{m}_{ch,k}''' \tag{4.18}$$

where

$\dot{m}_{ch,p.k}'''$ production rate of species k due to reactions in the gas phase.

For example, k=V (which may be either V_I or V_{II}) then,

$$\dot{w}_V''' = \dot{m}_V + \dot{m}_{ch,V}''' \tag{4.19a}$$

Where, for global one step oxidation of volatile, assuming a first order reaction,

$$\dot{m}_{ch,V} = -A_V Y_V Y_{O_2} \rho^2 \exp\left(\frac{-E_V}{R_u T}\right) \tag{4.19b}$$

If k=O_2, then O_2 is consumed due to heterogeneous and homogeneous reactions, Thus,

$$\dot{w}'''_{O_2} = \dot{m}_{C,I}\,\upsilon_I + \dot{m}_{C,II}\,\upsilon_{II} + \dot{m}_{V,S}\,\upsilon_{V,S} - \dot{m}'''_{ch,O_2} \tag{4.19c}$$

where

$$\dot{m}_{ch,O_2} = \dot{m}_{ch,V}\,\upsilon_V + \dot{m}_{ch,CO}\,\upsilon_{CO} \tag{4.19d}$$

And for wet oxidation of CO,

$$\dot{m}'''_{ch,CO} = -A_{CO}\,Y_{CO}\,Y_{O_2}^{0.5}\,Y_{H_2O}^{0.5}\,\rho^2 \exp\left(\frac{-E_{CO}}{R_u T}\right) \tag{4.19e}$$

Similarly, for k=CO and CO_2, the source term $\dot{w}'''_{CO}$ and $\dot{w}'''_{CO_2}$ can be calculated.

4.4.2.5.3 Heat Source ($\dot{w}'''_h$)

The heat source in the gas phase is given as

$$\dot{w}'''_h = \dot{q}'''_{conv} + \dot{q}'''_{ch} + \dot{q}'''_m \tag{4.20}$$

The first term $\dot{q}'''_{conv}$ equation (4.20) represents the heat sink or source in the gas phase due to the transient heating or cooling of coal particles; the second term $\dot{q}'''_{ch}$ in the equation (4.20) represents the heat generation per unit volume due to chemical reactions in the gas phase; the third term $\dot{q}'''_m$ in equation (4.20) represents the heat added to the bulk gas from the particle due to mass transfer.

4.4.3 Mercury and Chlorine Pyrolysis

Due to competing reactions, Hg will be release through V_I and V_{II}; However the Hg fractions in V_I and V_{II} differ. If $f_{Hg,I}$ and $f_{Hg,II}$ are fractions of Hg mass in V_I and V_{II} then

$$\dot{m}_{Hg} = f_{Hg,I}\,\dot{m}_{v,I} + f_{Hg,II}\,\dot{m}_{v,II} \tag{4.21}$$

Defining,

$$f_{Hg,v} = \frac{\dot{m}_{Hg}}{\dot{m}_{v}} \tag{4.22}$$

One can show that $f_{Hg,v}$ is fraction of Hg in volatiles given by

$$f_{Hg,v} = \mathrm{M_{Hg}}\ \mathrm{x}\left[\frac{Hg_{V,I}}{M_{V,I}}\times VK_I + \frac{Hg_{V,II}}{M_{V,II}}\times VK_{II}\right]/\left(VK_I + VK_{II}\right) \tag{4.23}$$

Similarly with Cl,

$$\dot{m}_{Cl} = f_{Cl,I}\,\dot{m}_{v,I} + f_{Cl,II}\,\dot{m}_{v,II} \tag{4.24}$$

One can show that,

$$f_{Cl,v} = \mathrm{M_{Cl}}\ \mathrm{x}\left[\frac{Cl_{V,I}}{M_{V,I}}\times VK_I + \frac{Cl_{V,II}}{M_{V,II}}\times VK_{II}\right]/\left(VK_I + VK_{II}\right) \tag{4.25}$$

where $VK_i = \alpha_i$ x $A_{V,i}$ exp(-$E_{V,i}$ / RT) , i= I, II indicate two different competing reactions for the pyrolysis

4.4.4 Initial and Boundary Conditions

The boundary conditions at r = *a* are as follows:

Mass

$$\dot{m}_w = \dot{m}_v + \dot{m}_c + \dot{m}_{Hg} + \dot{m}_{HCl} \tag{4.26}$$

The mass flow rate at the interface must equal the mass loss rate by the particle via volatiles ($\dot{m}_v$), carbon oxidation ($\dot{m}_c$), mercury ($\dot{m}_{Hg}$) and chlorine ($\dot{m}_{HCl}$).The liberation rate of volatiles is modeled using a competing reaction model [42].

Species

Oxygen:

$$\dot{m}_w Y_{O_2,w} - \rho D \left(\frac{\partial Y_{O_2}}{\partial r} \right)_{r=a} 4\pi a^2 = \dot{m}_C \upsilon \tag{4.27}$$

CO_2:

$$\dot{m}_w Y_{CO_2,w} - \rho D \left(\frac{\partial Y_{CO_2}}{\partial r} \right)_{r=a} 4\pi a^2 = \dot{m}_C (1+\upsilon) \tag{4.28}$$

Volatile (V_I):

$$\dot{m}_w Y_{V,I} - \rho D \left(\frac{\partial Y_{V,I}}{\partial r} \right)_{r=a} 4\pi a^2 = \dot{m}_{V,I} \tag{4.29}$$

Volatile (V_{II}):

$$\dot{m}_w Y_{V,II} - \rho D \left(\frac{\partial Y_{V,II}}{\partial r} \right)_{r=a} 4\pi a^2 = \dot{m}_{V,II} \tag{4.30}$$

Trace Species (Mercury and Chlorine)

The proposed changes made to the boundary conditions in order to incorporate the mercury and chlorine chemistry are,

$$\dot{m}_w Y_{Hg,w} - \rho D \left(\frac{\partial Y_{Hg}}{\partial r} \right)_{r=a} 4\pi a^2 = \dot{m}_{Hg} \tag{4.31}$$

$$\dot{m}_w Y_{HCl,w} - \rho D \left(\frac{\partial Y_{HCl}}{\partial r} \right)_{r=a} 4\pi a^2 = \dot{m}_{HCl} \tag{4.32}$$

The coal particle releases Hg and HCl which react in gas phase reactions (Table 4.1) producing $HgCl_2$. The total rate of production of $HgCl_2$ at any time t within the film is estimated by using (Fig 4.2)

$$\dot{w}_{HgCl_2}(t) = \int_{r=a}^{\infty} \dot{w}'''_{HgCl_2} 4\pi r^2 dr \tag{4.33}$$

while total production during life time of the particle is given as

$$w_{HgCl_2} = \int_0^{t_b} \dot{w}_{HgCl_2} dt \tag{4.34}$$

where, t_b is the burning time. The time to burn 90% of mass is assumed to be the burning time. The Hg is released during pyrolyis and integrated amount of Hg released is given as

$$m_{Hg} = \int_0^{t_v} \dot{m}_{Hg}(t)\,dt \tag{4.35}$$

where, t_v is the volatile release time.

It is noted that the Hg in $HgCl_2$ can be estimated as

$$m_{Hg,\,HgCl2} = w_{HgCl_2} \times M_{Hg}/M_{HgCl2} \tag{4.36}$$

The percentage of Hg (0) converted to $HgCl_2$ is

$$= (w_{HgCl_2} \times M_{Hg}/M_{HgCl2}) \times 100/ m_{Hg} \tag{4.37}$$

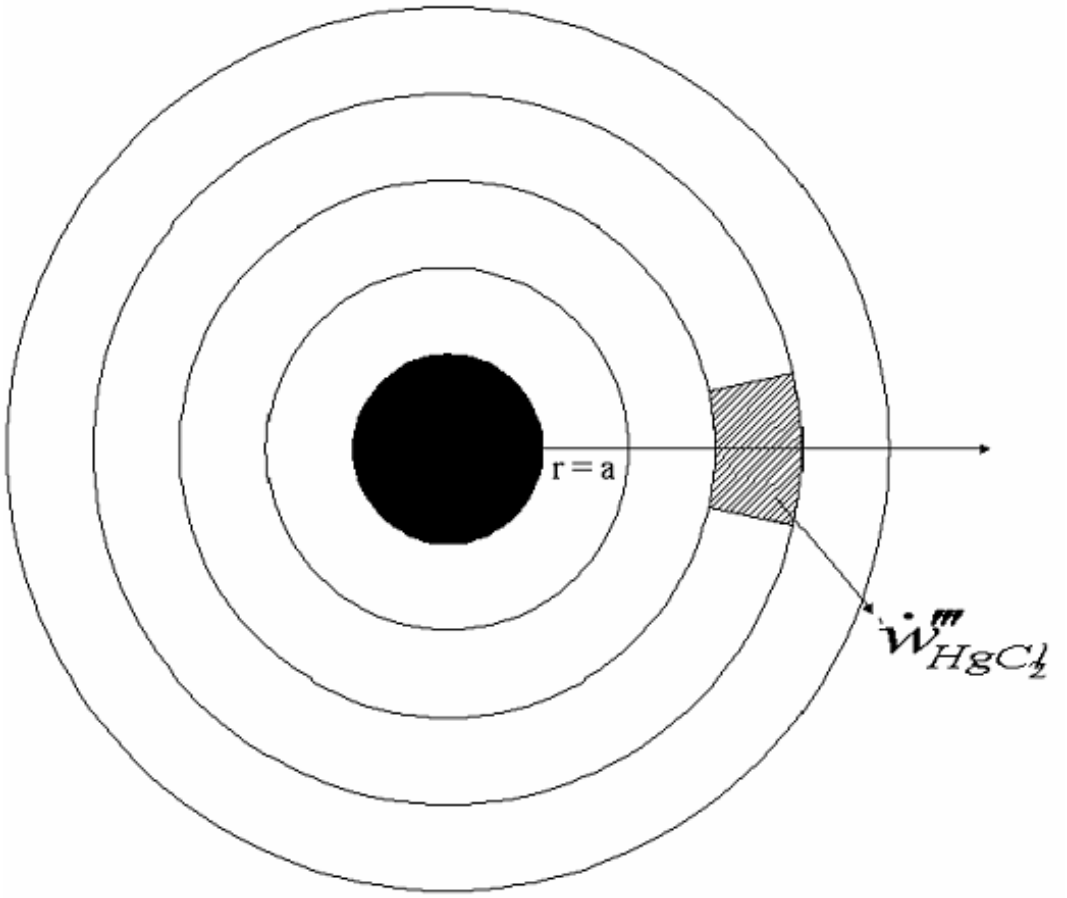

Fig. 4.2. Illustration of conversion of Hg to $HgCl_2$

Energy

$$\left\{\lambda \frac{dT}{dr}|_{r=a} 4\pi a^2\right\} + \dot{m}_C\, h_C + \dot{m}_{V,I}\, h_{V,I} + \dot{m}_{V,II}\, h_{V,II} + \varepsilon\sigma 4\pi a^2 \left(T_{rad}^4 - T_p^4\right) = m_p c\left(\frac{dT_p}{dt}\right) \tag{4.38}$$

The transient conditions are given below,

At t = 0

Gas phase

$T = T_\infty$ (4.39a)

$\rho = \rho_\infty$ (4.39b)

$Y_k = Y_\infty$ (4.39c)

Solid phase

$m_p = m_{p,0}$ (4.40a)

$d_p = d_{p,0}$ (4. 40b)

$\rho = \rho_{p,0}$ (4. 40c)

$T_p = T_{p,0}$ (4. 40d)

At any time t > 0

As $r \rightarrow \infty$

$T = T_\infty$ (4.41a)

$\rho = \rho_\infty$ (4.41b)

$Y_k = Y_\infty$ (4.41c)

4.5 Non-dimensional Form of the Conservation Equations

The system of governing equations can be rewritten in non-dimensional form by introducing the reference quantities and non-dimensional variables in the following sections.

4.5.1 Reference Quantities

$$\rho_{ref} = \frac{P}{RT_{ref}} \tag{4.42a}$$

where $R=R_u/W$ and W is the molecular weight

$$t_{ref} = \frac{\rho_{ref} a_0^{\,2}}{RT_{ref}} \tag{4.42b}$$

$$\dot{m}'''_{ref,g} = \rho D / a_0^{\,2} = \left(\frac{\rho_{ref}}{t_{ref}} \right) \tag{4.42c}$$

where ρ is the density of the gas (determine ρ at $T = T_\infty$ and D at $T = T_\infty$).

$$\dot{m}_{ref,g} = 4\pi\rho D a_0 \tag{4.42d}$$

$$h_{ref} = c_p T_{ref} \tag{4.42e}$$

$$\dot{m}_{ref,g} = \left(\frac{m_{p,0}}{t_{ref}} \right) \tag{4.42f}$$

4.5.2 Non-dimensional Variables

4.5.2.1 Gas Phase

$$\xi = \frac{a}{r} \tag{4.43a}$$

$$\tau = \frac{t}{t_{ref}} \tag{4.43b}$$

$$\rho^* = \frac{\rho}{\rho_{ref}} \tag{4.43c}$$

$$\alpha = \frac{\dot{m}}{\dot{m}_{ref,g}} \tag{4.43d}$$

$$q^*_{conv} = \frac{q_{conv} t_{ref}}{h_{ref} m_{p,0}} \tag{4.43e}$$

$$h^*_T = \frac{h_T}{h_{T,ref}} \tag{4.43f}$$

$$w_m = \frac{\dot{w}'''_m}{\dot{m}'''_{ref}} \tag{4.43g}$$

$$w_k = (\dot{m}'''_{p,k} + \dot{m}'''_{ch,k}) \Big/ \dot{m}'''_{ref} \tag{4.43h}$$

$$w_h = (\dot{q}'''_{conv} + \dot{q}'''_{ch} + \dot{q}'''_{m}) \Big/ (\dot{m}'''_{ref,g}\, h_{T,ref}) \tag{4.43i}$$

4.5.2.2 Solid Phase

The solid phase non-dimensional quantities are defined as follows

$$m_p^* = \frac{m_p}{m_{p,0}} \tag{4.44a}$$

Where $m_{p,0}$ is the mass of the particle at time t = 0

$$d_p^* = \frac{d_p}{d_{p,0}} \tag{4.44b}$$

where $d_{p,0}$ is the diameter of the particle at time t = 0

$$D_V = \frac{B_{V,I} m_{p,0}}{4\pi\rho D a_0}, \text{ Damkohler number for volatile releases} \tag{4.44c}$$

$$E_V^* = \frac{E_V / R_u}{T_{ref}} \tag{4.44d}$$

$$D_C = \frac{B_C d_p^2 \rho_{ref}}{4\pi\rho D a_0}, \text{ Damkohler number for carbon reactions} \tag{4.44e}$$

$$m_V^* = \frac{\dot{m}_V}{\dot{m}_{ref,p}} \tag{4.44f}$$

$$m_C^* = \frac{\dot{m}_C}{\dot{m}_{ref,p}} \tag{4.44g}$$

$$q_{conv}^* = \frac{\dot{q}_{conv}\, t_{ref}}{h_{ref}\, m_{p,0}} \tag{4.44h}$$

$$q_{rad}^* = \frac{\dot{q}_{rad}\, t_{ref}}{h_{ref}\, m_{p,0}} \tag{4.44i}$$

$$q_{ch,p}^* = \frac{\dot{q}_{ch,p}\, t_{ref}}{h_{ref}\, m_{p,0}} \tag{4.44j}$$

4.5.3 Non-dimensional Gas Phase Conservation Equations

4.5.3.1 Mass

$$\frac{\partial \rho^*}{\partial \tau} + \xi^4 \left(\frac{\partial \alpha}{\partial \xi} \right) = 0 \tag{4.45}$$

4.5.3.2 Species

$$\rho^* \frac{\partial Y_k}{\partial \tau} - \alpha \xi^4 \left(\frac{\partial Y_k}{\partial \xi} \right) - \xi^4 \left(\frac{\partial^2 Y_k}{\partial \xi^2} \right) = w_k \tag{4.46}$$

4.5.3.3 Energy

$$\rho^* \frac{\partial h_T^*}{\partial \tau} - \alpha \xi^4 \left(\frac{\partial h_T^*}{\partial \xi} \right) - \xi^4 \left(\frac{\partial^2 h_T^*}{\partial \xi^2} \right) = w_h \tag{4.47}$$

4.5.4 Non-dimensional Solid Phase Equations

4.5.4.1 Particle Mass

$$\frac{dm_p^*}{d\tau} = -(m_V^* + m_C^*) \tag{4.48}$$

4.5.4.2 Particle Diameter

$$\rho_p^* \left(\frac{d(d_p^*)^3}{d\tau} \right) = -m_C^* \tag{4.49}$$

4.5.4.3 Particle Density

$$d_p^{*3} \left(\frac{d\rho_p^*}{d\tau} \right) = -m_V^* \tag{4.50}$$

4.5.4.4 Particle Temperature

$$m_p^* \left(\frac{d\theta_p}{d\tau} \right) = (q_{ch,p}^* - q_{conv}^* - q_{rad}^*) \tag{4.51}$$

4.5.5 Normalized Boundary Conditions

The normalized boundary conditions are:

Mass

$$\dot{m}_w^* = \dot{m}_{V,I}^* + \dot{m}_{V,II}^* + \dot{m}_C^* + \dot{m}_{Hg}^* + \dot{m}_{Cl}^* \tag{4.52}$$

Species

Oxygen:

$$\alpha_w Y_{O_2,w} + \left(\xi^2 \frac{dY_{O_2}}{d\xi} \right)_{\xi=1} = \left(\frac{\dot{m}_{ref,p}}{\dot{m}_{ref,g}} \right) (\dot{m}_C^* \upsilon) \tag{4.53}$$

CO_2:

$$\alpha_w Y_{CO_2,w} + \left(\xi^2 \frac{dY_{CO_2}}{d\xi} \right)_{\xi=1} = \left(\frac{\dot{m}_{ref,p}}{\dot{m}_{ref,g}} \right) \dot{m}_C^* (1+\upsilon) \tag{4.54}$$

Volatile (V_I):

$$\alpha_w Y_{V,I,w} + \left(\xi^2 \frac{dY_{V,I}}{d\xi} \right)_{\xi=1} = \left(\frac{\dot{m}_{ref,p}}{\dot{m}_{ref,g}} \right) \dot{m}_{V,I}^* \tag{4.55}$$

Volatile (V_{II}):

$$\alpha_w Y_{V,II,w} + \left(\xi^2 \frac{dY_{V,II}}{d\xi} \right)_{\xi=1} = \left(\frac{\dot{m}_{ref,p}}{\dot{m}_{ref,g}} \right) \dot{m}_{V,II}^* \tag{4.56}$$

Trace species (Mercury and Chlorine):

$$\alpha_w Y_{Hg,w} + \left(\xi^2 \frac{dY_{Hg}}{d\xi} \right)_{\xi=1} = \left(\frac{\dot{m}_{ref,p}}{\dot{m}_{ref,g}} \right) \dot{m}^*_{Hg} \tag{4.57}$$

$$\alpha_w Y_{HCl,w} + \left(\xi^2 \frac{dY_{HCl}}{d\xi} \right)_{\xi=1} = \left(\frac{\dot{m}_{ref,p}}{\dot{m}_{ref,g}} \right) \dot{m}^*_{HCl} \tag{4.58}$$

Energy

$$-\left(\frac{\dot{m}_{ref,g}}{\dot{m}_{ref,p}} \right)(Le)\left(\xi^2 \frac{dh^*_T}{d\xi} \right)_{\xi=1} + \dot{m}^*_C h^*_C + \dot{m}^*_{V,I} h^*_{V,I} + \dot{m}^*_{V,II} h^*_{V,II}$$
$$+ \frac{\dot{m}_{ref,g}}{\dot{m}_{ref,p}}(Ra)(h^{*\,4}_{rad} - h^{*4}) = m^*_p \frac{dh^*_T}{d\tau} \tag{4.59}$$

The transient conditions are given below,

At $\tau = 0$,

Gas phase

$$h^*_{T,\infty} = h_{T,\infty} / h_{T,ref} \tag{4.60a}$$

$$\rho^*_\infty = T_{ref} / T_\infty \tag{4.60b}$$

$$Y_k = Y_{k,\infty} \tag{4.60c}$$

Solid phase

$$m_p^* = 1 \tag{4.61a}$$

$$d_p^* = 1 \tag{4.61b}$$

$$\rho_p^* = 1 \tag{4.61c}$$

$$\theta_p = T_{p,0} / T_{ref} \tag{4.61d}$$

At any time $\tau > 0$,

As $\xi \rightarrow 0$

$$\rho^{*} = \rho_{p,\infty} \tag{4.62a}$$

$$h_T^{*} = h_{T,\infty} \big/ h_{T,ref} \tag{4.62b}$$

$$Y_k = Y_{k,\infty} \tag{4.62c}$$

It should be noted that gas phase conservation equations are first order with respect to non-dimensional time τ, and second order with respect to non-dimensional radius, ξ, and as such, one need two boundary conditions and one initial condition for each variable, equations are parabolic. The solid phase conservation equations are first order respect to τ and hence one needs only the initial condition.

5 NUMERICAL PROCEDURE

This section describes the numerical scheme used in solving the governing equations for the transient ignition and combustion of an isolated coal particle followed by the program description, the listing of input variables.

5.1 Numerical Method

The present version of the code COALPILE has been developed to simulate the transient pyrolysis, ignition and combustion process of an isolated coal particle. The present code also simulates the mercury and chlorine behavior during the pyrolysis and combustion of the coal particle.

5.1.1 Eulerian Equations

Eulerian equations (4.45), (4.46) and (4.47) for gas phase can be written in general form as follow:

$$A\rho^{*}\left(\frac{\partial\psi}{\partial\tau}\right)-B\xi^{4}\left(\frac{\partial\psi}{\partial\xi}\right)-C\xi^{4}\left(\frac{\partial^{2}\psi}{\partial\xi^{2}}\right)=DW_{\psi} \tag{5.1}$$

where $W_\psi = W_m$, W_k and W_h

The property ψ and the constant A, B, C and D for the conservation equations are tabulated in Table 5.1. An explicit finite difference upwind scheme is used to solve the gas phase governing differential equations. The generalized Eulerian equation 5.1 can be expressed in simple form as

$$TRANS + ADVECT - DIFFUS = SOURCE \tag{5.2}$$

Table 5.1

Conserved quantity ψ for Eulerian equations

	Mass	**Species**	**Energy**
	α	**Y_k**	**h_T^***
A	0	1	1
B	1	α	α
C	0	1	1
D	1	1	1
W_ψ	0	W_k	W_h

Where TRANS is the transient (or accumulation) term, ADVECT is the advection term, DIFFUS is the diffusion term and SOURCE is the source term. The upwind scheme was used to represent the advection term and a central difference formulation for the diffusion term. The expanded forms of these terms are as follows

$$TRANS = A\rho^*\left(\frac{\psi_i^{\tau+\Delta\tau} - \psi_i^{\tau}}{\Delta\tau}\right) \tag{5.3a}$$

$$DIFFUS = C\xi^4\left(\frac{\psi_{i+1}^{\tau} + \psi_{i-1}^{\tau} - 2\psi_i^{\tau}}{\Delta\xi^2}\right) \tag{5.3b}$$

$$ADVECT = B\xi^4\left(\frac{\psi_{i+1}^{\tau} - \psi_i^{\tau}}{\Delta\xi}\right) \qquad B > 0 \tag{5.3c}$$

$$ADVECT = B\xi^4\left(\frac{\psi_i^\tau - \psi_{i-1}^\tau}{\Delta\xi}\right) \qquad B < 0 \qquad (5.3d)$$

where the subscript I refers to nodal location. The source term can be expanded into chemical consumption (CHEM) and production (PROD) terms. Expressing the transient term in explicit form as well, equation (5.2) can be re written as

$$A\rho^*\left(\frac{\psi_i^{\tau+\Delta\tau} - \psi_i^\tau}{\Delta\tau}\right) + ADVECT + DIFFUS = CHEM + PROD \qquad (5.4)$$

Rearranging this equation gives

$$\psi_i^{\tau+\Delta\tau} = \psi_i^\tau + \frac{\Delta\tau}{A\rho^*}(CHEM + PROD - ADVECT + DIFFUS) \qquad (5.5)$$

This is the form of the equations used in the numerical model to determine the current values of the dependent variables for gas phase.

5.1.2 Numerical Methods

Although the governing equations used in the code are generalized non-dimensional form, it is convenient to use the dimensional form of conservation equations in order to illustrate the numerical method. A brief description of the method used is given below.

(1) Determine the properties at t = 0:

Gas phase source terms

With the given initial conditions at t = 0 for T_g, Y_k, m_p, Tp, ρ_p and d_p, calculate the source terms $\dot{w}_m'''$, $\dot{w}_k'''$, $\dot{w}_h'''$ for mass, species and energy conservation equations (4.1),

(4.2) and (4.3). The bulk gas mass loss rate ($\dot{m}$) is set to zero at the beginning of the time by the initial condition.

(2) Determine the properties at t = Δt:

Gas phase properties

Using the source terms in the equations (4.2) and (4.3) and explicit method, determine the Y_k and T_g at each location for the next time step. With the ideal gas law, find gas phase density ρ by the ideal gas law (ρ= (P/RT)) at t = Δt. Since ρ at Δt is different from ρ at t = 0, find ($\partial\rho/\partial t$). Using the mass source term $\dot{w}_m'''$ and ($\partial\rho/\partial t$), find the gas mass flow rate $\dot{m}$ at t = Δt by the mass conservation equation (4.1).

Solid phase properties

With estimated gas temperature T at t = Δt, determine the heat transferred via convection to or from particle ($\dot{q}_{conv}$), the chemical heat liberated due to reactions at the coal particles ($\dot{q}_{ch,p}$) and radiative heat transfer ($\dot{q}_{rad}$) between particle and ambience within Δt using equations (4.14a), (4.16) and (4.15). Then, using equation (4.13), find particle temperature $(T_p)_{t=\Delta t}$. Determine the mass loss rate of the volatiles($\dot{m}_V$), mass loss rate of the trace species ($\dot{m}_{Hg}$ and $\dot{m}_{HCl}$) and the mass loss rate ($\dot{m}_C$) due to heterogeneous reactions within Δt using equations (4.13) and (4.10c). The particle diameter and density can be determined after ($\dot{m}_V$) and ($\dot{m}_C$) are known. Then, with

equation (4.4b), total mass loss rate is evaluated. Using the estimated total mass loss rate ($\dot{m}_p$) and equation (4.4), determine particle mass m_p at $t = \Delta t$.

Interpolate ρ_p, d_p and T_p for particles into nodal positions by using particle properties at Δt.

(3) Properties at $t = 2\Delta t, 3\Delta t$ ……., etc.

With knowledge of T_p at $t = \Delta t$, d_p at Δt, Y_k at $t = \Delta t$, $\dot{m} = \Delta t$, etc., repeat steps (1) and (2) for gas phase and solid phase properties.

5.2 Program Description

The overall organization of the generalized model is best understood by studying the program flow chart in Fig. 5.1, which illustrates the linkage between the various program subroutines. The main program controls the frequency and order of calling subroutines that comprise the general model. Program COALPILE is the main program. It reads the input variables, initializes the gas phase variables, steps in time and space, calls subroutines separately with a flag, order that data be read and processed and post processes the output data. Various subroutines may not be need and may be eliminated in a straight forward by simply setting the corresponding flag equal to 0. Such a technique was in the development of this generalized model and resulted in many useful entities such as: CHAR = 1 for char combustion model, IADIAB = 1 for adiabatic conditions and ISOLATE = 1 for isolated combustion model, etc. Since only the isolated coal particle combustion is involved in this dissertation, the program structure and subroutines for coal combustion are introduced in following sections. The subroutines

called in the main program for isolated coal particle combustion are ALPA, CLOMP, CLPROD, DELTOU, EQUATION, HCLOH, HGCL, HGCL2, HGPROD, HVVOL, MASSP, PRINTOUT, QFACT, RADN, SOURCE, STCVOL, THETAP, VELOCITY, VLCOMP, VOLFRAC AND VOLINT. More description of each of the subroutines and description of the input data are given in Appendix A.

5.3 Justification of Input Data for the Base Case

Justification for the values chosen for the base case is as follows.

The ambient temperature (TINF) was selected as 1500 K for ignition and combustion since this representative of typical experimental ambient temperature for the ignition and boiler burner temperature for combustion. A temperature of 300 K was selected for the for the particle temperature (TP0) since the gas film surrounding the particle was assumed to be approximately at same temperature as particle initially. The ambient oxygen mass fraction (YO2INF) and the initial oxygen mass fraction in gas phase were chosen as 0.23 since this is the oxygen mass fraction of air. The pressure (PRESS) was chosen to be atmospheric pressure. The coal mass fraction (C, H and O), trace elements (Hg and Cl), coal density (RHOP0), and the coal heating value (HCOAL) were selected to represent Wyoming Sub-bituminous coal. The initial particle diameter was chosen as 100 μm. Typical air properties were selected for the gas phase properties. The competing reaction pyrolysis kinetics was taken from [41]. The heterogeneous char oxidation kinetics were taken from [43]. The CO oxidation kinetics is used for the volatile oxidation kinetics and data was taken from [44, 45]. Mercury oxidation kinetics is taken from [23, 38].

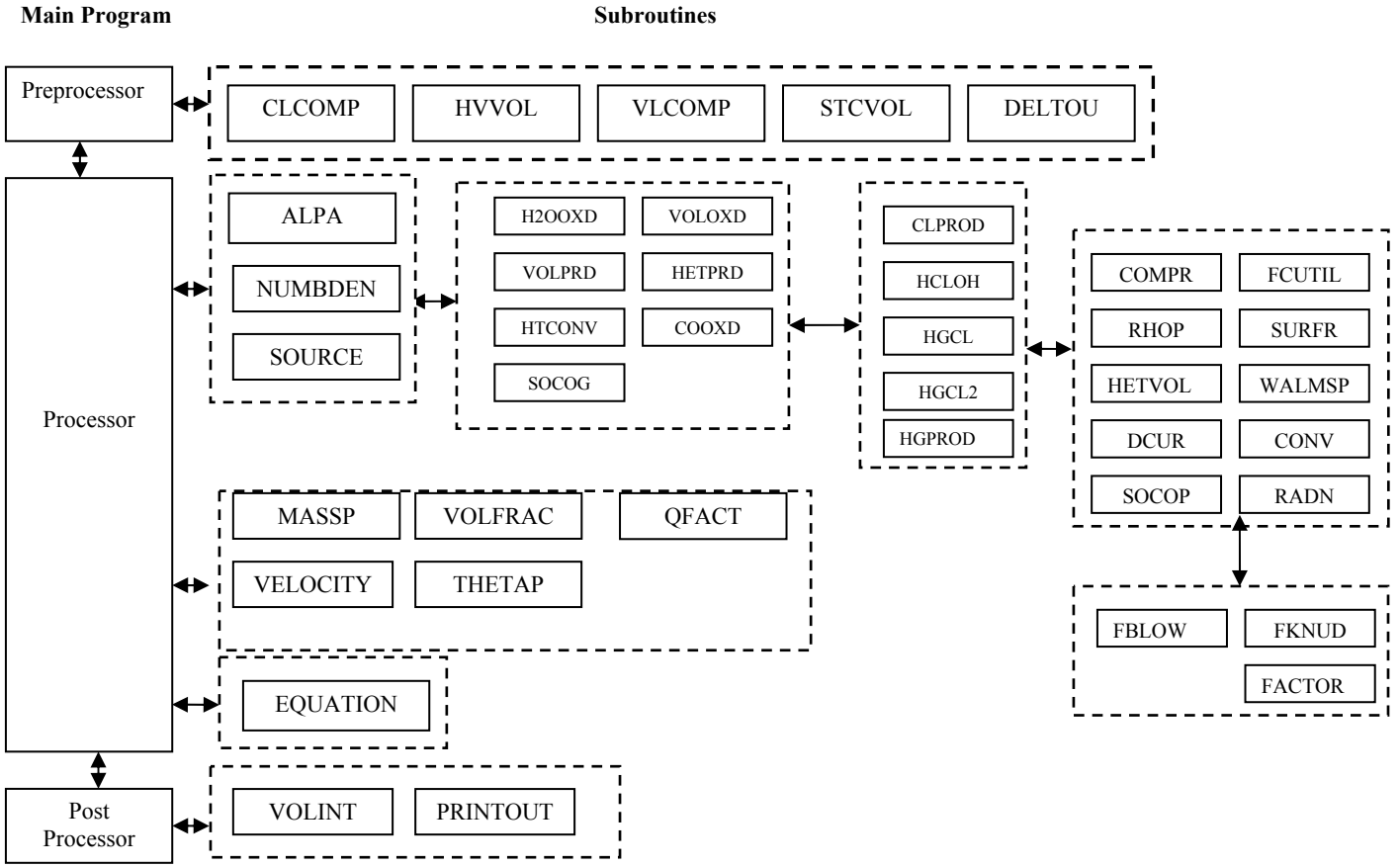

Fig. 5.1. Program structure

6 RESULTS AND DISCUSSION

6.1 Overall Coal Combustion Process

Prior to presenting the detailed results, the physical process occurring during the heat up, ignition and combustion of a isolated particle can described. Consider a single particle at $T \approx 300K$. As soon as the particle placed in a hot furnace, a thermal wave propagates into the particle. When the temperature of the particle reaches pyrolysis level, thermal decomposition occurs and the particle start releasing volatiles. If the local volatiles and oxygen concentrations and local temperature are such that a flammable mixture can be formed, the ignition occurs. Once ignited, the local temperature rises rapidly and subsequently a thin flame is formed. Combustion continues until all volatiles are consumed, then char combustion occurs. The schematic of the ignition and combustion process of a coal particle is shown in Fig 6.1.

In the next few sections, the results will be presented in the following order:

1. Equilibrium calculations
2. Mercury loading
3. Parametric studies
    - *Ambient Temperature*
    - *Chlorine content in fuel*
    - *Particle Diameter*
    - *Volatile matter*

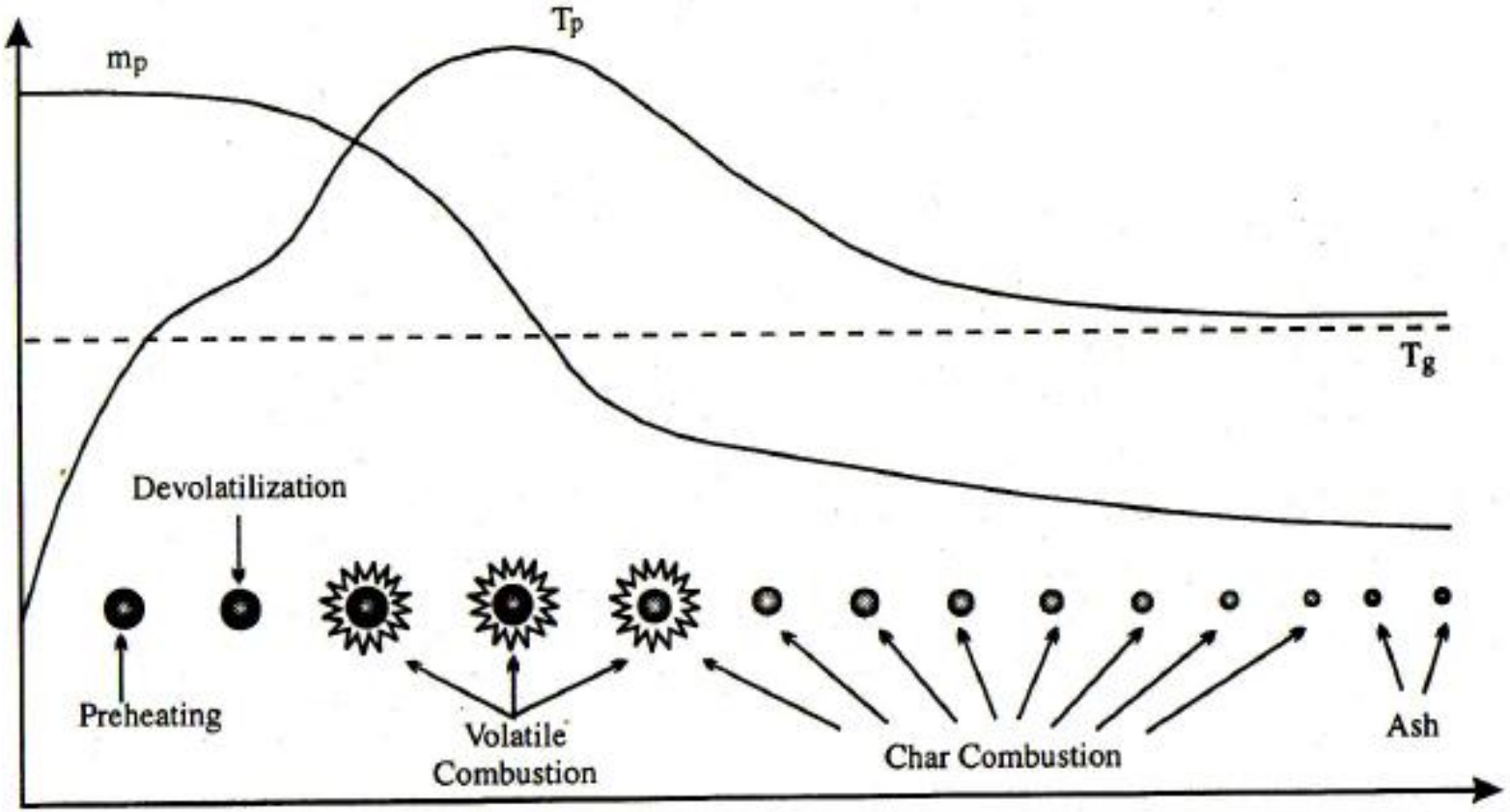

Fig. 6.1. Ignition and Combustion process of isolated coal particle [46]

- *Effect of changing kinetics*
- *Effect of blending with Feedlot Biomass, but heating the fuel as a single fuel particle with an equivalent Chemical formula.*
- *Effect of Varying Ambient Temperature and Oxygen concentration with time.*

6.2 Equilibrium Studies

The Chlorine chemistry wit Hg can be both heterogeneous and homogenous. Equilibrium calculations on distribution of mercury species in coal combustion flue gases has been calculated using equilibrium reactions. The calculations are done for three different equilibrium reactions. The three equilibrium reactions which are considered are:

$$Hg + Cl_2 \Leftrightarrow HgCl_2 \quad \text{I}$$

$$Hg + Cl_2 \Leftrightarrow HgCl + Cl \quad \text{II}$$

$$Hg + Cl_2 \Leftrightarrow ½\ HgCl + ½\ HgCl_2 + ½\ Cl \quad \text{III}$$

The concentrations of mercury and chlorine in the above equilibrium reactions are similar to the respective concentrations present in flue gas. The atomic concentrations of mercury and chlorine are 1.6E-08 and 1E-04 moles. The results are show in Fig 6.2. It can be inferred that almost all of the Hg is converted into $HgCl_2$ below 750 ^{0}K while HgCl is more dominant than $HgCl_2$ at higher temperatures. The amount of Hg oxidized depends on the amount of chlorine present in the coal. Mercury content of the coal has no control on the distribution of mercury species. The calculations demonstrated that the

gas phase equilibrium for mercury-containing species in coal-fired power plant exhaust may not valid at temperatures below 800^0K [16], since kinetic time scale could be longer due to lower temperature.. The most important for the oxidation of mercury in the post-combustion gases is the chlorine-containing species. It should be noted that equilibrium is not attained in flue gas due to fact that flue gas cools rapidly as heat is transferred from water to steam. The detailed equilibrium calculations are given in APPENDIX B.

6.3 Mercury Loading

Mercury loading is defined as the amount of Hg (kg) per Giga joule. The Hg in the exhaust gases is treated with chlorine. The amount of Hg left after the reaction helps in calculating mercury loading. Usually the volume of exhaust gases is typically 350 m^3/GJ. This value depends on the type of coal. It depends on H/C and O/C ratio. These ratios are calculated by finding out the empirical formula of the coal being used. Figure 6.3 shows the effect of chlorine concentration in coal on mercury loading at different temperatures. Excess chlorine is defined as $\left(Cl\ \ Con - Stoic\ \ Cl\ \ Con\right) \times 100 \Big/ Stoic\ \ Cl\ \ Con.$

From the graph it can be seen that an increase in chlorine concentrations has a positive effect on mercury loading at low temperatures. But at high temperatures, the high concentration of chlorine has no effect on mercury loading. Mercury loading is normalized with respect to initial concentration of coal. Mercury loading increases with increase in temperature. This is due to the reaction kinetics between mercury and chlorine, which are dormant at high temperatures. The analytical calculations of mercury loading are described briefly in APPENDIX B.

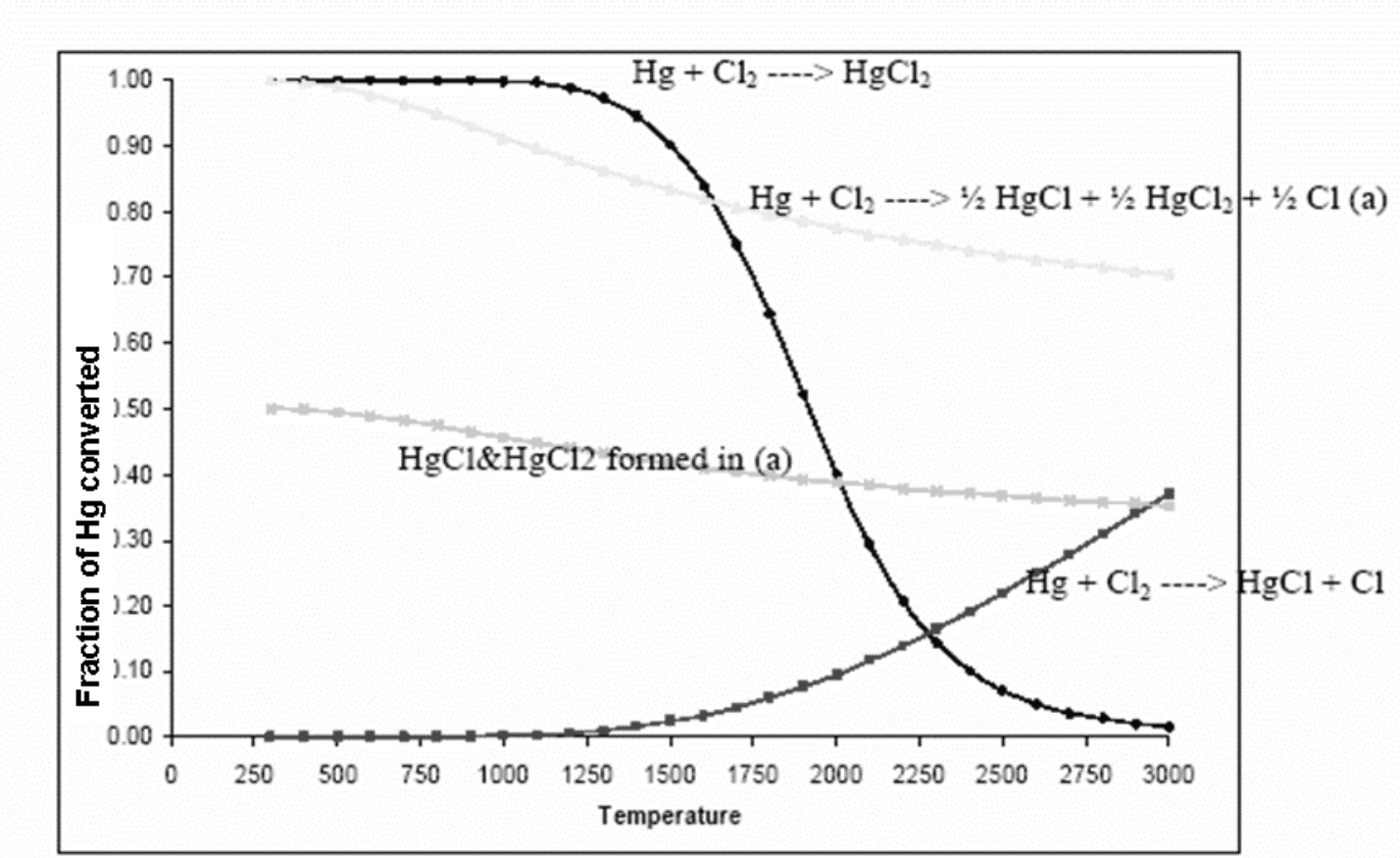

Fig. 6.2. Equilibrium mercury speciation in flue gas as a function of temperature (atomic concentrations of Hg and Cl are 1.6E-08 and 1E-04 moles)

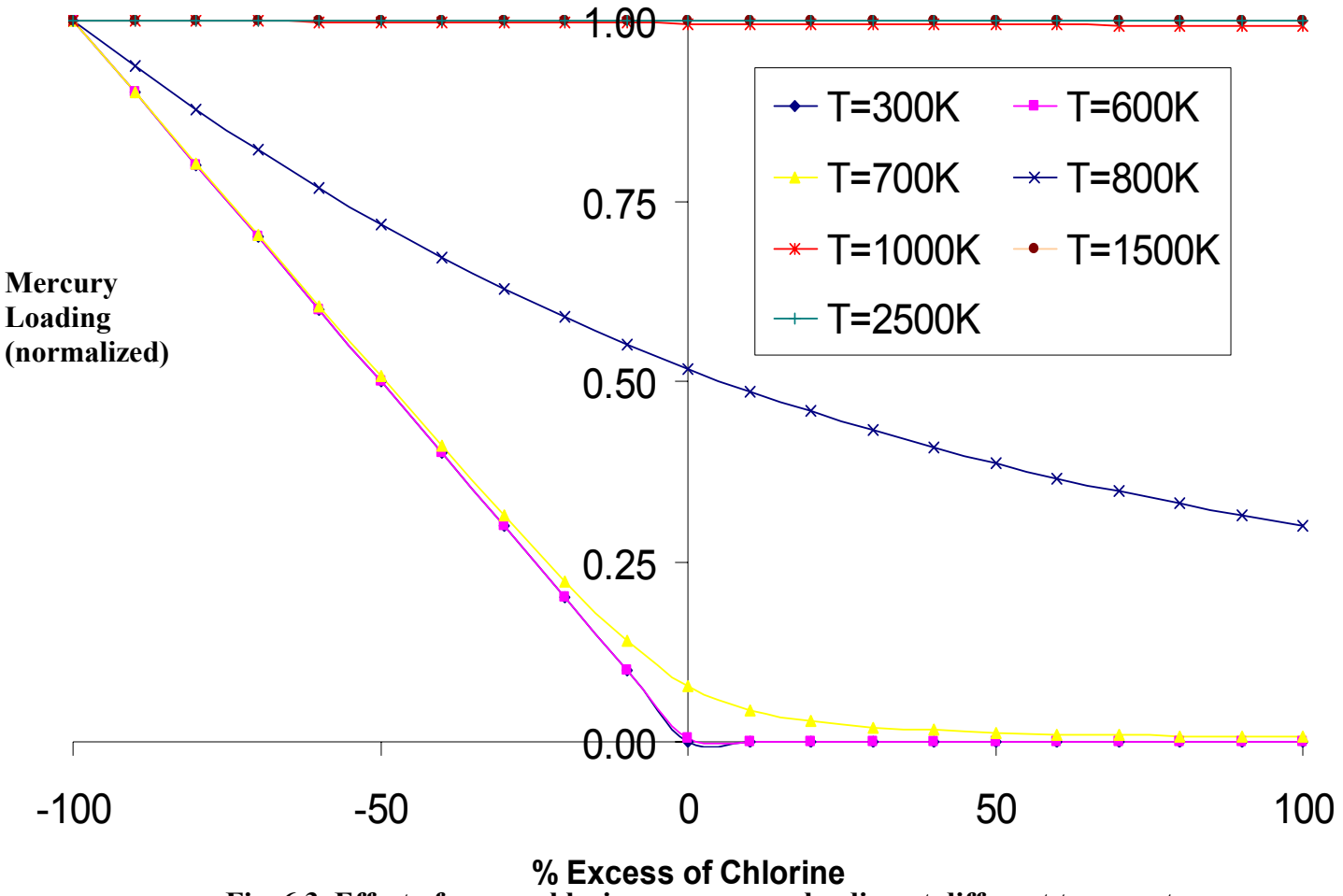

Fig. 6.3. Effect of excess chlorine on mercury loading at different temperatures

From the equilibrium and mercury loading analysis, it can be inferred that temperature and concentration of chlorine play an important role in mercury and chlorine chemistry. So, in order to control mercury emissions from coal fired power plants, the above said parameters, have a vital part to participate how mercury behaves in the coal fired boilers.

6.4 Global Oxidation Reaction Mechanism

Different parameters have been considered to study their effect on the mercury and chlorine oxidation. For the base case Wyoming Sub-bituminous coal is considered. Analysis is also done to study the mercury oxidation behavior when the above fuel is blended with fuels like Feedlot Biomass. The proximate and ultimate analyses of the fuel are given in Table 6.1.

Firstly attempts have been made to two different global oxidation reaction mechanism have been considered for numerical simulation. The two different global reactions which are considered are given below:

$$Hg + Cl_2 \rightarrow HgCl_2 \qquad \text{(IV)}$$

$$Hg + 2HCl \rightarrow HgCl_2 + H_2 \qquad \text{(V)}$$

For the above two global reactions, it was assumed that the pyrolysis product of coal results in release of Cl_2 for (IV) and HCl for reaction (V). The kinetics for the reactions has been taken from [16]. The simulations are carried at ambient temperature 1500K. Figures 6.4 and 6.5 shows the effect of different chlorine concentration on mercury oxidation at different time steps for the two different global mercury oxidation with chlorine (IV) and (V) respectively. It can be seen that the amount of mercury converted

Table 6.1

Proximate and ultimate analyses of the fuel

	Wyoming	Feedlot Biomass FB	Wyoming - Biomass(90:10)	Wyoming - Biomass(80:20)
Proximate (%)				
Volatile	49.38	81.84	52.63	55.87
Fixed C	50.62	18.19	47.38	44.13
Ultimate (%)				
Carbon	74.06	52.55	71.91	69.76
Hydrogen	4.40	6.35	4.60	4.79
Nitrogen	1.35	4.71	1.69	2.03
Sulfur	1.22	1.03	1.20	1.18
Oxygen	19.14	35.36	20.76	22.39
Chlorine (ppm)	140	9096	1089	1979
Mercury (ppb)	120	6	108	97
HHV(kJ/kg)	23200	7861	21639	20108

to mercury chloride is negligible. Even though the conversion is not much, but at fixed chlorine concentrations, the mercury oxidized increases with time. This is due to favorable temperatures towards the end of combustion process in the gas phase. When the chlorine concentration is changed from 50ppm to 176ppm, there is considerable change in mercury conversion relatively, even though on a larger picture, the amount of mercury converted is not noticeable.

From the above results obtained from the numerical simulations carried out by implementing the global oxidation reactions, it can be understood that global oxidation does not appear to provide a feasible reaction mechanism for the mercury oxidation mercury. The OH and Cl radicals seem to promote Hg oxidation. In combustion process high temperatures regions occur, which produce OH and Cl radicals. Hence, a three step reaction mechanism has been implemented. The reaction mechanism is mentioned in Section 4, Table 4.1. Equilibrium reaction chemistry is considered for H_2O which breaks down into OH and ½ H_2. The radicals which are more reactive will help in the formation of atomic chlorine. The OH radical formed during equilibrium results in atomic chlorine when reacted with HCl. This atomic chlorine sets the rate oxidation of mercury. Note that the CO oxidation requires OH. Since the concentration of Hg and Cl is very small, the OH consumption by CO is not expected to affect the Hg oxidation magnificently.

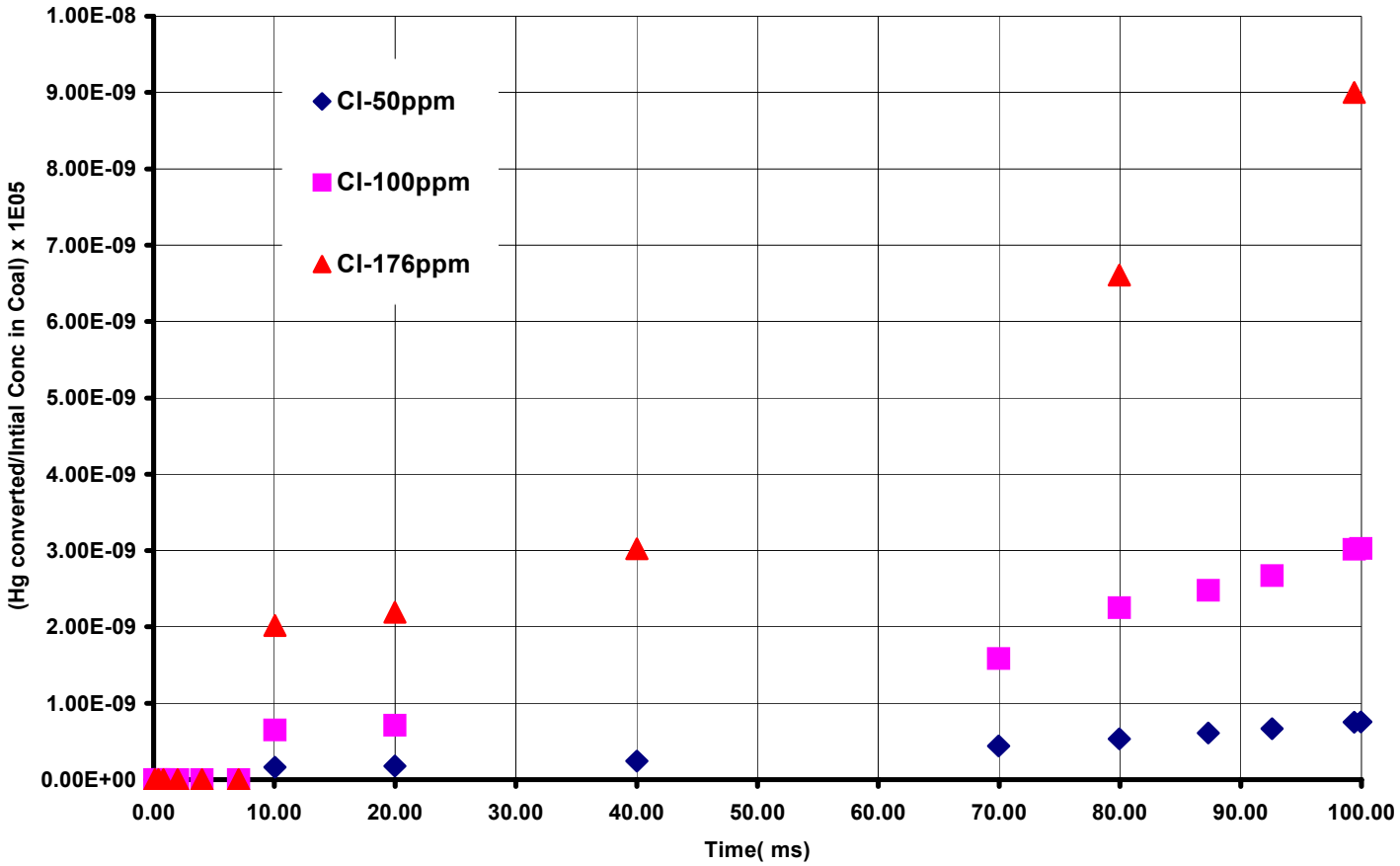

Fig. 6.4. Mercury oxidized, $Hg + Cl_2 \rightarrow HgCl_2$

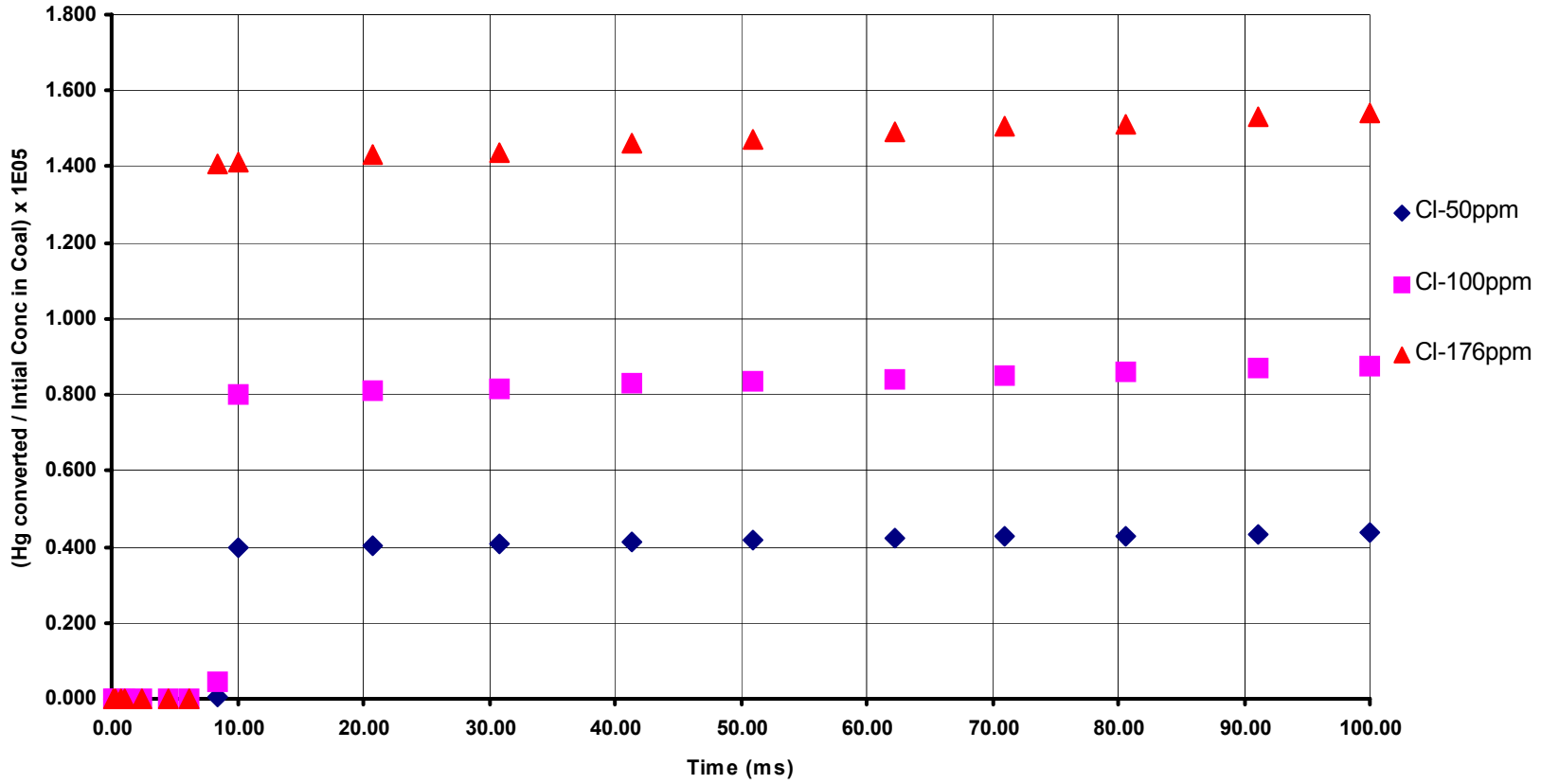

Fig. 6.5. Mercury oxidized, $Hg + 2HCl \rightarrow HgCl_2 + H_2$

6.5 Parametric Studies

The base case for the proposed study will be Wyoming Sub-bituminous Coal of diameter 100 μm initially at 298 K and suddenly exposed to an ambient temperature of 1500 K and O_2 concentration of 23% (by mass) with Hg and Cl concentration at 120 ppb and 140 ppm. The proximate and ultimate analyses of the coal are given in Table 6.1. The base case data used in this study and the values assigned to each input variable for the base case are given in Table 6.2.

Table 6.2

Base case data and kinetics data

Data Card 1: Ambient Data

Variables	Values	Units
TINF	1500.00	K
YO2INF	0000.23	
YCO2IN	0000.00	
YCOINF	0000.00	
YVlINF	0000.00	
YV2INF	0000.00	
YH20INF	0000.00	
TGCO	0300.00	K
TPO	0300.00	K
YO2CO	0000.23	

Table 6.2 continued

PRESS	0001.00	bars
PGSAT	0000.03	bars
Data Card 2: Coal Data		
Variables	Values	Units
C	0.7568	
H	0.0443	
N	0.000	
O	0.1873	
Hg	120	ppb
Cl	140	ppm
ASH	0.0	
HCOAL	30.0	MJ/kg
Data Card 3: Particle Size		
Variables	Values	Units
DPO(1)	100 E-06	m
NPS(I)	1	
RHOPO(1)	1300.00	kg/ m^3
Data Card 4: Competing Reaction Pyrolysis Data		
Variables	Values	Units
VM(1)	0.464	
VM(2)	0.800	

Table 6.2 continued

EV(1)	1.34E05	s^{-1}
EV(2)	1.46E05	s^{-1}
BV(1)	74.10	MJ/kmol
BV(2)	251.00	MJ/kmol
HPYR(1)	-837.00	kJ/kg
HPYR(2)	-1670.00	kJ/kg

Data Card 5: Char Kinetics Data

Variables	Values	Units
EC(1)	6.64 E04	kJ/kmolK
EC(2)	0.0	kJ/kmolK
EC(3)	1.09E05	kJ/kmolK
EC(4)	0.0	kJ/kmolK
NO21	1.0	
NO22	1.0	
NCO2	1.0	
NH2O4	1.0	
BC(1)	450.00	m/s
BC(2)	0.0	m/s
BC(3)	390.00	m/s
BC(4)	0.00	m/s

Table 6.2 continued

Data Card 6: CO-oxidation Kinetics Data

Variables	Values	Units
ACO	5.0E9	m^3/kgs
ECO	1.26E05	kJ/kmolK
NCO	1.0	
NO2CO	0.5	
NH2OCO	0.5	
ACOB	1.5715E13	
ECOB	3.9416E05	

Data Card 7: Volatiles Oxidation Kinetics Data

Variables	Values	Units
AVG	5.0E09	m^3/kgs
EVG	1.26E05	kJ/kmolK
NV	1.0	
N02V	1.0	

Data Card 8: Mercury Oxidation with Chlorine radical

Variables	Values	Units
AHCl	7.43E02	m, kmol,sec
EHCl	-920.7	kJ/kmol
NHCl	1.0	
NOHHCL	1.0	

Table 6.2 continued

AHG	1.19E03	m, kmol,sec
EHG	-60289.0	kJ/kmol
NHG	1.0	
NCLHG	1.0	
AHGCL	9.28E12	m, kmol, sec
EHGCL	12979.0	kJ/kmol
NHGCL	1.0	
NCLHGCL	1.0	

Data Card 9: Numerical Data

Variables	Values	Units
XIMAX	1.0	
FNXI	31 0	
DTEMPL	3.0	
DTGLMT	20.0	
DTPLMT	2.0	
DTSET	1.0E-03	
FBO	0.01	

Data Card 10: Program Control Data

Variables	Values	Units
ICHAR	0	
IFREEZE	0	

Table 6.2 continued

IOXDV	1
IOXDCO	1
JFLAG	0
IVOLS	0
ICOVOLS	0
INSTCO	0
INSTV	0
NSIZE	1
NITERN	9,999,999
ISTEP	10,000
ISPACE	11
IPRINT	1
IMETHD	1
LSTART	1
IADIAB	0
IIGN	0
INOX	0
IADHEAT	0
IPEAK	0
ICOORD	3
IEQUIL	1

Table 6.2 continued

IEXPAN	1	
ISOLATE	1	
Data Card 11: Free Stream Gas properties		
Variables	Values	Units
RHOD	5.0E-05	kg/ms
CP	1.18	kJ/kgK
LAMBDA	5.9E-05	kW/mK
NU	2	
FREEL	4.1 E-09	m

6.5.1 Effect of Ambient Temperature

The coal particle travels through different temperature regions as it burns in the boiler. This parameter study was conducted at different ambient temperatures on mercury oxidation. From the equilibrium studies conducted, it has been inferred that temperature is crucial when mercury and chlorine reactions are involved. For the base case, the ambient temperature is 1500 K, where the concentration of mercury and chlorine are 120 ppb and 140 ppm, the percentage of the mercury oxidized to mercury chloride is 9% shown in Fig 6.6. When the ambient temperature is reduced to 950K, the percentage of mercury oxidized is increased to 25%. On the other side, when the ambient temperature is increased to 2000 K, the mercury oxidized percentage dropped. This is possible due to two effects i) kinetics of the reactions and ii) reduced combustion

time. Two of the three reactions which are used to simulate the mercury oxidation have negative activation energy. The burning time for the gas phase combustion for different temperatures is plotted in Fig 6.7. Burning time is reduced from 1.8 s to 0.2 s as ambient temperature is increased from 900 K to 1200 K. In order to understand the effects of kinetics and combustion times, the characteristic half time scales are plotted in Fig 6.8.

From these results, it can be understood that even in real time cases, where equilibrium reactions are not feasible, temperature is important factor which determines the extent of mercury oxidation.

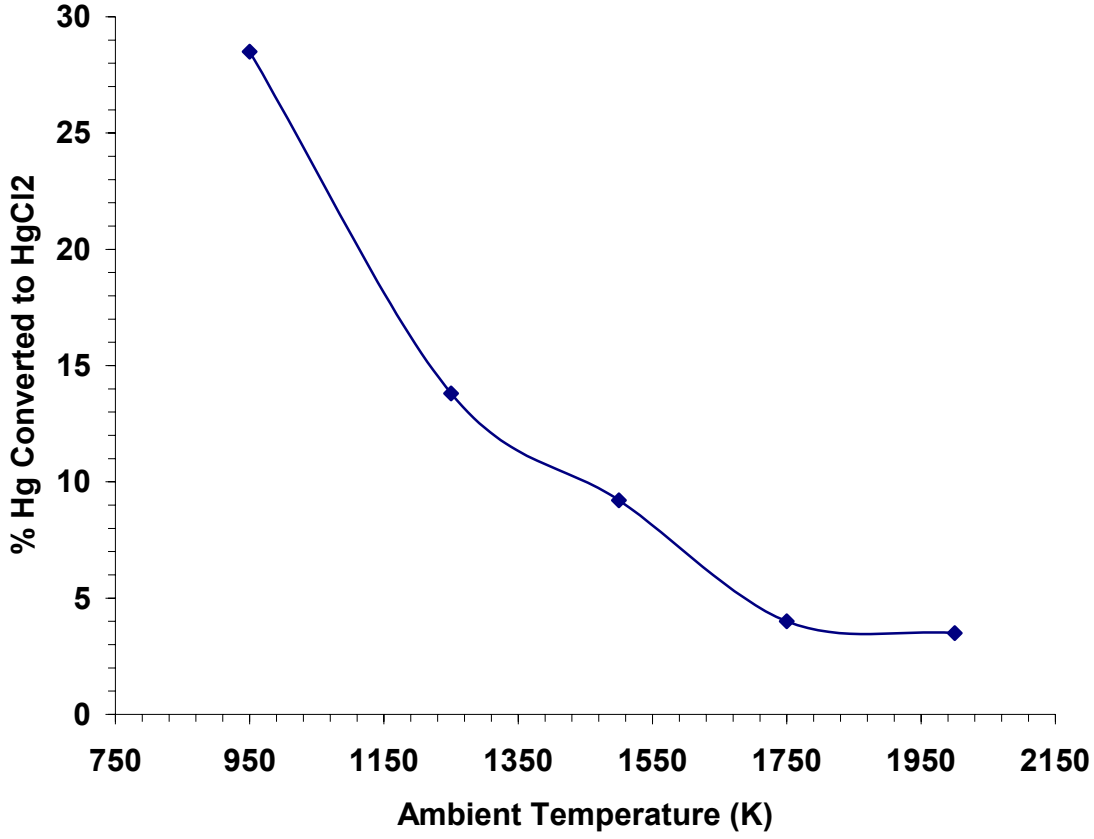

Fig. 6.6. Variation of mercury oxidation with ambient temperature

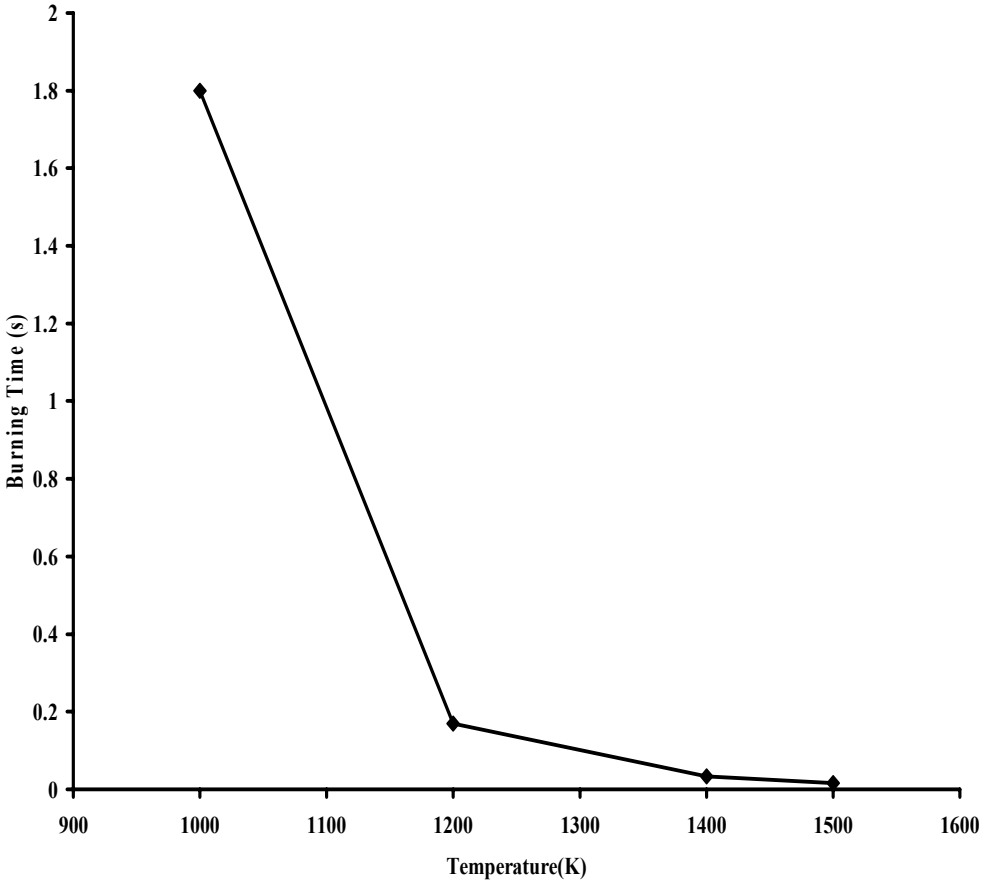

Fig. 6.7. Burning time (s) at different temperatures

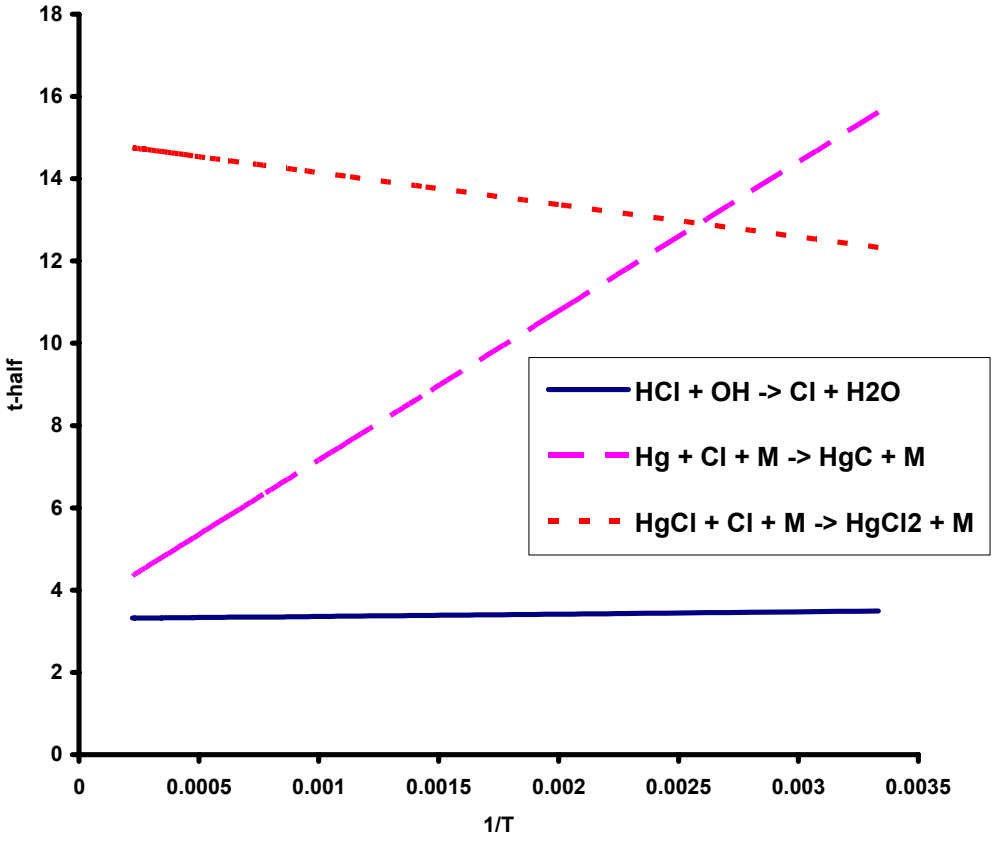

Fig. 6.8. Characteristic half time scales

6.5.2 Effect of Chlorine Concentration

The initial amount of chlorine in coal depends on the coal type. Usually, lignite and sub-bituminous coals have less amount of chlorine when compared to bituminous coal. The whole thought of considering chlorine concentration as one of the parameter is that chlorine concentration has considerable effect on mercury oxidation when it exists in adequate amount. Numerical simulations are done by varying concentration of chlorine in coal from 50 ppm to 1000 ppm keeping other concentrations of elements constant including mercury. This results in increasing the concentration of chlorine species in flue gases.

Figure 6.9 shows the effect of change of chlorine concentration on mercury oxidation. From the figure, mercury oxidation increases with the increase in chlorine concentration. One of the assumptions considered for the pyrolysis of chlorine is that the release rate is in proportion with volatiles release rate and all of the chlorine initially present in coal is released during pyrolysis. Figure 6.10 shows the fraction of chlorine in volatiles at the end of pyrolysis for different chlorine concentration in coal. For the base case, where the chlorine concentration is 140ppm, the percentage of mercury oxidized is around 7%. At really high concentrations around 1000ppm more than 50% of mercury is oxidized. Even though the experimental results for the mercury emission from isolated coal particle are sparsely available, various experimental data on mercury emission shows that the increase of chlorine concentration in flue gases results in increase in mercury oxidation [17].

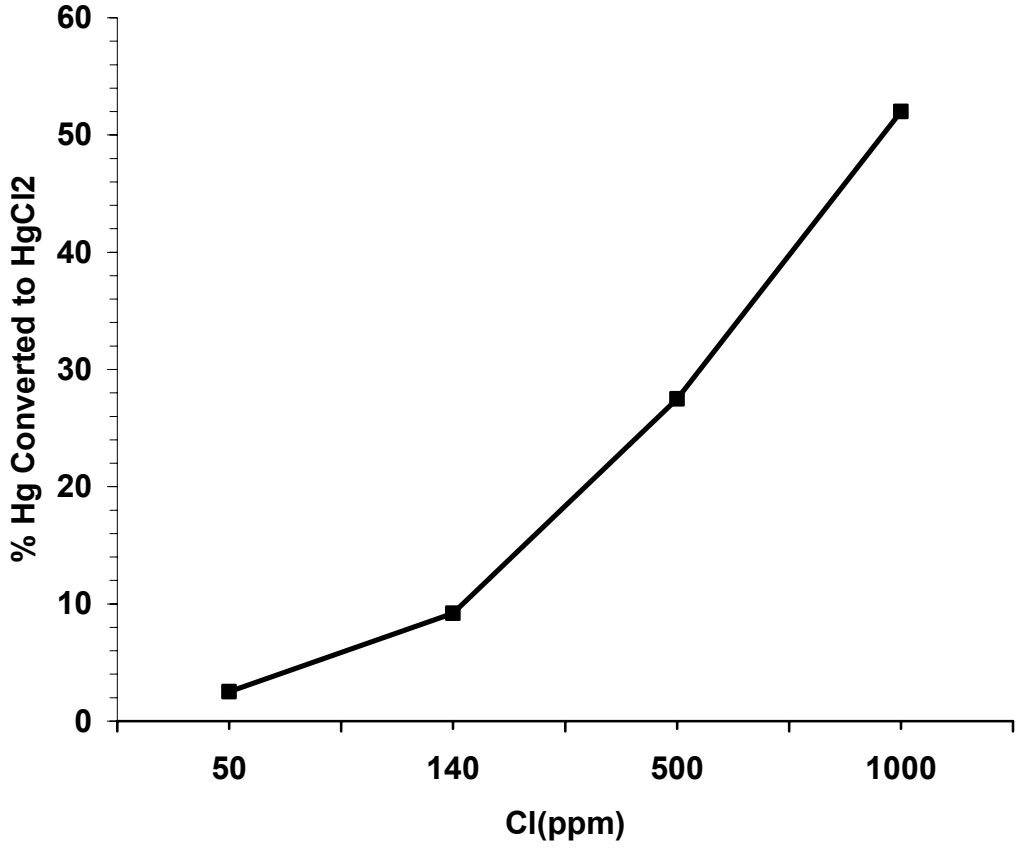

Fig. 6.9. Effect of chlorine concentration on mercury oxidation

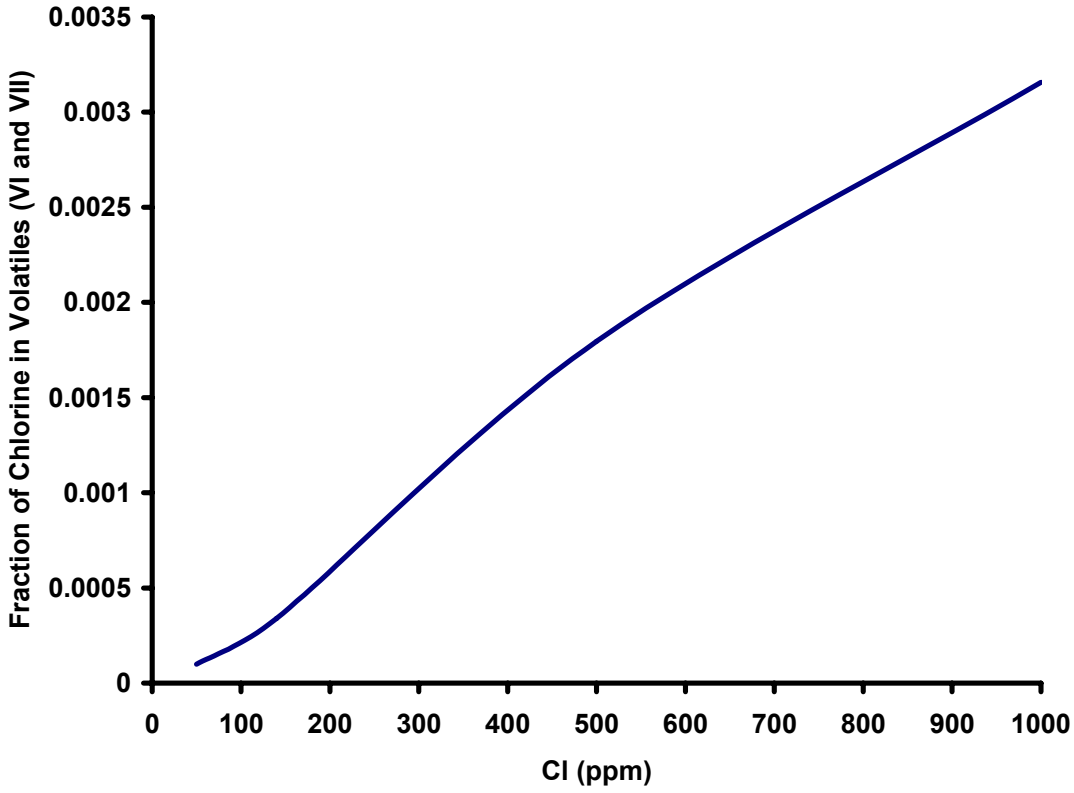

Fig. 6.10. Varying fraction of chlorine in volatiles with chlorine concentration

6.5.3 Effect of Particle Diameter

The effect of particle size on mercury oxidization is studied. Usually, the pulverized coal has a particle size distribution. In this study, since it is a isolated coal particle study, particle size distribution is not considered. But, some of the values of the diameter of the coal particle have been considered to be the Sauter mean diameter (SMD) of the particle size distribution. Fig 6.11 shows that when particle size is decreased, the amount of elemental mercury oxidized is also reduced. When the size of the particle is increased,

increased time is available for reaction which results in an increased mercury oxidation. Fig 6.12 shows the variation of characteristic diffusion time scales with particle size.

When the diameter of the coal particle is increased, the particle takes more time to release volatiles (including trace elements chlorine and mercury) as the particle gets heated slowly when compared to smaller size particle. This slow process of releasing volatiles and longer diffusion time gives more time for the reactions to occur. Further volume of reaction zone scales as d^3 and hence larger particle provides more reaction volume and less residence time.

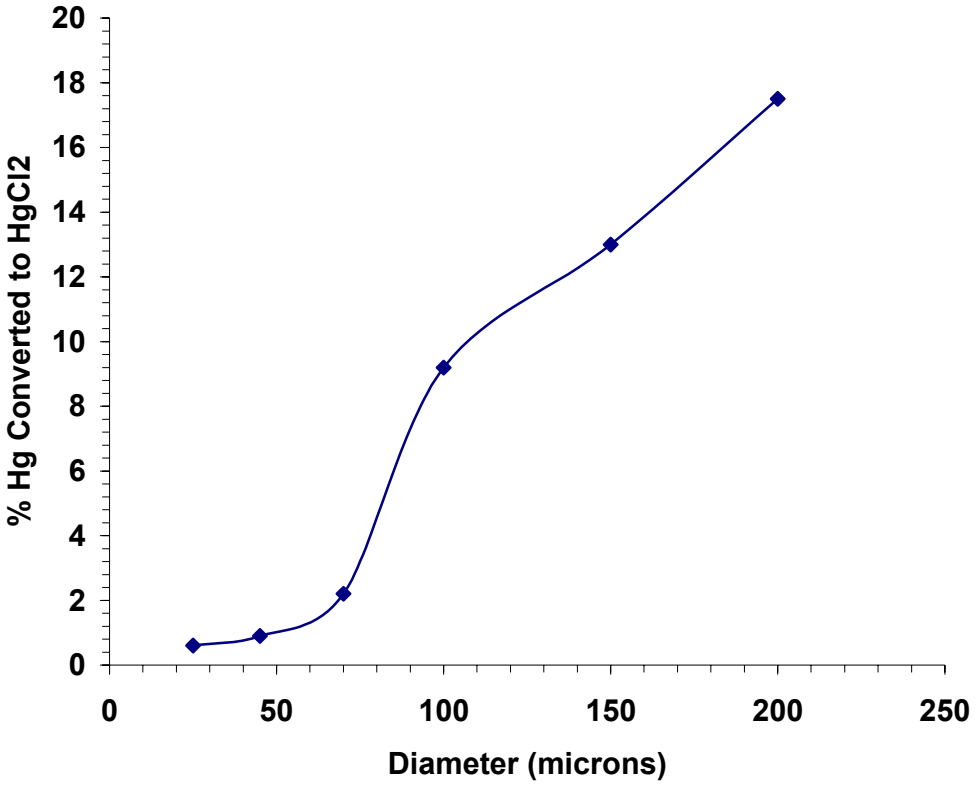

Fig. 6.11. Effect of particle size on mercury oxidation

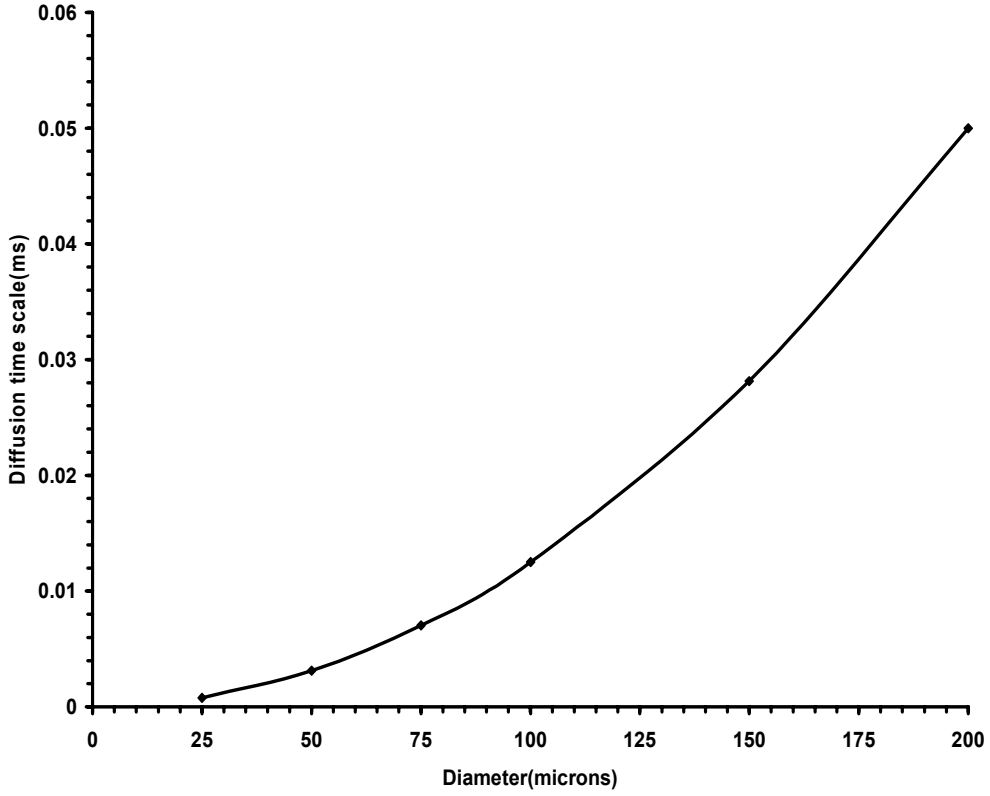

Fig. 6.12. Variation characteristic diffusion time with diameter

6.5.4 Effect of Volatile Matter

Numerical simulations are performed by varying the proximate volatile matter present in the coal. For the pyrolysis process, competing reaction model is considered. The values of V_I are varied from 30% to 80%. The value of V_{II} is kept constant 80%. The effect of the volatile matter on mercury oxidation is studied.

According to the competing reaction model, there are two reactions proceeding simultaneously and competing for hydrogen atoms. One reaction follows a low

temperature path and other one follows the high temperature. Due to this reaction model, the total volatile yield will be more than the proximate volatile matter. Figure 6.13 shows the Q factor for two different particle sizes, 25μm and 100μm for varying proximate volatile matter. The Q factor is defined as the ratio of total volatile yield produced by the two reactions to the volatile yield produced by following low temperature reaction path (V_I). From the figure, it can be seen that the Q factor for the smaller particle is size is more than 2.0 at lower proximate volatile matter. This shows that for smaller size particles, even though for less proximate volatile matter, by the end of pyrolysis, the total volatile yield is twice that of proximate. This is because smaller particles have a higher heating rate, due to which they follow the high temperature reaction path (V_{II}) and release more volatiles. Figure 6.14 shows the variation of total volatile yield with respect to proximate volatile matter for two different particle sizes.

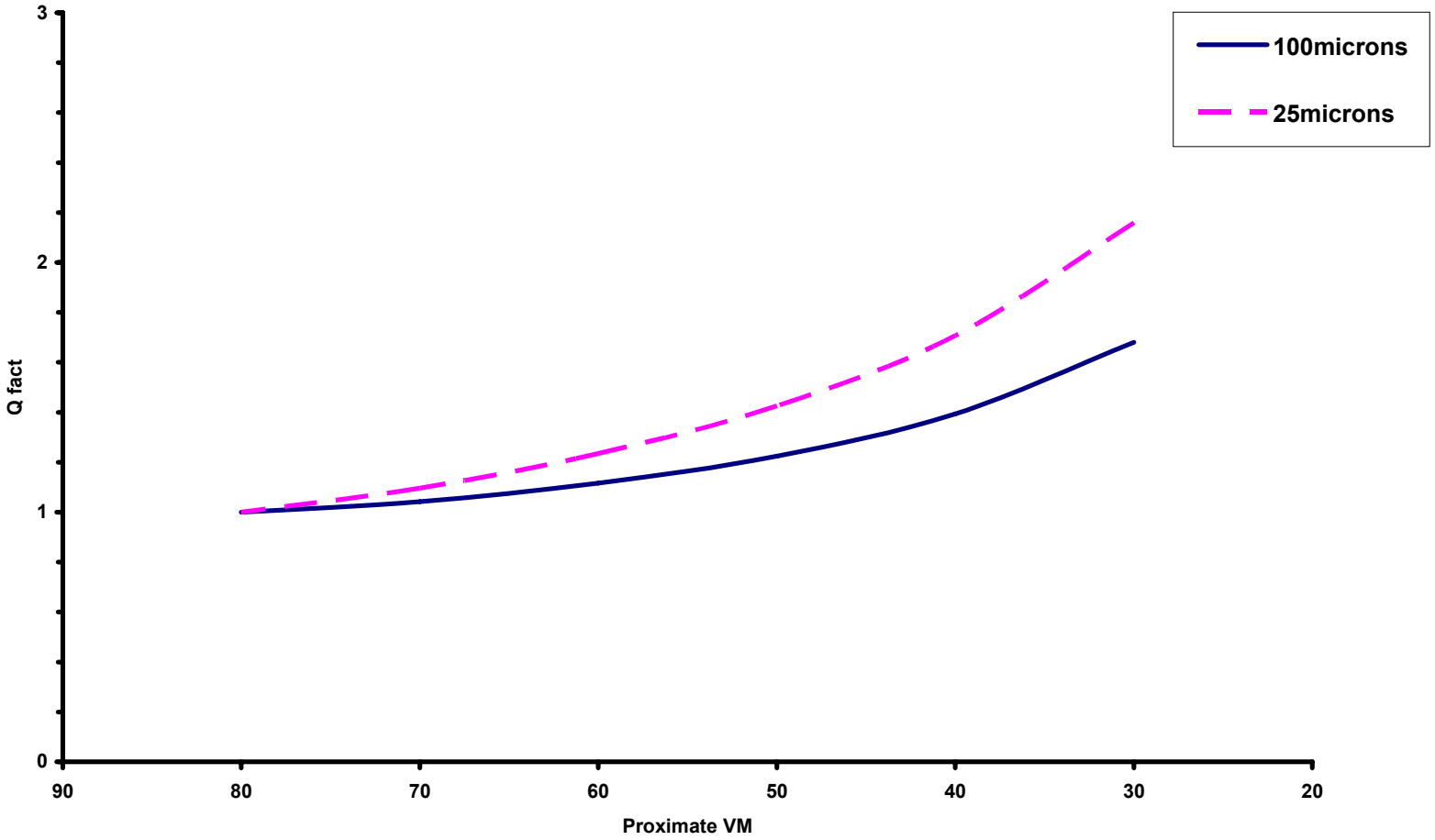

Fig. 6.13. Variation of Q factor with proximate volatile matter

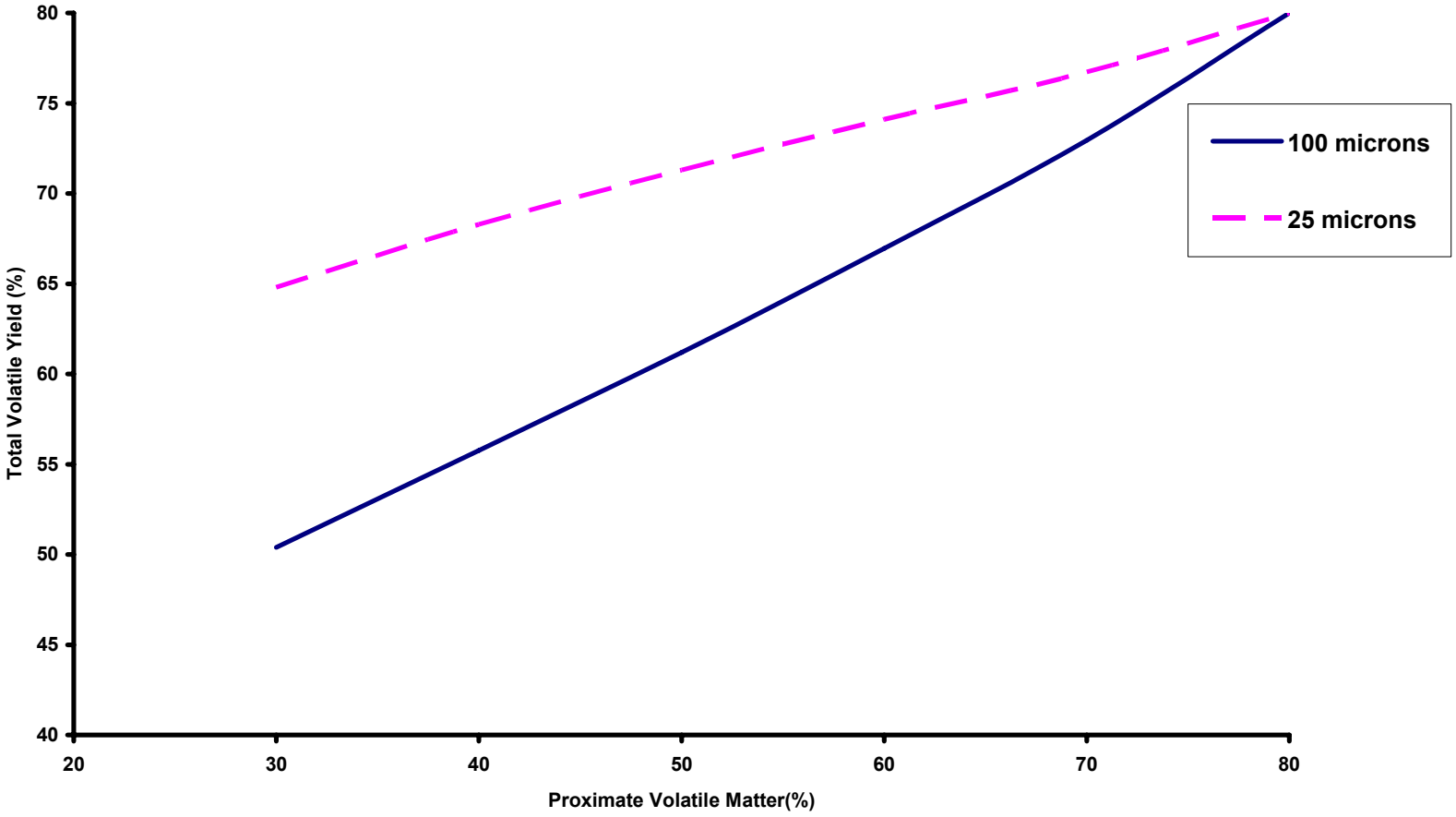

Fig. 6.14. Variation of total volatile with proximate volatile matter

Figure 6.15 shows the effect of volatile matter on mercury oxidation. There is very minor change in mercury oxidation when the proximate volatile matter is changed for a given particle size. In the model, it has been assumed that mercury and chlorine follow devolatilisation kinetics during pyrolysis. They are released in proportion with volatiles and are released completely into the gas phase by the end of pyrolysis.

Figure 6.16 shows the mass fraction of chlorine at the particle surface for varying volatile matter. From the graph, it can be seen that initially the chlorine released in the gas phase increases and later when the there is no chlorine release, the slope gradually decreases due to diffusion and consumption in gas film surrounding the particle. Even though, the model assumes that release of chlorine depends on the volatile kinetics and volatile matter present coal, but from the results obtained show that volatile matter does not show much effect on the amount of chlorine release with respect to time.

Similarly Fig 6.17 shows similar trend for mass fraction of mercury at the particle surface with respect to time for varying proximate volatile matter.

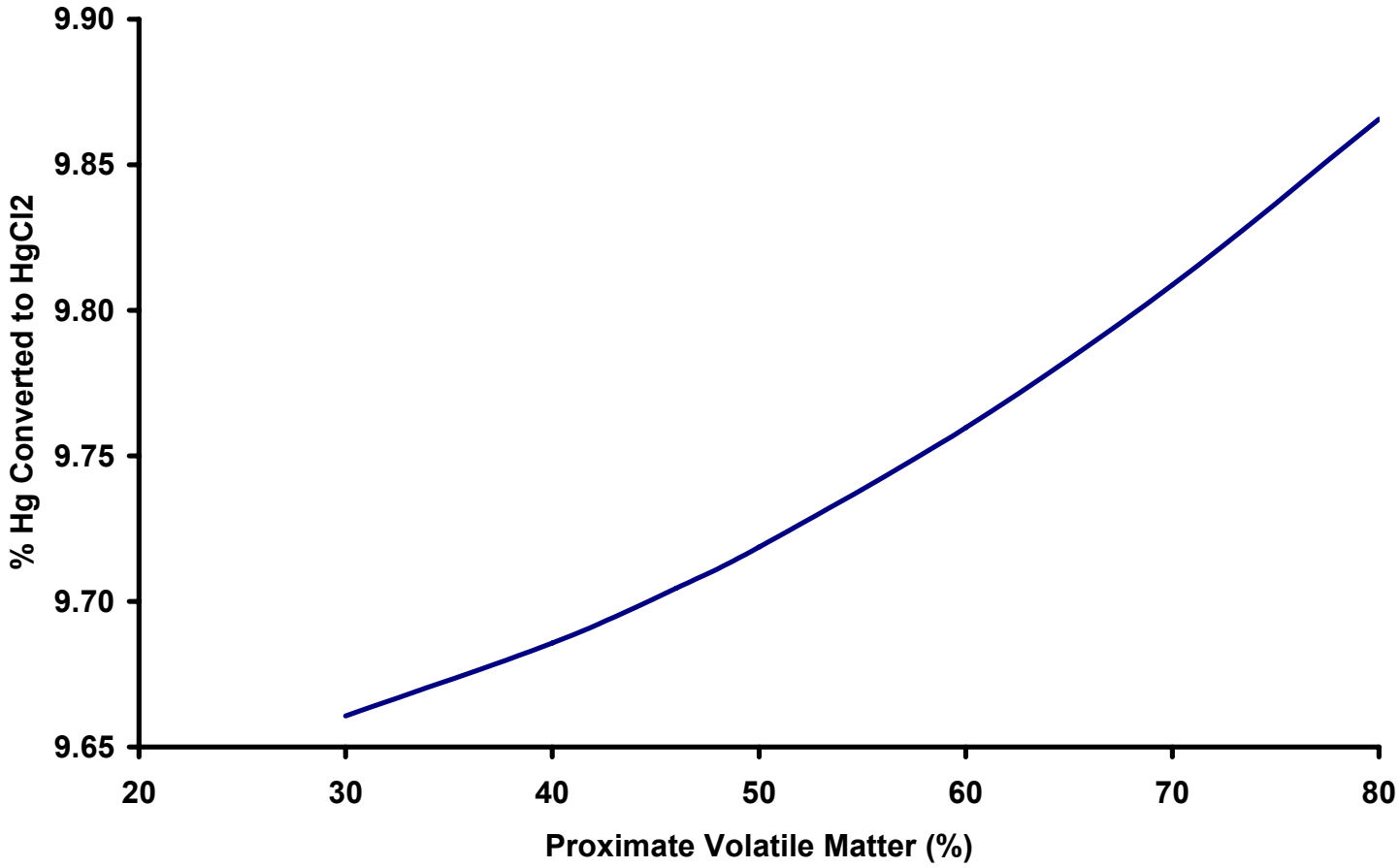

Fig. 6.15. Effect of proximate volatile matter on mercury oxidation

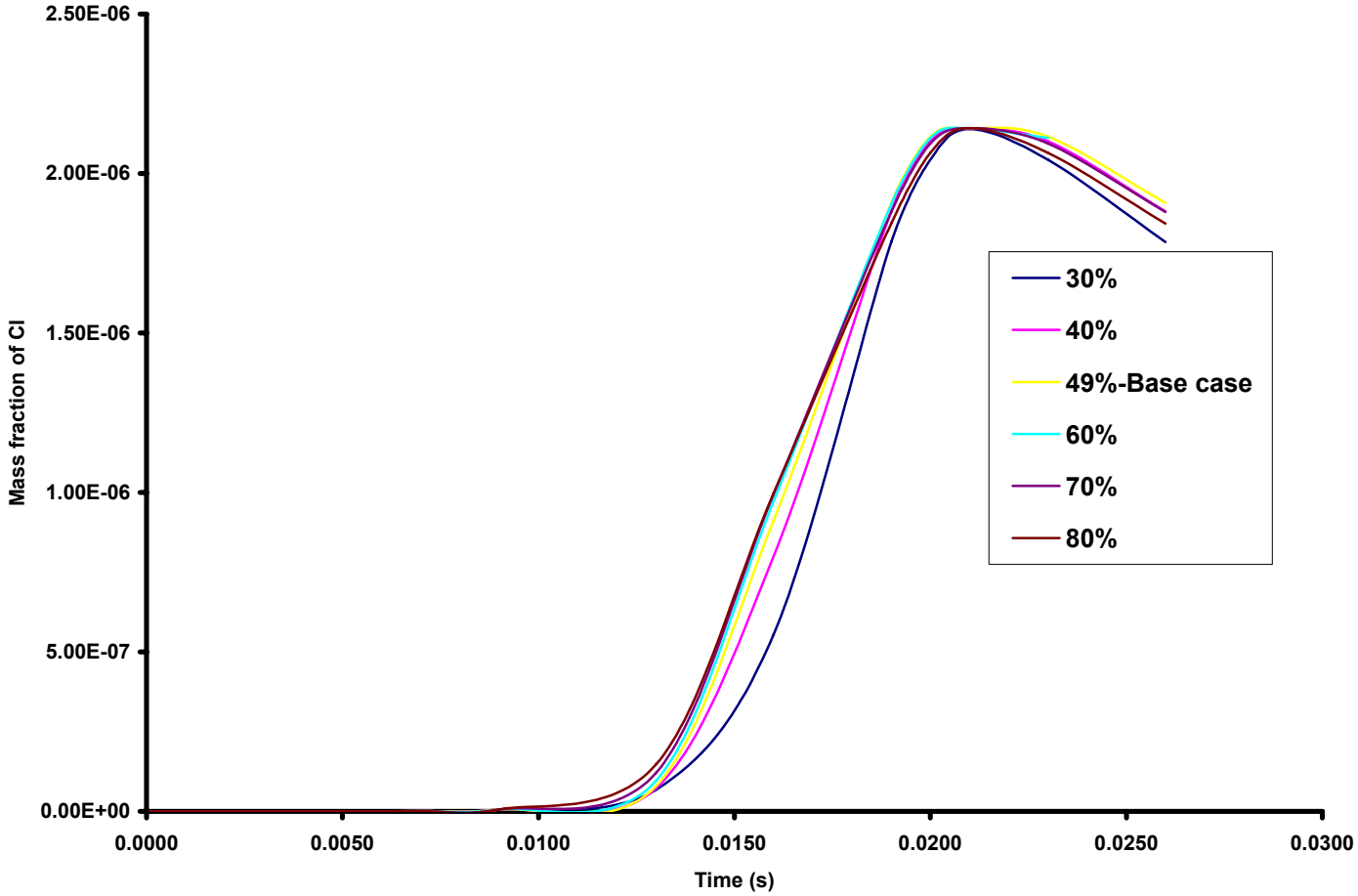

Fig. 6.16. Mass fraction of chlorine at particle surface for different volatile matter

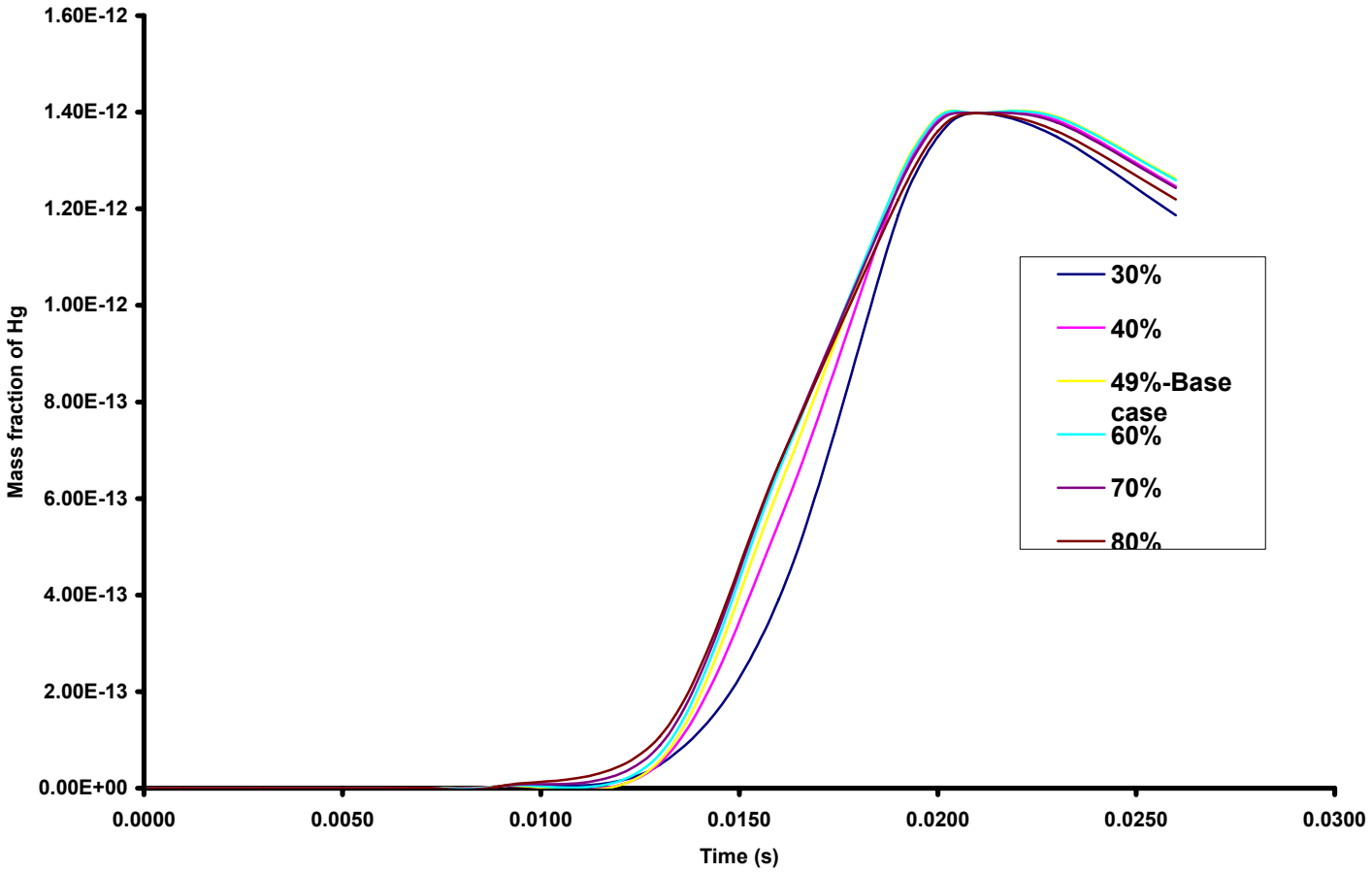

Fig. 6.17. Mass fraction of mercury at particle surface for different volatile matter

6.5.5 Effect of Kinetics of Reactions

The sensitivity of the results on the chemical kinetics was investigated by changing pre-exponential term in the Arrhenius equation for the mercury oxidation reaction mechanism. The reaction mechanism is mentioned in Table 4.1 of Section 4.

The effect of chlorine radical kinetics (Table 4.1, Reaction VIII) was investigated by dividing the pre-exponential factor (A_{HCl}) by 10 and then increasing by 10. Figure 6.18 shows the results. The percentage of mercury oxidized to mercury chloride is reduced by 3% compared to the base case when A_{HCl} is reduced. This is a result of the decrease in the production of chlorine radical species. The chlorine radical is the most significant species in the flue gases which assists in formation of mercury chloride. Enhancing the chlorine radical kinetics by a factor of ten (A_{HCl}x10) results an increase in the percentage of mercury oxidized by 4%.

6.5.6 Effect of Blending Coal

For the present numerical simulations, dry ash free Wyoming Sub bituminous coal is considered as base case. The composition of coal on DAF basis is given Table 6.1. It is noted that VM %, and Cl are higher for FB compared to coal. Thus for coal:FB blend more the % of FB in the blend, more the % of Cl in blend. Blending coal with feedlot biomass is considered in order to study their effect on mercury speciation. The deduced empirical chemical formulae for fuel and volatiles V_I and V_{II} are shown in Table 6.3.

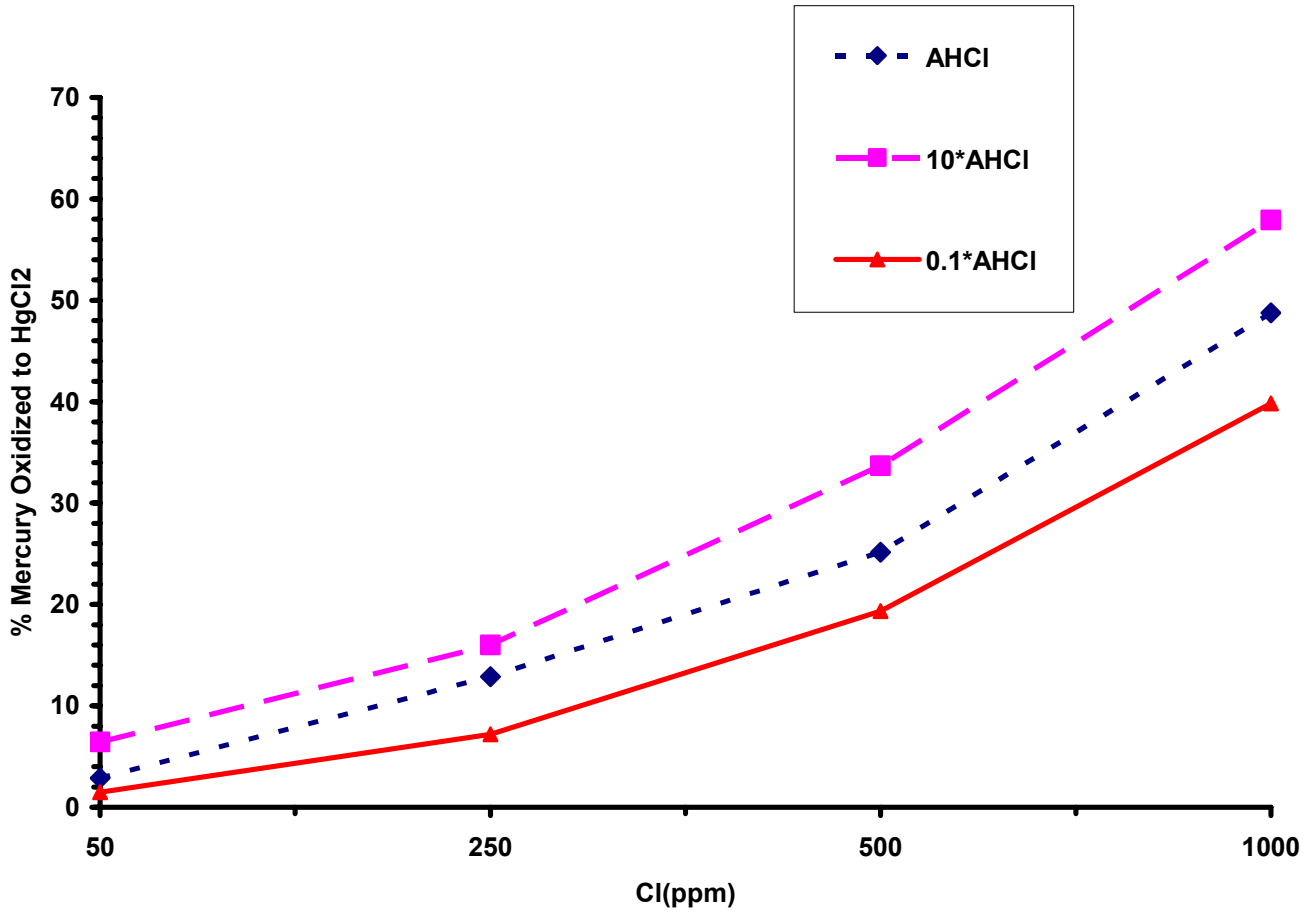

Fig. 6.18. Effect of chlorine radical kinetics on mercury oxidation

It is known from the literature studies that increase in chlorine concentration in flue gases will result in increase oxidation of mercury. The FB has much higher VM, higher Cl, lower HV compared to Wyoming. Coal is blended with FB in the ratios of 90:10 and 80:20. The chlorine concentration in blend increases with increase in % FB.

Table 6.3

Empirical formulae for the coal, blend and volatiles

	Wyoming	**Wyoming-FB(90:10)**	**Wyoming-FB(80:20)**
Fuel	$CH_{0.7}N_{0.015}O_{0.194}S_{0.006}$	$CH_{0.76}N_{0.020}O_{0.21}S_{0.006}$	$CH_{0.82}N_{0.025}O_{0.21}S_{0.006}$
Volatiles, V_I	$CH_{2.18}N_{0.048}O_{0.599}S_{0.019}$	$CH_{2.19}N_{0.0579}O_{0.623}S_{0.018}$	$CH_{2.18}N_{0.066}O_{0.64}S_{0.0170}$
Volatiles, V_{II}	$CH_{0.96}N_{0.021}O_{0.2649}S_{0.0084}$	$CH_{1.05}N_{0.027}O_{0.299}S_{0.0086}$	$CH_{1.142}N_{0.035}O_{0.336}S_{0.0088}$

Figure 6.19 shows the effect of increasing % of FB in the blend on the total volatile yield. It is noted that the competing reactions model is only for coal. The blended fuel is treated like a single fuel particle with an empirical chemical formulae presented in Table 6.3 with proximate yield equal to the weighted proximate yield. Competing reaction model is used for the pyrolysis. As the percentage of feedlot biomass is increased, there is an increase in the total volatile yield essentially due to higher proximate VM.

Figure 6.20 shows the variation of fraction of mercury and chlorine contained in the volatiles. The fraction of chlorine in volatiles increases due to an increase in the concentration of chlorine in the fuel blend. But in the case of mercury, the fraction decreases with increase percentage FB in the fuel blend since FB contains negligible Hg.

Figure 6.21 shows the percentage of mercury oxidized to $HgCl_2$ with increase in % FB. The chlorine liberated as HCl with FB, promotes the oxidation of Hg. For the base case, where the chlorine concentration is 140 ppm, the percentage of mercury oxidized is around 9%. At 20% of FB causes 90% of Hg gets oxidized to $HgCl_2$ from 9% to 90%(a ten fold increase). It is to note that FB has more volatiles; hence temperatures profiles for blend particle will be different compared to temperature profiles of a pure coal. Higher volatiles may lead to earlier ignition and higher gas phase temperature which effects the OH and Cl concentrations and hence Hg reactions

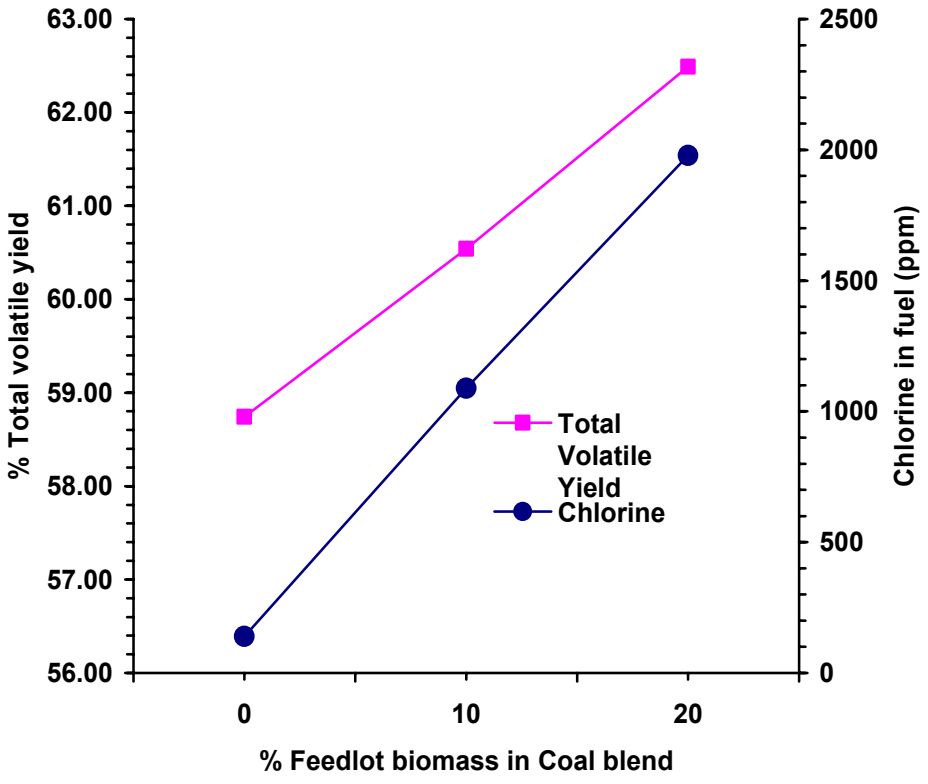

Fig. 6.19. Variation of total volatile yield and chlorine with coal blend

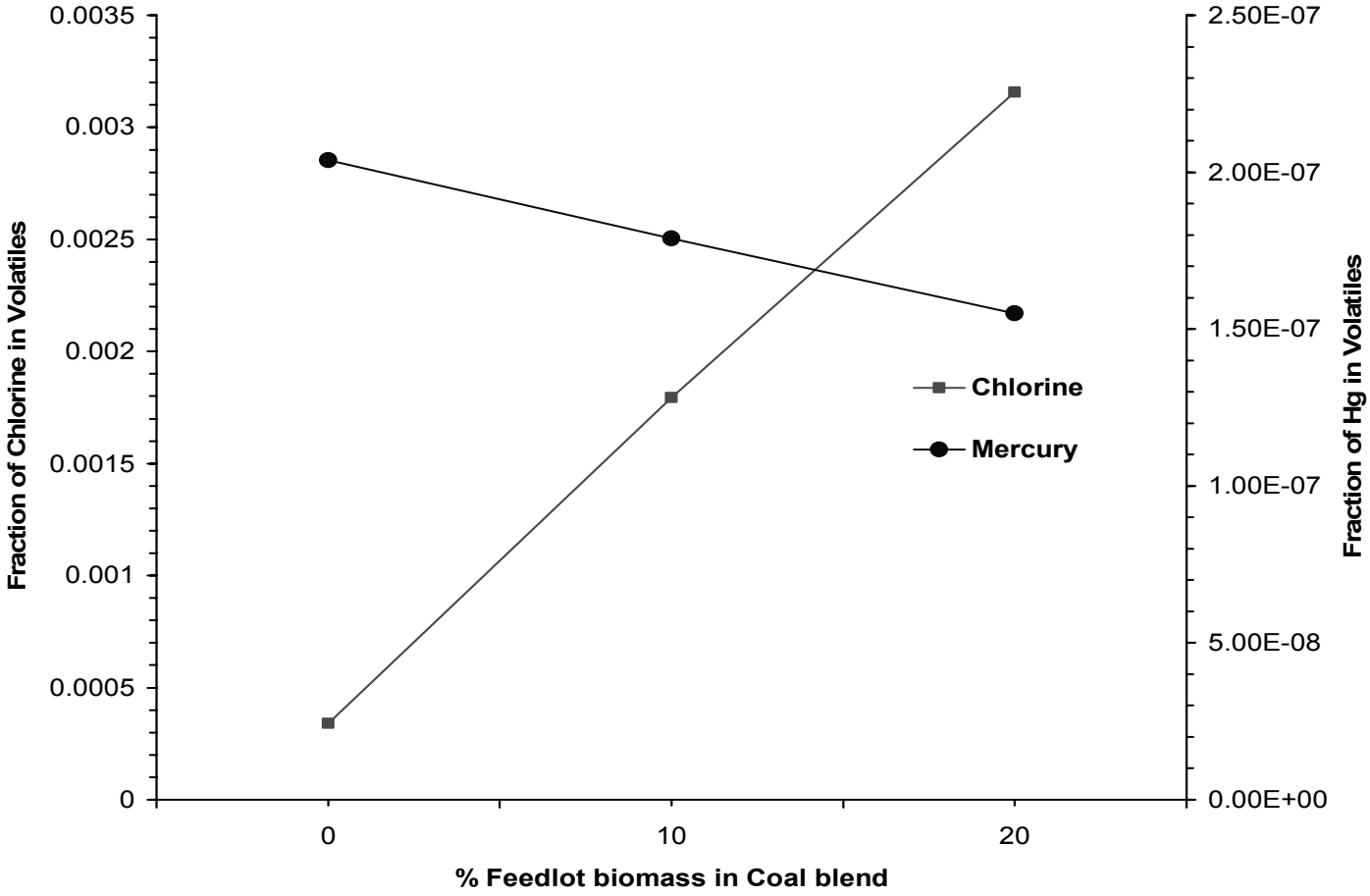

Fig. 6.20. Fraction of mercury ($f_{Hg,v}$) and chlorine ($f_{Cl,v}$) contained in volatiles

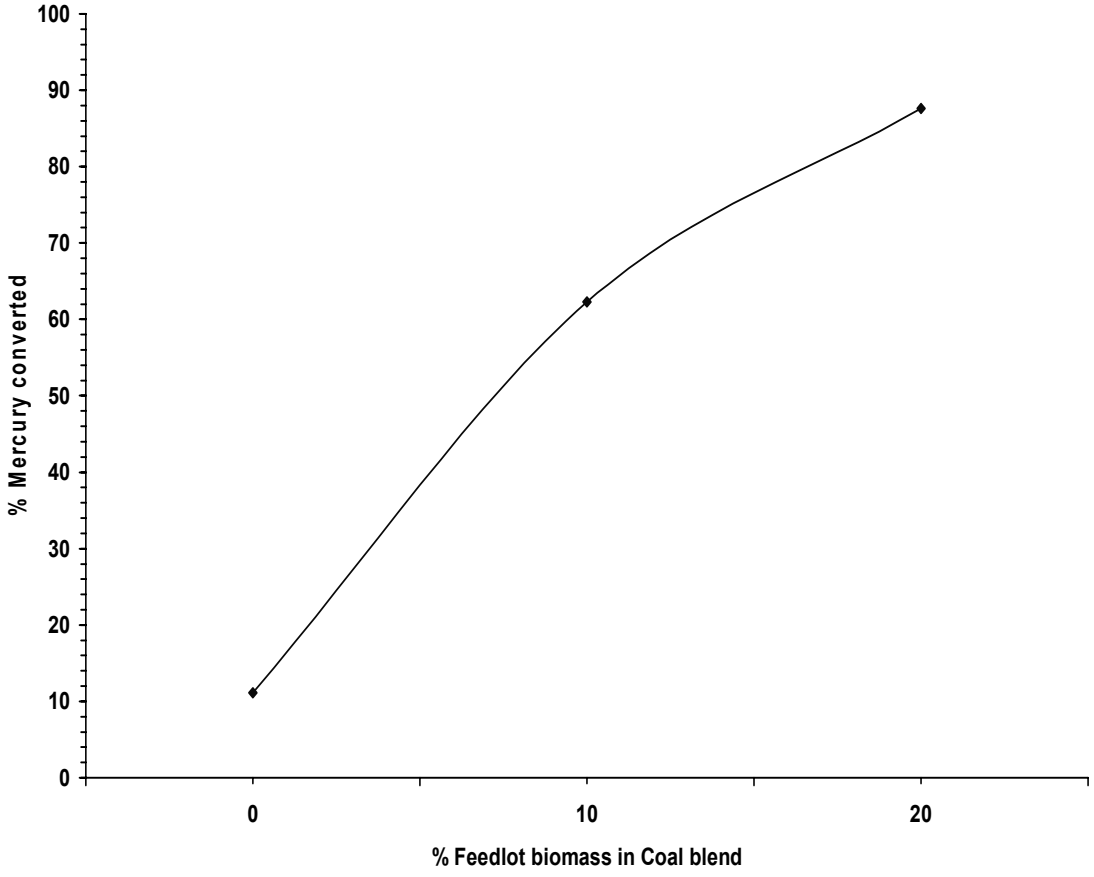

Fig. 6.21. Effect of blending coal on mercury oxidation

6.5.7 Effect of Different Temperature Profiles

For the base case study, analysis has been done for a constant ambient temperature. In this parametric study, analysis is done for varying temperature profiles. The temperature profiles used are obtained from the experimental studies. Figure 6.22 shows the different temperature profiles used for the analysis

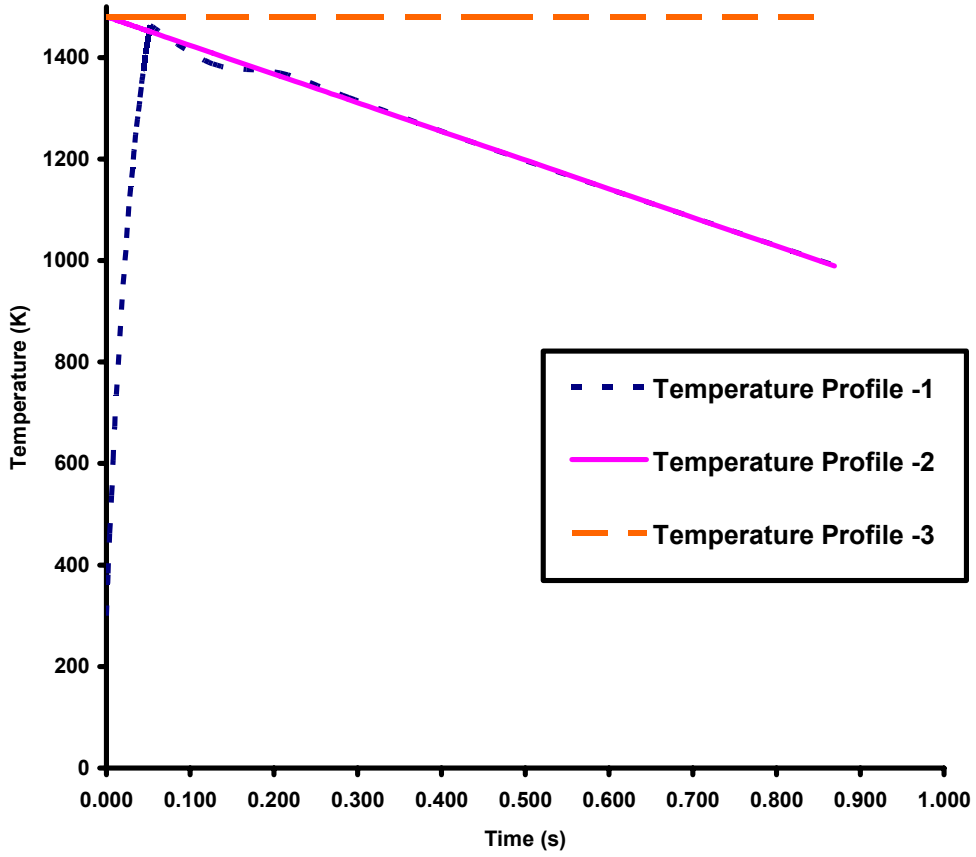

Fig. 6.22. Different temperature profiles

In the above graph, temperature profile-1 starts at temperature 300 K. This profile is similar to the temperature profile during reburn. Temperature profile-2 is similar to the temperature values obtained along the boiler with no reburn. And temperature profile-3 is the constant temperature profile, used in the analysis of base case.

The effect of different temperature profiles on the mercury oxidation are investigated. Figure 6.23 shows the result. The effect of temperature profile on mercury oxidation is found out to be in the following order, 1>2>3. Mercury oxidation chemistry is very

sensitive to the temperature. The average temperature in the gas phase region when temperature profile 1 is used is lesser when compared to profiles 2 and 3. Due to lower temperatures in the gas phase, the negative activation energy causes more oxidation of mercury.

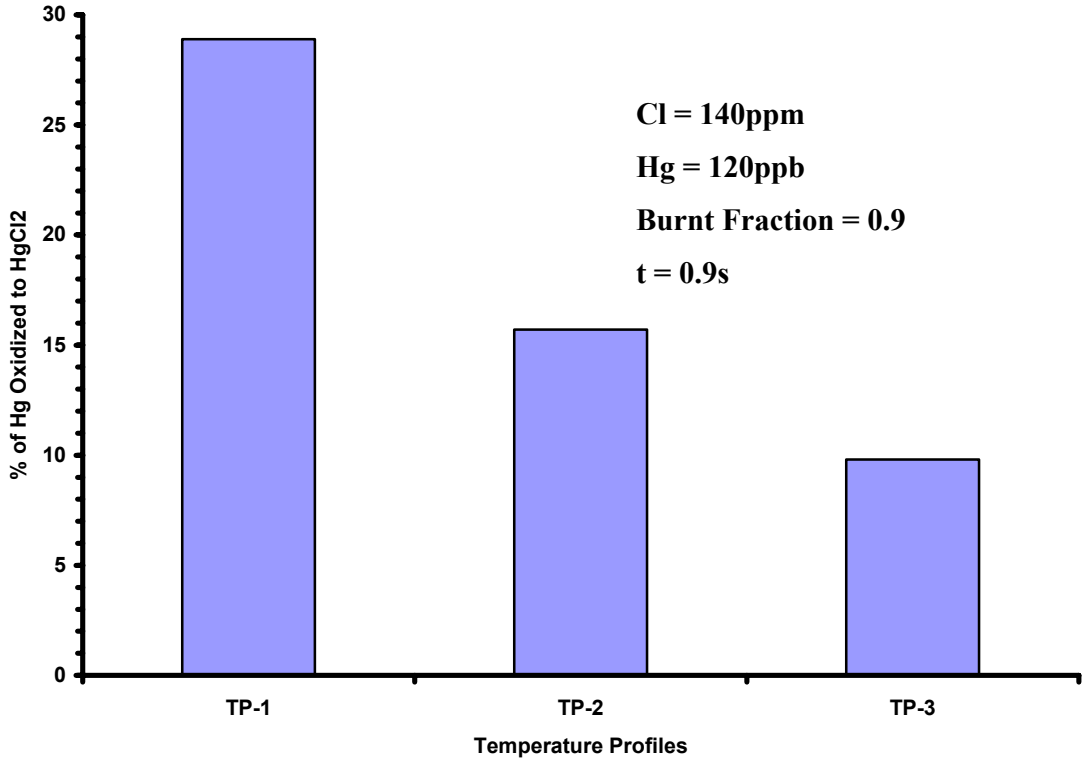

Fig. 6.23. Effect of temperature profile on mercury oxidation

6.5.8 Effect of Actual Diffusion Coefficient of Mercury

Previously, simulations have been performed considering the same diffusion coefficient for all the gas species. But actually species having higher molecular weight

diffuses less when compared to lighter species. Mercury and its species have larger molecular weight, so they diffuse relatively less than other gas species.

To include this change, changes have been made to numerical code. A detailed formulation is given in APPENDIX C. The values of diffusion coefficient of mercury are calculated experimentally and theoretically [47]. Figure 6.24 shows the change in percentage of mercury oxidized when actual diffusion coefficient of mercury is used. From the figure, it can be said that, the percentage of mercury oxidized has reduced when actual diffusion coefficient of mercury is used. For the base case, reduce in percentage of mercury oxidized is around 3%. At 1000 ppm of Cl, the reduce is around 7%. Figure 6.25 shows the mass fraction of mercury at two different time periods a) 50% volatiles release b) 100% volatiles release. It shows the effect the on mercury diffusion. When actual diffusion coefficient is used, mercury is diffused very slowly. The reason for reduce in percentage is because; the amount of mercury coming in to contact with chlorine is less. Chlorine which is lighter, diffuse faster than mercury species.

6.6 Experimental Validation

To validate the results and the accuracy of the numerical code, analysis has been done by using the values used in experiments [48]. Experiments are conducted by co-firing bituminous coal and sewage sludge in entrained flow reactor at constant temperature of 1370 K. The objective of the above experiments was to determine the behavior of the mercury in the flue gases. During co-combustion, HCl was added to simulate the effect of it on mercury oxidation.

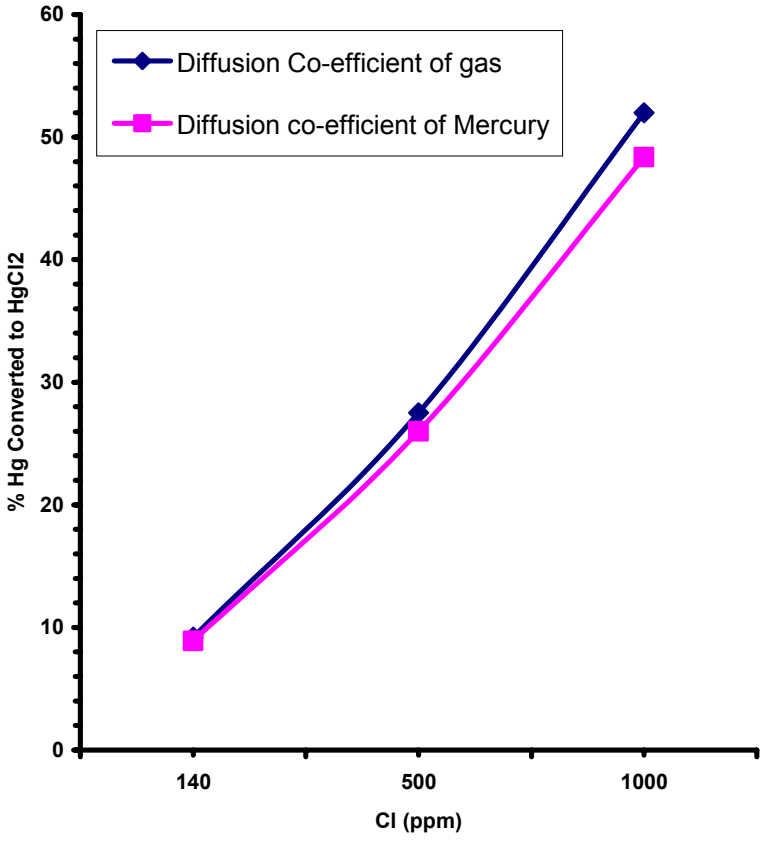

Fig. 6.24. Effect of diffusion coefficient on mercury oxidization

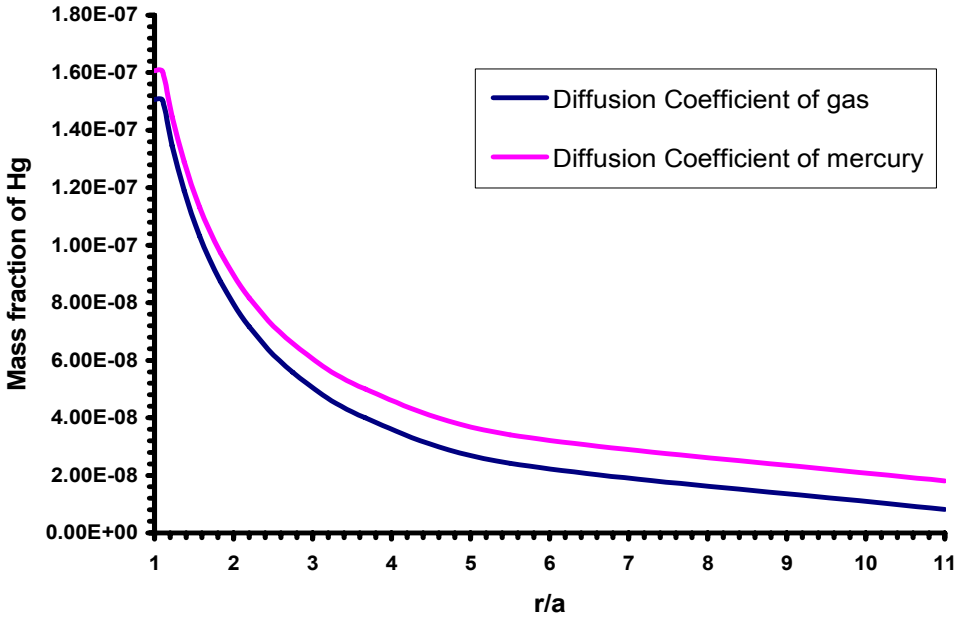

(a)

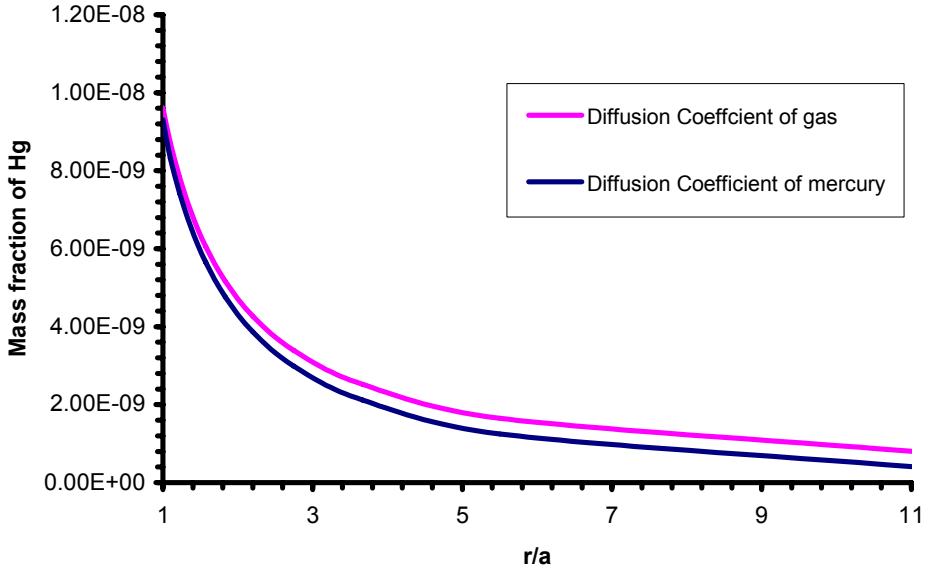

(b)

Fig. 6.25. Mass fraction of Hg a) 100% volatiles b) 50% volatiles

The ultimate and proximate analysis of the above fuels is given in Table 6.4. Analysis has been performed for coal blend of ratio 90:10 (no HCl spiking), 90:10 (with 12.41 ppm HCl spiking) and 90:10 (with 50.29 ppm HCl spiking). For the numerical studies, HCl spiking is simulated by adding HCl in the ambient.

Figure 6.26 shows the results obtained by the numerical analysis. Experimental results show that around 52% is converted of mercury is converted to mercury chloride. When the experiments are carried with spiking of HCl, for amounts of 12.41ppm, the oxidized mercury has increased by 4%. But when it is spiked by 50.29 ppm of HCl, the oxidized amount of mercury is reduced but the particulate mercury has increased. The excess amount of chlorine and the unburned carbon in the ash act as an activated carbon, which aids in adsorbing mercury and its compounds.

The numerical results obtained seem to agree with experimental values for the case a) coal blend, b) coal blend 90:10 with 12.5 ppm of HCl spiking. The results for the case c) coal blend with 50.29 ppm HCl spiking vary. This is because, in the simulations only homogeneous oxidation reactions have been considered. Due to this, the amount of mercury oxidized to mercury chloride in more when compared to experimental values.

Table 6.4

Proximate and ultimate analyses of the fuel

	Bituminous	**Sewage Sludge**	**Bituminous –Sew Sludge(90:10)**
Proximate (%)			
Volatile	36.5	93.68	42.21
Fixed C	63.5	6.31	57.78
Ultimate (%)			
Carbon	81.0	51.54	78.06
Hydrogen	5.39	8.39	5.67
Nitrogen	1.53	6.8	2.06
Sulfur	0.89	2.8	1.07
Oxygen	11.19	30.48	13.12
Chlorine (ppm)	2206	1193	2104
Mercury (ppb)	182	1642	328
HHV(kJ/kg)	27030	9480	25275

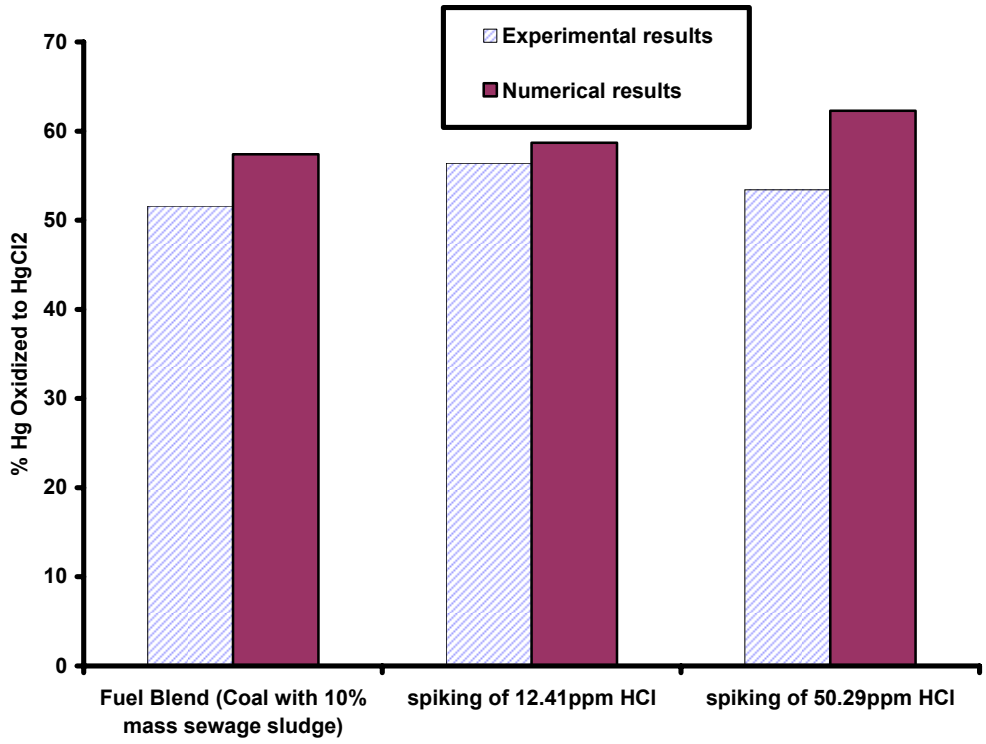

Fig. 6.26. Effect of co-combustion on mercury oxidation

6.7 Grid Independency

Numerical simulations are performed in order to study the independency of the solution on the grid size. Two different parameters are considered i) ignition time and ii) percentage of mercury oxidized for varying chlorine concentrations. Table 6.5 shows the varying of ignition time with respect to grid size. When the grid is very fine, there is not much of variation in ignition time. Figure 6.27 shows the percentage of mercury oxidized for different grid size. At higher grid size number, the change in the percentage is very less when compared to lower grid size number.

Table 6.5

Varying of ignition time with grid size

Grid Size	Ignition Time (s)
10	0.011810
15	0.011730
20	0.011725
25	0.011723
30	0.011722
35	0.011721

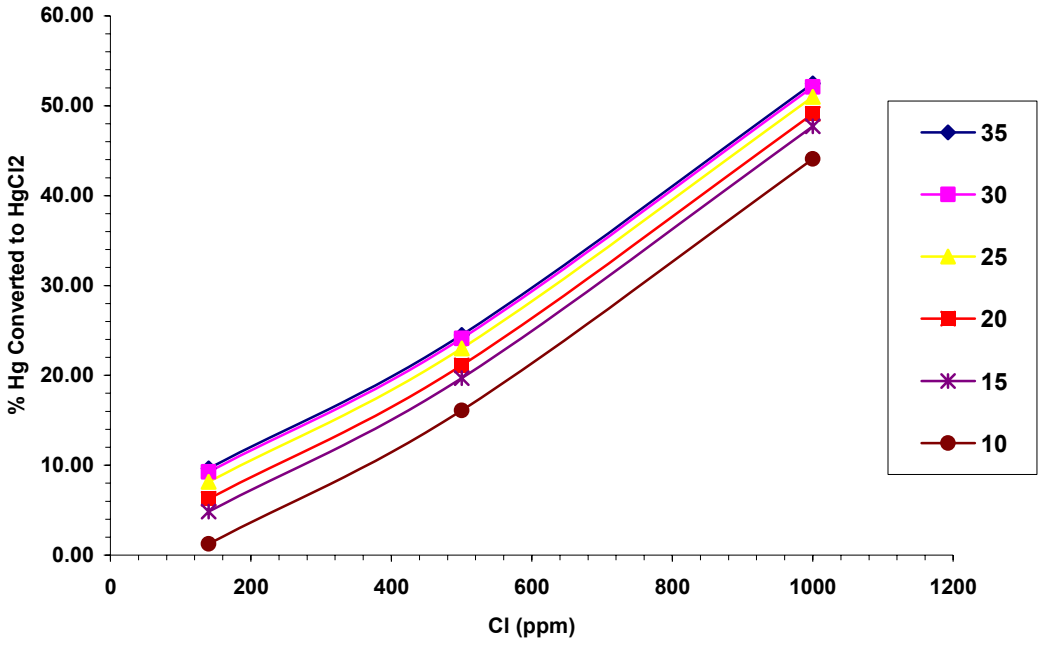

Fig. 6.27. Varying of mercury oxidation with grid size

7 CONCLUSIONS

An isolated coal particle combustion model is presented which includes pyrolysis of mercury and chlorine and mercury oxidation reaction mechanism.

1. The equilibrium calculations demonstrated that the most important factor for the oxidation of mercury in the post-combustion gases is the chlorine-contained species. The results show that all of the Hg exists in the form $HgCl_2$ below 750°K. From the equilibrium studies, HgCl is more dominant than $HgCl_2$ at higher temperatures. The amount of Hg oxidized depends on the temperature of the gas species.
2. Temperature was found to be a significant aspect in mercury oxidation. The extent of mercury oxidation depends on the temperature at which the reaction takes place. Due to the negative activation energy of the two reactions involving Cl, OH in the three step reaction mechanism and large time scales at lower temperatures, an increase in mercury oxidation is noticed at low ambient temperatures.
3. Particle size has a small effect on the mercury oxidation. Particles of larger size tend to increase the percentage of mercury oxidized to mercury chloride. This is attributed to the point that when the particle size is increased, increased time and reaction volume zones are available for the reactions which results in an increase in mercury oxidation. When the diameter is increased from 100 microns to 200 microns, the percentage of mercury oxidized increased from 8 to 18.

4. Similar to temperature, chlorine concentration in flue gases has a substantial effect on mercury oxidation. Coals which have high concentration of coal tends to emit fewer amounts of mercury emissions when compared coals which have very less amount of coal. It has also been seen, addition of chlorine to flue gases also assists in reducing mercury emissions.
5. Volatile matter was found to be a weak factor for promoting mercury oxidation. There is not a significant change in numbers when volatile matter is varied from 30% to 80%.
6. Parametric study of the effect of chlorine radical kinetics revealed that atomic chlorine is plays an important role in mercury oxidation. An increase in the concentration of atomic chlorine in the flue gas, promotes mercury oxidation. This increase is obtained by the changing the kinetics of the Reaction VIII.
7. The idea of blending coal with feedlot biomass is to reduce the mercury emissions. Chlorine which is present in large amounts in FB will help in converting elemental mercury to mercury chloride. Results have shown that by blending coal with FB in the ratios of 90:10 and 80:20 will result in around 65%-80% of mercury converting to mercury chloride. While for pure coal the Hg converted is only 9%.

8 RECOMMENDATIONS FOR FUTURE RESEARCH

Recommendations for future work in this area include:

1. Expand the isolated combustion model to incorporate the group combustion of coal particles which includes the detailed mercury and chlorine reaction chemistry.
2. Both homogenous and heterogeneous reactions contribute in reducing the mercury emissions. The present model only studies homogeneous reactions involving mercury and chlorine species. Include heterogeneous reactions into the model in order to give an accurate representation.
3. Present studies reveal that ash plays an important role in reducing mercury emissions. Many compounds present in ash aid in adsorbing mercury. Including heterogeneous kinetics in the numerical model will help in carrying Hg speciation in particulate phase.
4. Even though chlorine and its species have a major effect on mercury oxidation, it would be reasonable if other components of flue gas are added to the mercury oxidation reaction to study their effect.

NOMENCLATURE

a	radius of the particle
B	pre-exponential frequency factor, m/s
c	coal particle specific heat, kJ/kg K
D	diffusion coefficient, m^2/s
d_p	particle diameter, m
E	activation energy, kJ/kmol
$f_{Hg,v}$	fraction mercury contained in volatiles
$f_{Cl,v}$	Fraction of mercury contained in volatiles
h_m	mass transfer coefficient
h_T	thermal enthalpy, kJ/kg
$h_{T,ref}$	reference enthalpy = C_pT_{ref}, kJ/kg
h^*	non dimensional enthalpy = $h/h_{T,ref}$
k	specific reaction rate constant, m/s
$\dot{m}$	mass flow rate, kg/s
m_{cu}	undecomposed particle mass, kg
$\dot{m}_C$	heterogeneous mass burning rate, kg/s
$\dot{m}_{Cl}$	mass loss rate due to chlorine, kg/s

$\dot{m}_{Hg}$	mass loss rate due to mercury, kg/s
m_p	particle mass
$\dot{m}_p$	particle mass loss rate, kg/s
$\dot{m}_{ref,g}$	reference mass loss rate = $4\pi\rho Da$, kg/s
$\dot{m}_{ref,p}$	reference particle mass loss rate = $m_{p,0}/t_{ref}$, kg/s
$\dot{m}_V$	mass loss rate due to pyrolysis, kg/s
n	particle number density, m^{-3}
P	Pressure
$\dot{q}'''_{conv}$	convective heat transfer between gas phase and the particle, kJ/kg
$\dot{q}'''_{ch}$	enthalpy produced as a result of chemical reactions in the gas phase, kJ/kg
$\dot{q}'''_m$	enthalpy gained by the gas phase due to the addition of mass from the particles, kJ/kg
R_u	universal gas constant, kJ/kmol K
T	temperature, K
T_{ref}	reference temperature, K
t	time, s
t_{ref}	reference time = $\rho_{ref}\, a^2 / \rho D$
V	volatiles

w_k	non dimensional source of species = $\dot{w}_k''' \Big/ \dot{m}_{ref,g}'''$
w_h	non dimensional source of enthalpy = $\dot{w}_h''' \Big/ \dot{m}_{ref,g}''' h_{T,ref}$
w_m	non dimensional volumetric mass source = $\dot{w}_m''' \Big/ \dot{m}_{ref,g}'''$
$\dot{w}_h'''$	volumetric gas phase enthalpy source, kW/m^3
$\dot{w}_k'''$	volumetric gas phase of species k, kg/m^{3}s
$\dot{w}_{k,ch}'''$	species addition due to gas phase chemical reaction, kg/m^{3}s
$\dot{w}_{k,pp}'''$	species addition due to chemical reactions at the particle, kg/m^{3}s
$\dot{w}_m'''$	volumetric mass source, kg/m^{3}s
Y	species mass fraction

Greeks

α	non dimensional mass flow = $\dot{m} \Big/ \dot{m}_{ref}$
α_I, α_{II}	maximum volatile matter via pyrolysis routes I and II
ν_{O2}	stoichiometric mass of oxygen per unit mass of carbon
ξ	non dimensional inverse radius = a/r
ρ	gas phase density, kg/m^3
ρ_{ref}	reference density = $P/R_u T_{ref}$, kg/m^3
ρ^*	non dimensional density = ρ/ρ_{ref}
τ	non dimensional time = t/t_{ref}

Subscipts

C	carbon, char
Cl	chlorine
ch	gas phase chemical reaction
ch,p	particle chemical reaction
cu	coal undecomposed
Hg	mercury
$HgCl_2$	mercury chloride
k	species
I	volatiles due to route I
II	volatile due to route II
O_2	oxygen
ref	reference
T	thermal
V	volatile
W	surface of the particle
0	at time t = 0
∞	infinite

Superscripts

‴	per unit volume
*	non dimensional variable

Acronyms

FB	feedlot biomass
PCD	polluting control devices
SMD	sauter mean diameter
VM	volatile matter

REFERENCES

[1] Endress+Hauser, Coal Fired Power Plant, http://www.endress.com, Sept 2006.

[2] United Nations Environment Programme, Civil Society, http://www.unep.org, June 2005.

[3] D. K. James, C. B. Sedman, R. K. Srivastava, J. V. Ryan, C. W. Lee, and S. A. Thorneloe, Control of Mercury Emissions from Coal Fired Electric Utility Boilers: Interim Report; No: EPA-600/R-01-109.; USEPA, Office of Research and Development, 2002.

[4] J. F. Thomas, Mercury Control Technology Field Phase II Testing Status Report; NETL, US DOE, 2005.

[5] United States Geological Survey, Mercury, http://www.usgs.gov, June 2005.

[6] Environmental Protection Agency, Mercury,, http://www.epa.gov/mercury, June 2005.

[7] C. L. Senior, D. Lignell, B. Shiley, Z. Chen, A. Sarofim, Kinetic Models for Predicting the Behavior of Mercury in Coal-Fired Power Plants, in: ACERC Annual Conference, Salt Lake City, UT, Feb 19-20, 2003.

[8] W. P. Linak, J. V. Ryan, B. S. Ghorishi, J. O. L. Wendt, J. Air Waste Manage. Assoc. 51 (2001) 688-698.

[9] S. M. Wilhelm, Mercury in Petroleum and Natural Gas: Estimation of Emissions from Production, Processing, and Combustion; EPA-600/R-01-066; Office of Air Quality Planning and Standards: 2001.

[10] D. Xiangyang, K. Annamalai, Combust. Flame 97 (1994) 339-354.

[11] R. Meij, Water, Air, Soil Pollut. 56 (1991) 21-23.

[12] P. Chu, D. B. Porcella, Water, Air, Soil Pollut. 80 (1995) 135-144.

[13] P. Chu, B. Nott, W. Chow, Results and Issues from the Pisces Field Tests, in: 2nd International Conference on Managing Hazardous Air Pollutants, Washington, DC, 1993.

[14] R. Meji, H. J. V. Leo, W. Henk, J. Air Waste Manage. Assoc. 52 (2002) 912-917.

[15] F. Fransden, K. Dam-Johanses, P. R. Ramussen, Prog. Energy Combust. Sci. 20 (1994) 115-138.

[16] C. L. Senior, A. F. Sarofirm, T. Zeng, J. J. Helble, R. Mamani-Paco, Fuel Process. Technol. 63 (2000) 197-213.

[17] M. S. De Vitto, W. A. Rosnhoover, Flue Gas Mercury and Speciation at Coal-Fired Utilities Equipped with Wet Scrubbers, in: 15th International Pittsburgh Coal Conference, Pittsburgh, PA, Sept 15-17, 1998.

[18] B. Hall, P. Schanger, J. Wesmaa, Chemosphere 30 (1995) 611-627.

[19] Y. Otani, C. Kanaoka, C. Usui, S. Matsui, H. Emi, Environ. Sci. Technol. 20 (1986) 735-738.

[20] P. Schanger, B. Hall, O. Lindqvist, Retention of gaseous mercury on fly ashes, in: 2nd International Conference on Mercury as Global Pollutant, Monterey, CA, 1992.

[21] W. H. Gibb, F. Clarke, A. K. Mehta, Fuel Process. Technol. 65-66 (2000) 365-377.

[22] L. Kunlei, Ying Gao, John T. Riley, Wei-Ping Pan, Arun K Mehta, Ken K Ho, Stephen R Smith, Energy Fuels 5 (2001) 1173-1180.

[23] N. C. Widmer, J. West, Thermochemical Study of Mercury Oxidation in Utility Boiler Fuel Gases, in: 93rd Annual Meeting, Air & Waste Management Association, Salt Lake City, UT, 2000.

[24] S. Niksa, N. Fujiwara, The Impact of Wet FGD Scrubbing on Hg Emissions from Coal-Fired Power Stations, in: Joint EPRI DOE EPA Combined Utility Air Pollution Control Symposium, The Mega Symposium, Washington, DC, Aug 30-Sept 2, 2004.

[25] P. Nolan, W. Downs, R. Bailey, S. Vecci, Use of Sulfide Containing Liquors for Removing Mercury from Flue Gases. US Patent # 6,503,470, Jan 7, 2003.

[26] P. Chu, D. Laudal, L. Brickett, C. W. Lee, Power Plant Evaluation of the Effect of SCR Technology on Mercury, in: DOE-EPRI-U.S. EPA -A&WMA Combined Power Plant Air Pollutant Control Symposium - The Mega Symposium, Washington, DC, May 19-22, 2003.

[27] H. P. John, Everett A. Sondreal, Michael D. Mann, Edwin S. Olson, Kevin C. Galbreath, Dennis L. Laudal, Steven A. Benson, Fuel Process. Technol. 82 (2003) 89-165.

[28] M. Antonia Lopez-Anto´n, Juan M.D. Tasco´n, M. Rosa Martı´nez-Tarazona, Fuel Process. Technol. 77-78 (2002) 353-358.

[29] Z. Hancai, Feng Jin, Jia Guo, Fuel 83 (2004) 143-146.

[30] H. P. John, M. J. Holmes, S. A. Benson, C. R. Crocker, K. C. Galbreath, Fuel Process. Technol. 85 (2004) 563-576.

[31] J. M. Stanley, E. D. Grant, S. O. Edwin, D. B. Thomas, Fuel Process. Technol. 65-66 (2000) 343-363.

[32] F. D. Guffey, A. E. Bland, Fuel Process. Technol. 85 (2004) 521-531.

[33] B. Hall, P. Schanger, E. Ljungstrom, Water, Air, Soil Pollut. 81 (1-2) (1995) 121-134.

[34] S. Niksa, J. J. Helble, N. Fujiwara, Environ. Sci. Technol. 35 (2001) 3701-3706.

[35] A. N. Glenn, H. Yang, R. C. Brown, D. L. Laudal, G. E. Dunham, J. Erjavec, Fuel 82 (2003) 107-116.

[36] M. Rostam-Abadi, Y. Lu, B. G. Miller, S. F Miller, Combustion of Sewage Sludge and Coal Fines in a Pilot-Scale Circulating Fluidized-Bed Combustor; Electric Power 2005, in: 7th Annual Conference and Exhibit, Chicago, Illinois, April 5-7, 2005.

[37] D. Dajnak, F. C. Lockwood, International Flame Research Foundation Combustion Journal, http://www.journal.ifrf.net (2001)

[38] J. F. Roesler, R. A. Yetter, F. L. Dryer, Combust. Flame 100 (1995) 495-504.

[39] D. B. Anthony, J. B. Howard, H. P. Meissner, Fuel 55 (1976) 121-128.

[40] D. B. Stickler, R. E. Gannon, H. Kobayashi, Rapid Devolatilization Modeling of Coal, in: Easter States Meeting of the Combustion Institute, Silver Spring,MD, 1974.

[41] S. K. Ubhayakar, D. B. Stickler, C. W. Von Rosenberg, R. E. Gannpon, Rapid Devolatilization of Pulverized Coal in Hot Combustion Gases, in: 16th Symposium (International) on Combustion, The Combustion Institute, Pittsburgh, 1977.

[42] K. Annamalai, I. Puri, Combustion Science and Engineering Technology, Taylor & Francis, Oxford, UK, 2006.

[43] I. W. Smith, Combust. Flame 13 (1971) 303-314.

[44] F. L. Dryer, I. Glassman, High temperature oxidation of CO and CH4, in: 14th International Symposium on Combustion, The Combustion Institute, Pittsburgh, PA, 1973.

[45] H. Vandenabeele, R. Corbeels, A. Vantiggelen, Combust. Flame 4 (1960) 253-260.

[46] D. Xiangyang, Ignition and Combustion of a Dense Stream of Coal Particles, Ph.D., dissertation, Texas A&M University, College Station, 1995.

[47] J. G. Peter, P. Peter, R. P Steven, J. Chem. Eng. Data 36 (1991) 265-268.

[48] H. Michael, S. Unterberger, K. R. G. Hein, Chem. Eng. Technol. 24 (12) (2001) 1267-1272.

APPENDIX A

DESCRIPTION OF SUBROUTINES AND INPUT DATA

A.1 Subroutine Description

Each subroutine used in the man program for group combustion of coal particles and its functions are described as follows:

ALPA	This subroutine is used to determine the nondimensional radial mass flow rate. It is called by program COALPILE for each time step after all gas phase variables have been determined at each location.
CLCOMP	This subroutine IS used to determine the coal composition on a molar basis from the input coal composition on mass basis. It is called by program COALCOMP once the input data has been read and before the variables are initialized.
CLPROD	This subroutine is used to determine the chlorine volatile source per unit volume of the gas phase. It calls subroutines VLPROD. It is called by subroutine SOURCE at each time step.
COMPR	This subroutine is used to determine the pyrolysis rates of variables I and II using the competing reaction model. It is called by subroutine VOLPRD at each time step.

CONV	This subroutine is used to determine the convective heat transfer between the gas phase and a single particle. It is called by subroutine HTCONV at each time step and each location.
COOXD	This subroutine is used to determine the mass consumption rate of carbon monoxide and oxygen and the production rate of carbon dioxide due to the gas phase oxidation of carbon monoxide. It is called subroutine SOURCE at each time step and location.
DCUR	This subroutine is used to determine the new particle diameter from the previous particle diameter and the heterogeneous oxidation rate of a fixed carbon. It is called by subroutine HETPRD at each time step and each location within the cloud.
DELTOU	This subroutine is used to determine the new time step for use in the calculations. The new time step is based on three criteria. The first criterion involves the gas phase temperature rise. More specifically, if the gas phase temperature at any location raises more than a specified amount during a single time step, then a new time step is found that would limit the temperature to the specified temperature rise. Similarly, the second criterion involves limiting the particle temperature

	rise. The third criterion is based on the stability criteria. The subroutine chooses the minimum of these three time steps for use over the next time interval. It is called by program COALPILE at the end of each time step.
EQUATION	This subroutine is used to use to solve for the values of the gas phase dependent variables at the current time. It is called by program COALPILE at each time step and location after the source terms for the gas phase variables have been determined.
FACTOR	This subroutine is used to determine the radiative view factor between the surroundings and the particles. Currently, this value is assumed to be one. It is called by subroutine RADN at each time step and each location.
FBLOW	This subroutine is used to determine the blowing correction factor to the particle Nusselt number for use in determining the convective heat transfer to the particle and drag force. It is called by subroutine CONV at each time step and location within the cloud.
FCUTIL	This subroutine is used to determine the fraction of coal undecomposed for use in the competing reaction model. It is called by subroutine VOLPRD at each time step and each

	location within the cloud.
FKNUD	This subroutine is used to determine the Knudsen factor and Nusselt number for use in determining the convective heat transfer to the particle. It is called by subroutine CONV for each time step and each location within the cloud.
H2OOXD	This subroutine is used to determine the dissociation rate of H_2O to OH and H_2 and the subsequent recombination rates. It is called by subroutine SOURCE at each time step and location.
HCLOH	This subroutine is used to determine the chlorine radical source term. It is called by the subroutine SOURCE.
HETPRD	This subroutine is used to determine the total consumption rates of fixed carbon and in-situ volatiles due to the heterogeneous reactions and finds the total gas phase source terms for gas phase mass fractions and enthalpy due to heterogeneous reactions. It calls subroutines SURFR, HETVOL, WALMSF and DCUR. It is called by subroutine SOURCE at each time step and location within the cloud.
HETVOL	This subroutine is used to determine the heterogeneous oxidation rate of insitu volatiles assuming that the volatiles oxide to water vapor and carbon monoxide. It is called by subroutine HETPRD at each time step and each location

	within the cloud.
HGPROD	This subroutine is used to determine the mercury volatile source per unit volume of the gas phase. It calls subroutines VLPROD. It is called by subroutine SOURCE at each time step.
HGCL, HGCL2	These two subroutines determine the mercury oxidation with chlorine. It is called by the subroutine SOURCE.
HTCONV	This subroutine is used to determine the heat transfer from the gas phase to the particles per unit volume of the gas phase. It calls subroutine CONV and RADN. It is called by subroutine SOURCE; it each time step and each location.
HVVOL	This subroutine is used to determine the heating values of volatiles I and II using the heating value of the coal, the latent heat of pyrolysis, and the mass fraction of the parent coal that can be released as volatiles I or II. It assumes that volatiles are combusted to carbon dioxide and water vapor. It is called by program COALPILE once the input data have been read and before the variables are initialized.
MASSP	This subroutine is used to determine the new particle mass from the previous particle mass, the time step, and the mass loss rates due pyrolysis and heterogeneous oxidation of fixed carbon and in-situ volatiles. It called by program COALPILE

	at each time step and location within the cloud.
PRINTOUT	This subroutine is used to determine the print formats of the output from the program. It is called from program COALPILE as necessary.
QFACT	This subroutine is used to determine the instantaneous Q' factor for the coal particles from the volatile kinetics and the instantaneous particle temperature. It is called by program COALPILE at each time step and each location within the cloud.
RADN	This subroutine is used to calculate the radiative heat transfer. It is called by subroutine CONV at each time step.
RHOP	This subroutine is used to determine the particle density using the mass loss rate due to pyrolysis predicted by the competing reaction model. It is called by subroutine VOLPRD at each time step and each location within the cloud.
SORCOG	This subroutine is used to determine the correction factor for the gas phase reactions. It is called by subroutine HETPRD at each time and each location within the cloud.
SORCOP	This subroutine is used to determine the correction factor for the gas phase reactions. It is called by subroutine HETPRD at each time and each location within the cloud.

SOURCE	This subroutine is used to determine the source terms for the gas phase variables due to gas phase oxidation and heterogeneous reactions. It calls subroutines COOXD, H2OOXD, HETPRD, HTCONV, VOLOXD and VOLPRD to determine the various contributions to the source terms from each mechanism. It then finds the total source term for each gas phase variable from the individual contributions. It then calls subroutine SORCOR to correct the total source terms. It is called by program COALPILE at each time step and location.
STCVOL	This subroutine is used to determine the stoichiometric combination coefficient for the volatiles with respect to diatomic oxygen using the coal molar compositions. It is called by program COALPILE once the input data have been read and before the variables are initialized.
SURFR	This subroutine is used to determine the consumption rate of the fixed carbon, the consumption rate of oxygen, and the production rates of carbon monoxide, carbon dioxide, water vapor and enthalpy due to heterogeneous oxidation of fixed carbon and in-situ volatiles. It is called by subroutine HETPRD at each time step and location within the cloud.
THETAP	This subroutine is used to determine the current particle

	temperature. It uses the radiative heat transfer to the particles, the convective heat transfer to the particle, the latent heat of vaporization and the heat generation from heterogeneous oxidation of fixed carbon and in-situ volatiles. It is called by the program COALPILE at each time step.
VLCOMP	This subroutine is used to determine the composition of volatiles I and II from the coal molar composition and the maximum mass fraction of volatiles I and II that can be released according to the competing reaction model. It is called by program COALPILE after the input values have been read in and before the variables are initialized.
VOLINT	This subroutine is used to perform volumetric integrations to determine such things as total coal mass, total mercury oxidized etc. It is called by program COALPILE as necessary.
VOLFRAC	This subroutine is used to determine the instantaneous coal mass fraction that could be released as volatiles I. It is called by program COALPILE at each time step and each location within the cloud.
VOLOXD	This subroutine is used to determine the volatiles oxidation rate in the gas phase. It is called by subroutine SOURCE at each time step and each location.

VOLPRD	This subroutine is used to determine the volatile source per unit volume of the gas phase. It calls subroutines COMPPR, FCUTIL and RHOP. It is called by subroutine SOURCE at each time step and location within the cloud.
WALMSP	This subroutine is used to determine the mass fraction of the gas phase components at the particle surface. It is called by subroutine HETPRD at each time step and each location.

The program begins by reading the input data card (described in the following section) and, then, it prints out the problem types under consideration and the values of input data read in for the checking purpose. The coal composition on a mole basis is determined in subroutine CLCOMP from the input coal mass fractions. Then, subroutine HVVOL determines the heating values of the volatiles from the coal heating values and the latent heat of pyrolysis. The volatiles composition is then determined in subroutine VLCOMP from the coal composition and the mass fractions of volatiles I and II used in the competing reaction model. Next, subroutine STVOL determines the volatile stoichiometric combination coefficients from the volatiles composition. The gas phase properties, particle properties and other variables are then initialized. The loop that steps in time is entered next with the time step determined by subroutine DELTOU and values of global variables at the previous time step are saved for use in the current time step. The loop that steps in space is then entered. Values at the current location and previous time are stored for use in the current calculation.

Subroutine SOURCE is called to determine the source for mass, enthalpy and species mass fractions. It has many subroutines in order to accomplish this task (refer to Fig. 5.1). Subroutine H2OOXD is called to determine the dissociation and recombination of water vapor using finite kinetics. Subroutine HCLOH, HGCL and HGCL2 is called to determine the source terms for chlorine radical and oxidized forms of mercury. Subroutine VOLOXD is called to determine the source terms for volatiles, water vapor mass fraction, carbon dioxide, and enthalpy produced due to the combustion of volatiles. Subroutine COOXD is then called to determine the source terms for carbon monoxide, carbon dioxide, oxygen and enthalpy resulting from the combustion of carbon monoxide. Subroutine VOLPRD, which calls subroutine COMPR, FCUTIL and RHOP, is called to determine the production rate of volatiles and the consumption rate of enthalpy due to pyrolysis. Subroutine CLPROD and HGPROD are called to determine the chlorine and mercury production rate due to pyrloysis. Subroutine COMPR uses the finite competing reaction kinetics to determine the release rate of volatiles I and II**.** Subroutine FCUTIL determines the fraction of coal undecomposed (f_{cu}) for use in the competing reaction pyrolysis model. Subroutine RHOP determines the current density of the particles.

Subroutine SOURCE then calls subroutine HETPRD that determines the source terms from heterogeneous oxidation reactions. Subroutine HETPRD calls subroutines SURFR, HETVOL, WALMSP and DCUR. Subroutine SURFR uses finite oxidation kinetics to determine the total consumption and production rates of fixed carbon, in-situ volatiles, carbon monoxide, carbon dioxide, water vapor and enthalpy from heterogeneous reactions.

Subroutine HETVOL determines the rate of homogeneous in-situ volatiles combustion. Subroutine WALMSP determines the gas phase mass fractions at the particle surface. Subroutine DCUR determines the current particle diameter. Subroutine SOURCE now determines the total production and consumption rates of each gas phase component as a result of all reactions. Subroutine SOCOG is then called to correct gas phase reactions.

Subroutine SOCOP is called by subroutine HETPRD to correct solid phase reactions. Finally, subroutine HTCONV is called to determine the convective heat transfer from the cloud gas phase to a single particle. It calls subroutines FBLOW and FKNUD that determine the blowing correction factor and the Knudsen correction factor to the Nusselt number. The program flow now returns to program COALPILE and subroutine EQUATION is called to solve for the current values of enthalpy and gas phase mass fractions.

Program COALPILE now calls subroutine MASSP to determine the current particle mass. Subroutine RADN is called to determine the radiative heat transfer to the particle from the surroundings. Subroutine THETAP is called to determine the new particle temperature.

Once the particle properties have been determined, the program exits the space step loop and calls VOLINT to perform volumetric integration throughout the cloud of various parameters. Finally, subroutine DELTOU is called to determine the time step for use in the next time step and the program steps in time.

A.2 Description of Input Data

This section introduces each input data card to be used in running the program with a brief description of each variable in the input data card.

Data Card 1: Ambient Data

TINF= the ambient temperature surrounding the cloud, T_∞

YO2INF= the initial oxygen mass fraction in the ambience, $Y_{O2,\infty}$

YCO2INF= the initial carbon dioxide mass fraction in the ambience, $Y_{CO2,\infty}$

YVIINF= the initial low temperature volatile mass fraction in the ambience, $Y_{VI,\infty}$

YV2lNF= the initial low temperature volatile mass fraction in the ambience, $Y_{VII,\infty}$

YH2OINF= the initial water mass fraction in the ambience, $Y_{H2O,\infty}$

TGCO= the initial gas phase temperature, $T_{GC,0}$,

TPO= the initial particle temperature, $T_{p,0}$

PRESS= the pressure, p

PGSAT= the saturation pressure of water, p_{H2O}

YO2CO= the initial concentration of oxygen in gas phase, Y_{O2CO}

Data Card 2: Coal Data

C= the carbon mass fraction of the coal, C

H= the hydrogen mass fraction in the coal, H

N= the nitrogen mass fraction in the coal, N

O= the oxygen mass fraction in the coal, O

HG= the mercury mass fraction in the coal, HG

Cl= the chlorine mass fraction in the coal, Cl

ASH= the ash mass fraction in coal, AH

HCOAL= the heating value of the coal, h_{coal}

EMISS= the emissivity of the coal, a

Data Card 3: Particle Data

DPO(I) = the diameter of the particles for size group I, d

NPS(I) = the particle number density for size group I, n

RHOPO(I) = the coal density of size group I, ρ

Data Card 4: Competing Reaction Pyrolysis Data

VM(1) the maximum yield allowed via competing reaction route 1, a,

VM(2) the maximum yield allowed via competing reaction route 2, a,,

EV(1) the activation energy for competing route 1, $E_{V,I}$

EV(2) the activation energy for competing route 2, $E_{V,II}$

BV(1) the preexponential factor for competing route 1, $B_{V,I}$

BV(2) the preexponential factor for competing route 2, $B_{V,II}$

HPYR(1) the latent heat of reaction for pyrolysis route 1, $h_{p,I}$

HPYR(2) is the latent heat of reaction for pyrolysis route 2, $h_{p,I}$

Data Card 5: Char kinetics Data

EC(1)= the activation energy for heterogeneous reaction 1, $E_{C,1}$

EC(2)= the activation energy for heterogeneous reaction 2, $E_{C,2}$

EC(3)= the activation energy for heterogeneous reaction 3, $E_{C,3}$

EC(4)= the activation energy for heterogeneous reaction 4, $E_{C,4}$

NO21= the oxygen reaction order with respect to heterogeneous reaction 1, $n_{02.1}$

NO22= the oxygen reaction order with respect to heterogeneous reaction 2, $n_{O2,2}$

NCO23= the carbon dioxide reaction order to heterogeneous reaction 3, n_{CO}

NH2O4= the water reaction order with respect reaction 4, n_{H2O}

BC(1)= the preexponential factor for heterogeneous reaction 1, $B_{C,1}$

BC(2)= the preexponential factor for heterogeneous reaction 2, $B_{C,2}$

BC(3)= the preexponential factor for heterogeneous reaction 3, $B_{C,3}$

BC(4)= the preexponential factor for heterogeneous reaction 4, $B_{C,4}$

Data Card 6: CO Oxidation Kinetics Data

ACO= the preexponential factor for CO oxidation in the gas phase, A_{CO}

ECO= the activation energy for CO oxidation in the gas phase, E_{CO}

NCO= the order of CO reaction with respect to the oxidation, n_{CO},

NO2CO= the order of O_2, reaction with CO oxidation in the gas phase, $n_{O2,CO}$

NH2OCO= the order of water reaction with CO oxidation in the gas phase, $n_{H2O,CO}$

ACOB= the preexponential factor for CO, dissociation in the gas phase, $A_{CO,b}$

ECOB= the activation energy for CO, dissociation in the gas phase, $E_{CO,b}$

Data Card 7: Volatile Oxidation Kinetics Data

AVG= the preexponential factor for volatile oxidation in the gas phase, $A_{V,g}$

EVG= the activation energy for volatile oxidation in the gas phase, $E_{v,g}$

NV= the order of reaction for volatile oxidation in the gas phase, n_V

NO2V= the order of O_2, reaction to volatile oxidation in the gas phase, $n_{O2,V}$

Data Card 8: Mercury Oxidation with Chlorine radical

AHG= the preexponential factor for CO oxidation in the gas phase, A_{HG}

EHG= the activation energy for CO oxidation in the gas phase, E_{HG}

NHG= the order of CO reaction with respect to the oxidation, n_{HG},

NCLHG= the order of Cl, reaction with HG oxidation in the gas phase, $n_{Cl,HG}$

AHGCL= the preexponential factor for CO oxidation in the gas phase, A_{HGCL}

EHGCL= the activation energy for CO oxidation in the gas phase, E_{HGCL}

NHGCL= the order of CO reaction with respect to the oxidation, n_{HGCL},

NCLHGCL= the order of Cl, reaction with HG oxidation in the gas phase, $n_{Cl,HGCL}$

Data Card 9: Numerical Data

XIMAX= the maximum value of the reversal radius, ξ

FNXI= the number of space steps

DTEMPL= a switch to stop calculation for the current time step

DTGLMT= a switch to recalculates the time step

DTPLMT= the maximum particle temperature rise allowed per time step

DTSET= the initial time step specified

CRTIG= the criteria used to signal ignition

FBO= the fraction of the particle mass left at "burnout"

Data Card 10: Program Control Data

ICHAR= a switch that determines whether coal or char combustion is simulated

IFREEZE= a switch that specifies whether the gas phase is frozen or not

IOXDV= a switch that controls whether volatile oxidation is on or not

IOXDCO= a switch that controls whether CO oxidation is on or not

IFLAG= a switch that determines whether an initial time step is externally set or not

IVOLS= a switch that determines whether volatiles are consumed in-situ or not

ICOVOLS= a switch that specifies whether the volatiles are oxidized to CO or CO,

INSTCO= a switch that specifies if finite kinetics is used for CO oxidization

INSTV= a switch that specifies if finite kinetics is used for volatile oxidization

NSIZE= the number of size groups of particles within the cloud

NITERN= the maximum number of time steps allowed

ISTEP= the number of time steps between printouts

ISPACE= the number of space steps between printing

IPRINT= a switch that specifies whether subroutine PRINTOUT prints or not

IMETHD= a switch that specifies the numerical method used

ISTAT= the value that corresponds to the outer boundary of the calculation domain

IABIB= a switch that specifies whether the outer boundary is adiabatic or not

IIGN= a switch that specifies whether the run is made for ignition or not

INOX= a switch that determine. Whether NO, production is on or not

IQHEAT= a switch that specifies whether the adiabatic boundary is used or not

IPEAK= a switch that specifies that only peak values are printed

ICOORD= a switch that determines which coordinate is to be used

IEQUIL= a switch specifies whether backward reactions are included or not

IEXPAN= a switch that determines whether cloud expansion is included or not

ISOLATE= a switch that determines whether isolated coal or coal cloud

Data Card 11: Free Stream Gas Properties

RHOD= the product of pg and the diffusivity, ρD

CP= the specific heat of the gas phase, c_p

LAMBDA= the conductivity of the gas phase, λ

NU= Nusslet number, Nu

APPENDIX B

B.1 Mercury – Chlorine Equilibrium

Three different mercury oxidizing reactions are studied. Below are the three equilibrium reactions which are considered:

$Hg + Cl_2 \Leftrightarrow HgCl_2$ I

$Hg + Cl_2 \Leftrightarrow HgCl + Cl$ II

$Hg + Cl_2 \Leftrightarrow \frac{1}{2} HgCl + \frac{1}{2} HgCl_2 + \frac{1}{2} Cl$ III

For the above reactions, the equilibrium constants have been calculated at different temperatures ranging from 298K to 3000K.

$$k_{eq} = \exp(-\Delta G/RT) \quad (B.1)$$

Where ΔG is the Gibb's free energy and R is the universal gas constant. For the above reactions, the amount of mercury oxidized is calculated using the equilibrium constant and the partial pressures of the reactants and the products. From the equilibrium values calculated for the reactions (I, II and III) at different temperatures, a graph is plotted between ln (k_{eq}) vs. 1/T and they are linearly fitted. This graph is shown in Fig B.1. The values of the slope obtained from the curve fit gives you the values of Gibb's free energy.

Table B.1

Values of A and B

	A	B
I	-11.827	24773
II	-0.3386	4269.6
II	3.679	-16783

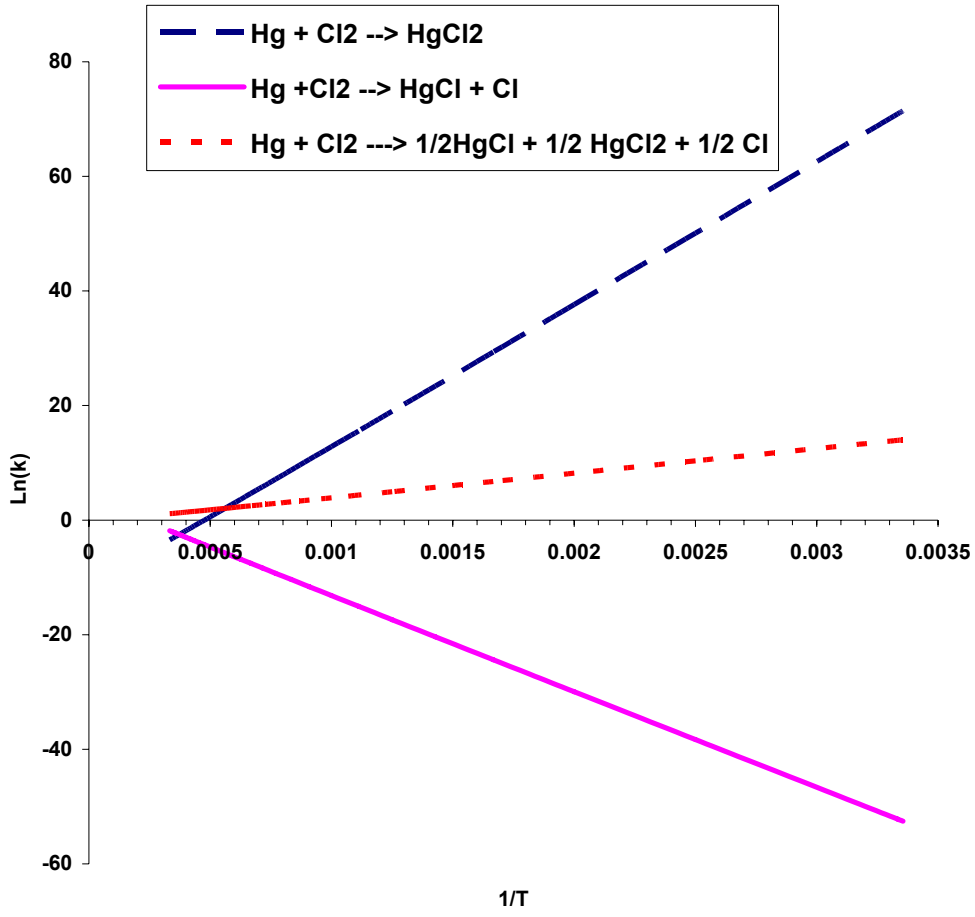

Fig. B.1. Plot of Ln (k) Vs 1/T

B.2 Mercury Loading

Mercury loading is defined as the amount of Hg (kg) per Giga joule. The Hg in the exhaust gases is treated with chlorine. The amount of Hg left after the reaction helps in calculating mercury loading. Usually the volume of exhaust gases is limited to 350 m^3/GJ. This value depends on the type of coal. It depends on H/C and O/C ratio. These ratios are calculated my finding out the empirical formula of the coal being used.

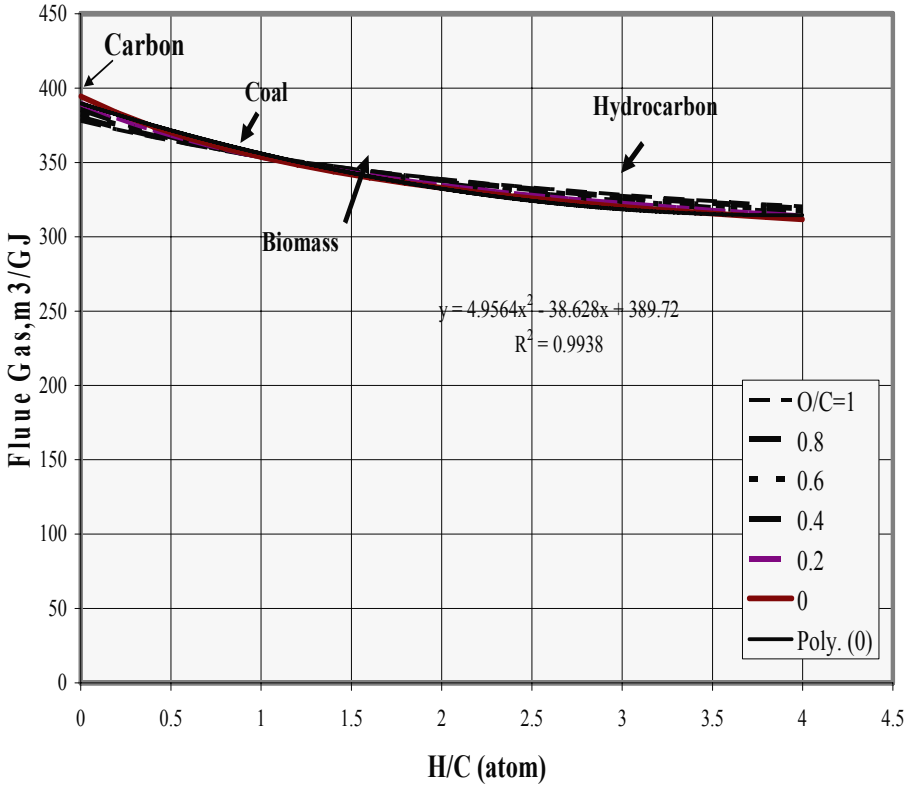

Fig. B.2. Variations of exhaust volume gas with H/C and O/C ratio

The following is the analytical method to calculate the mercury loading.

Let the Volume of the dry exhaust gas be V_{exh} m^3/GJ at STP conditions. V_{exh} for a coal industry is typically 350 m^3/GJ. To calculate the number of moles of exhaust gas, we use the ideal gas law.

$$PV = n_tRT \quad (B.2)$$

Where, P is pressure (atm), V is volume in litres, R is Universal Gas constant (atm.L/kmole.K). n_t is total moles of exhaust gas

At STP conditions, pressure is 1 atm, temperature is 273 K.

Now, $n_t = PV/RT$, substituting the values of P, V, R and T respectively,

$$n_t = (1*V_{exh}*10^3)/ (82.06*273)$$

n_t = 15.62 k moles.

The mercury vapor in the exhaust gas according to the experimental analysis is given in the range of 1-10 ppbv. For the present calculation, the value taken is 10ppbv. Now, the amount of mercury (V_m) in the given amount of exhaust gas is $V_{exh} * 10^{-08}$ m^3/GJ.Under STP conditions, the number of kmoles of mercury for the volume V_m is given by

$$n_m = PV/RT \quad (B.3)$$

$$n_m = (1*V_m)/RT$$

$$n_m= (1*V_{exh}*10^{-08})/ (82.06*273)$$

$n_m = 1.56 \times 10^{-07}$ k moles.

The chlorine is injected in to the exhaust gas in order to reduce the concentration of the elemental mercury. Considering that chlorine reacts with mercury to form mercuric chloride. According to the stoichometric reaction equation one kmole of chlorine reacts with one kmole of mercury to form one kmole of mercuric chloride.

$$Hg + Cl_2 \rightarrow HgCl_2 \quad \text{(B.5)}$$

Usually in experimental analysis excess of chlorine is injected (more than the required amount).Now considering the below chemical reaction.

$$n_m\,Hg + n_m(1+C/100)Cl_2 \text{ ---> } a\,HgCl_2 + b\,Hg + d Cl_2 \quad \text{(B.6)}$$

where 'C' is the excess % of Chlorine injected.

Now performing atom balance for the above reaction,

For Hg:

$$n_m = a + b \quad \text{(B.7)}$$

For Cl:

$$n_m\,(1+C/100) = a+d \quad \text{(B.8)}$$

There are three variables, namely a, b and d. The third equation is derived from the equilibrium reaction between mercury and chlorine.

$$Hg + Cl_2 \Leftrightarrow HgCl_2 \quad \text{(B.9)}$$

The equilibrium constant K (T) is given by:

$$k(T) = \frac{N_{HgCl2} * N_t}{N_{Hg} * N_{Cl2} * P} \quad \text{(B.10)}$$

where P = 1atm

Where, $N_{HgCl2} = a$; $N_{Hg} = b$; $N_{Cl2} = d$; $N_t = a + b + c + n_t$. Since n_t (exhaust moles) >> a, b, d Nt becomes equal to n_t and Eq. B.9 changes to

$$k(T) = (a * n_t)/(b*d) \quad \text{(B.11)}$$

Now rearranging the Eqs B.7, B.8 and B.11 and writing them in terms of the variable 'b' we get:

$$b\text{^}2 + b*\left(\frac{C*n_m}{100} + \frac{n_t}{K}\right) - \frac{n_m * n_t}{K} = 0 \quad \text{(B.12)}$$

The above equation is solved for various values of k_{eq} (equilibrium constant) for each value of C (excess % of chlorine).

The values of 'a' and 'd' are calculated from Eqs (B.7) and (B.8). The value of b is given in *kmoles/GJ*. Mercury loading (b) is normalized with respect to initial concentration of mercury in exhaust gases (n_m).

APPENDIX C

Diffusion coefficient of mercury species is less when compared to the air and other species Cl, HCl, O_2, N_2, CO_2 etc. In order to consider the diffusion coefficient of mercury species for the numerical simulations, the following changes have been made to the conservative equations.

Species

$$4\pi r^2 \rho\left(\frac{\partial Y_k}{\partial t}\right)+\dot{m}\left(\frac{\partial Y_k}{\partial r}\right)-\left[\frac{\partial}{\partial r}\left(4\pi r^2 \rho D_{Hg}\left(\frac{\partial Y_k}{\partial r}\right)\right)\right]=\dot{w}'''_{ch,k}\,4\pi r^2 \qquad \text{(C.1)}$$

where,

D_{Hg} Diffusion coefficient of mercury

Multiplying and diving the diffusion term in Equation C.1 by ρD , the equation can be written as follows:

$$4\pi r^2 \rho\left(\frac{\partial Y_k}{\partial t}\right)+\dot{m}\left(\frac{\partial Y_k}{\partial r}\right)-\left[\frac{\partial}{\partial r}\left(4\pi r^2\left(\frac{\rho D_{Hg}}{\rho D}\right)\rho D\left(\frac{\partial Y_k}{\partial r}\right)\right)\right]=\dot{w}'''_{ch,k}\,4\pi r^2 \qquad \text{(C.2)}$$

where,

D Diffusion coefficient of gas (assumed equal binary diffusion coefficient)

$$\left(\frac{\rho D_{Hg}}{\rho D} \right) = \beta \tag{C.3}$$

$$4\pi r^2 \rho \left(\frac{\partial Y_k}{\partial t} \right) + \dot{m} \left(\frac{\partial Y_k}{\partial r} \right) - \left[\frac{\partial}{\partial r} \left(4\pi r^2 \beta \rho D \left(\frac{\partial Y_k}{\partial r} \right) \right) \right] = \dot{w}'''_{ch,k} \, 4\pi r^2 \tag{C.4}$$

Non dimensionalizing Eq C.4 using the non-dimensional variables given in Section 4, equation can be written as

$$\rho^* \frac{\partial Y_k}{\partial \tau} - \alpha \xi^4 \left(\frac{\partial Y_k}{\partial \xi} \right) - \beta \xi^4 \left(\frac{\partial^2 Y_k}{\partial \xi^2} \right) = w_k \tag{C.5}$$

The property ψ and the constant A, B, C and D for the conservation equations are tabulated in Table C.1

Table C.1

Conserved quantity ψ for Eulerian equations

	Species (Y_k) **k = Hg, HgCl, $HgCl_2$**
A	1
B	α
C	β
D	1
W_ψ	W_k

Recollecting Eq. C.3,

$$\beta = \left(\frac{\rho D_{Hg}}{\rho D} \right)$$

ρD = 0.5 E-04 kg/m.s and ρD_{Hg} = 0.317 E-04 kg/m.s

β = 0.634

VITA

Madhu Babu Puchakayala was born in Hyderabad, India. He received his Bachelor of Technology and Master of Technology degrees in mechanical engineering from Indian Institute of Technology, Madras, India in May 2000 and 2002. The author may be contacted at L.I.G B 555, Dr A S Rao Nagar, Hyderabad, Andhra Pradesh, India, 500062 or by email at madhu_iitc@yahoo.com.